RESPONSE PROPERTIES OF DURATION-TUNED NEURONS IN THE BAT

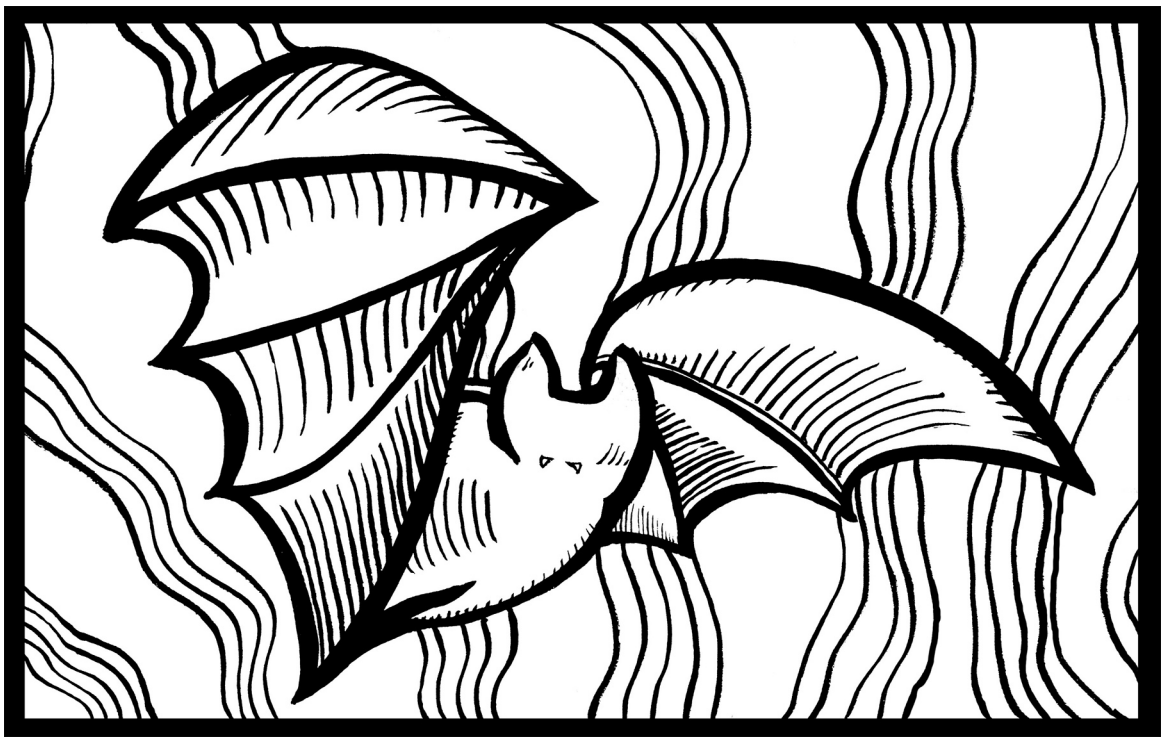

MONAURAL AND BINAURAL RESPONSE PROPERTIES OF DURATION-TUNED NEURONS IN THE BIG BROWN BAT

By RIZIQ SAYEGH, B.Sc.

A Thesis submitted to the School of Graduate Studies in Partial Fulfilment of the Requirements for the Degree Doctor of Philosophy

McMaster University DOCTOR OF PHILOSOPHY (2013) Hamilton, Ontario
Department of Psychology, Neuroscience & Behaviour

TITLE: Monaural and Binaural Response Properties of Duration-Tuned Neurons in the Big Brown Bat
AUTHOR: Riziq Sayegh, B.Sc. (McMaster University)
SUPERVISOR: Dr. Paul A. Faure
NUMBER OF PAGES: xiv, 195

Abstract

Neurons throughout the auditory pathway respond selectively to the frequency and amplitude of sound. In the auditory midbrain there exists a class of neurons that are also selective to the duration of sound. These duration-tuned neurons (DTNs) provide a potential neural mechanism underlying temporal processing in the central nervous system. Temporal processing is necessary for human speech, discriminating species-specific acoustic signals as well as echolocation. This dissertation aims to explore the role and underlying mechanisms of DTNs through single-unit *in vivo* electrophysiological recordings in the auditory midbrain of the big brown bat. The durations that DTNs are selective to in echolocating and non-echolocating species are first compared to the durations of each species vocalizations. This comparison reveals that the durations DTNs respond best to correlates to the durations of echolocation calls in echolocating species and to species-specific communication calls in non-echolocating species. The ability of DTNs in the bat to respond to stimulus parameters thought to be important for echolocation processing, such as pairs of pulses and binaural sound localization cues, are subsequently tested. The responses of DTNs to a paired tone spike suppressing paradigm presented monaurally and binaurally are also compared to characterize the role each ear plays in recruiting inhibition known to be involved in duration tuning. The results show that DTNs are able to respond to pairs of pulses at a timescale relevant to bat echolocation, and a majority also responded selectively to binaural sound localizing cues. Nearly half (48%) of DTNs did not show spike suppression to an ipsilaterally presented suppressing tone. When ipsilaterally evoked spike suppression occurred, the effect was significantly smaller than the suppression evoked by a contralateral suppressing tone. These findings provide evidence that DTNs may play a role in echolocation in bats as DTNs are able to respond to the outgoing pulse and returning echoes and localize the echo source and that the neural mechanism underlying duration tuning is monaural in nature.

This dissertation is dedicated to my wife, Michelle.

Thank you for your love, patience and support.

Acknowledgements

I recall the excitement I felt those first few times I managed to find a neuron and heard the action potentials popping through a set of computer speakers as they pierced through a sea of noise on the oscilloscope. I would pick up the lab phone and dial up my supervisor to tell him the good news, and he would drop whatever he was doing and rush down to the lab to share in the excitement. Even today the action potentials of a neuron responding to auditory stimuli that I've provided always seems to elicit an "excitatory" response in me. It took some time to get to the point where I could record neural activity in the bat brain. I had to put equipment together, solder wires, ground the rig, learn the surgical and electrophysiological procedures and create an appropriate microelectrode recipe to name a few hurdles, but I had a patient supervisor who always made time for me when I needed him. This dissertation would not have been possible without the guidance and encouragement of my supervisor, Dr. Paul A. Faure. I am also indebted to my committee members, Deda Gillespie, Hong-Jin Sun and Laurel J. Trainor for their support and guidance these past years and for helping me grow academically.

Many thanks to past and present lab mates, Brandon Aubie, Alejandra Ceballos-Vasquez, Natalie Cheng, Heather Mayberry, and Roberto Valdizon for the mutual support. It has been a pleasure working with Brandon Aubie these past years and I am eternally thankful for having a fellow student to talk to about the ups and downs of electrophysiology work. His custom software, SpikeDB, also proved to be a boon when it came time to analyze my data. In my time as a graduate student in the bat lab I have had the honour of supervising a number of graduate and undergraduate students in various stages of electrophysiology work: Brandon Aubie, Siavosh Fazel-Pour, James Morrison and Roberto Valdizon. Thanks for putting up with me.

Thank you Miroslav Cika and Jan Lewandowski for your countless hours spent plan-

ning, building and repairing custom hardware that proved invaluable to my research efforts.

Thank you Shannon Challis for providing me with a beautiful illustration of a bat in flight that appears as the frontispiece to this dissertation.

I would like to thank some past and present "gangroom" office mates: Kevin Abbott, Dan Case, Alan Cooper, Zachary Durisko, Lara Kujtan, Julie Marentette, Vicky Mileva, Sachin Sarin and Corrine Seeley along with some honourary members Rayna Friendly, Ashna Patel and Molly Pottruff. Over the years we've come to share more than just an office space and I cherish the time we've spent together. I would also like to thank a few friends outside of the ivory tower, Mike Daye, Jeff Kuronen, Mike Lazic and Brad Miller, for showing interest in my work and at times providing a much needed distraction.

A special thanks to my parents Adel and Rawieh Sayegh and my brother Samer Sayegh for their support throughout my academic career. I would not be here today without you.

Table of Contents

Abstract iii

Acknowledgements v

Table of Contents vii

List of Figures x

List of Tables xi

List of Abbreviations and Symbols xii

Declaration of Academic Achievement xiii

1 Introduction 1

2 Duration Tuning in the Auditory Midbrain of Echolocating and Non-Echolocating Vertebrates 7

2.1 Abstract . . . 7
2.2 Introduction . . . 8
2.3 Electrophysiology of duration tuning . . . 10
2.3.1 Response classes . . . 10
2.3.2 Response properties . . . 11
2.4 Mechanisms of duration tuning . . . 13
2.4.1 Coincidence detection mechanisms . . . 14
2.4.2 Anti-coincidence mechansisms . . . 16
2.4.3 Neural circuit implementations . . . 17
2.5 Duration tuning and echolocation . . . 19
2.6 Future studies . . . 22

3 Recovery Cycle Times of Inferior Colliculus Neurons in the Awake Bat Measured With Spike Counts and Latencies 43

3.1 Abstract . . . 43
3.2 Introduction . . . 45
3.3 Methods . . . 48
3.3.1 Surgical procedures . . . 48
3.3.2 Electrophysiological recordings . . . 49
3.3.3 Stimulus generation and data collection . . . 50

3.3.4 Measuring recovery times . . . 51
3.3.5 Data analysis . . . 54
3.4 Results . . . 55
3.4.1 Response properties . . . 55
3.4.2 Recovery cycle times . . . 56
3.4.3 Recovery cycles measured with spike counts and latencies . . . 59
3.4.4 Recovery cycles and response properties . . . 61
3.5 Discussion . . . 62
3.5.1 Recovery cycles and spike latencies . . . 62
3.5.2 Effect of stimulus amplitude and BEF on FSL and recovery times . . . 64
3.5.3 Spatial mapping of best duration . . . 65
3.5.4 Biological significance of recovery times . . . 66
3.5.5 Recovery cycles and neural inhibition . . . 69
3.6 Summary . . . 71

4 Monaural and Binaural Neural Inhibition Underlying Duration-Selective Responses in the Inferior Colliculus 102
4.1 Abstract . . . 102
4.2 Introduction . . . 104
4.3 Materials and Methods . . . 106
4.3.1 Surgical procedures . . . 106
4.3.2 Electrophysiological recordings . . . 107
4.3.3 Stimulus generation and data collection . . . 108
4.3.4 Data analysis . . . 110
4.4 Results . . . 110
4.4.1 Determining the timecourse of inhibition . . . 110
4.4.2 Comparing the timecourse of inhibition measured with spike counts and latencies . . . 113
4.4.3 Inhibition evoked with monotic and dichotic paired tone stimulation 115
4.4.4 Comparing monotic and dichotic inhibitory responses . . . 117
4.4.5 Relation of leading/lagging inhibition to BD, FSL and duration filter characteristic . . . 118
4.4.6 Effect of increasing NE tone amplitude in the dichotic condition . . . 120
4.5 Discussion . . . 121
4.5.1 Inhibitory inputs that create duration-tuned neurons are monaural . . . 121
4.5.2 Effect of increasing NE tone amplitude in the dichotic condition . . . 122
4.5.3 Role of inhibition recruited by the ipsilateral ear . . . 123
4.5.4 Monotic and dichotic temporal masking . . . 125

5 Dichotic Sound Localization Properties of Duration-Tuned Neurons in the IC of the Big Brown Bat 141
5.1 Abstract . . . 141

5.2 Introduction . . . 143
5.3 Methods . . . 145
5.3.1 Surgical procedures . . . 145
5.3.2 Electrophysiological recordings . . . 146
5.3.3 Stimulus generation and data collection . . . 147
5.3.4 Measuring neural responses to sound localization cues . . . 148
5.4 Results . . . 149
5.4.1 Response properties . . . 149
5.4.2 ILD selectivity . . . 151
5.4.3 ITD selectivity . . . 152
5.5 Discussion . . . 154
5.5.1 ILD selectivity . . . 155
5.5.2 ITD selectivity . . . 155
5.5.3 Time-intensity trade-off . . . 156
5.5.4 Comparing responses of temporally-selective and non-temporally-selective neurons . . . 158
5.5.5 Possible function(s) of DTNs in echolocation . . . 159
5.6 Summary . . . 161

6 Discussion **179**
6.1 Significance of dissertation . . . 179
6.2 Research limitations . . . 181
6.3 Alternate role of DTNs . . . 183
6.4 Future directions . . . 185

List of Figures

2.1 Echolocation calling sequences from two species of bats that employ different signaling strategies . . . 39
2.2 Example DTNs in the IC of *E. fuscus* . . . 40
2.3 Conceptual models of coincidence detection and anti-coincidence mechanisms of duration tuning . . . 41
3.1 Measuring recovery cycle times of IC neurons . . . 87
3.2 Temporal tuning and spatial topography or tonotopy in the IC . . . 89
3.3 Spike latency and tonotopy in the IC . . . 90
3.4 Response and recovery in a bandpass DTN . . . 91
3.5 Response and recovery in a shortpass DTN . . . 93
3.6 Response and recovery in a non-DTN . . . 95
3.7 Comparison of recovery time measures . . . 97
3.8 Comparison of mean recovery times measured with spike counts and spike latencies . . . 98
3.9 Mean recovery time as a function of stimulus duration at +20 dB above threshold . . . 100
3.10 Mean recovery time as a function of FSL at +10 dB above threshold . . . 101
4.1 Measuring the timecourse of inhibition with paired tone stimulation . . . 131
4.2 Comparing monotic and dichotic paired tone stimulation . . . 133
4.3 Onset of inhibition recruited monaurally and binaurally . . . 135
4.4 Histograms of the duration of inhibition minus the duration of the NE tone recruited monaurally and binaurally . . . 136
4.5 Comparing the latency and duration of inhibition in the monotic and dichotic condition . . . 137
4.6 Relation of leading inhibition to BD, FSL and duration filter characteristic . . . 138
4.7 Effect of increasing NE tone amplitude . . . 139
5.1 Example responses of IC neurons to binaural ILD stimuli . . . 173
5.2 ILD sensitivity of IC neurons . . . 175
5.3 Distribution histograms of ILD_{50} and slope factor values as a function of duration-selectivity and amplitude re theshold of the contralateral stimulus . . . 176
5.4 Example responses of IC neurons to dichotic ITD stimuli . . . 177

List of Tables

2.1 Neuronal best duration tuning in amphibians and mammals compared with typical species-specific acoustic vocalization durations 38
3.1 Mean ± SE first- and last-spike latency as a function of cell type and level above threshold 85
3.2 Mean ± SE spike count recovery time (and range) as a function of cell type and level above threshold 85
3.3 Mean ± SE first-spike latency (FSL) recovery time (and range) as a function of cell type and level above threshold 86
3.4 Mean ± SE last-spike latency (LSL) recovery time (and range) as a function of cell type and level above threshold 86
3.5 Mean ± SE recovery times as a function of the measured recovery parameter and level above threshold 86
5.1 Peak spikes per stimulus to ILD stimuli. 170
5.2 Peak spikes per stimulus to ITD stimuli. 170
5.3 Summary statistics of ILD-tuning in DTN and non-DTN neurons. 171
5.4 Summary statistics of ITD-tuning in DTN and non-DTN neurons. 172

List of Abbreviations and Symbols

AC	Auditory cortex
ANOVA	Analysis of variance
BD	Best duration
BEF	Best excitatory frequency
CF	Constant frequency
CNS	Central nervous system
D_{BD}	Duration of best duration tone
D_{NE}	Duration of non-excitatory tone
DTN	Duration-tuned neuron
FM	Frequency modulation
FSL	First spike latency
GABA	γ-Aminobutyric acid
IC	Inferior colliculus
ICc	Central nucleus of the inferior colliculus
ILD	Interaural level difference
IPI	Interpulse interval
ITD	Interaural time difference
L_{first}	First spike latency
L_{last}	Last spike latency
LSL	Last spike latency
MGB	Medial geniculate body
NE	Non-excitatory duration
OFF_E	Offset-evoked excitation
ON_E	Onset-evoked excitation
P1	First pulse
P2	Second pulse
PT	Pure tone
R1	Response to first pulse
R2	Response to second pulse
SD	Standard deviation
SE	Standard error
T_1	Onset of spike suppression
T_2	Offset of spike suppression
T_{end}	Effective end time of inhibition
T_{start}	Effective start time of inhibition
SPL	Sound pressure level
SUS_I	Sustained onset-evoked inhibition
TS	Torus semicircularis

Declaration of Academic Achievement

Chapter 1 - Introduction

Author: Riziq Sayegh

Chapter 2 - Duration Tuning in the Auditory Midbrain of Echolocating and Non-Echolocating Vertebrates

Authors: Riziq Sayegh, Brandon Aubie and Paul A. Faure

Publication: Journal of Comparative Physiology A (2011) 197:571-583

Comments: This manuscript was conceived by RS, BA and PAF. Data were collected by RS. The manuscript was written by RS and BA under supervision of PAF. Subsequent drafts were edited by RS, BA and PAF. Reprinted with permission.

Chapter 3 - Recovery Cycle Times of Inferior Colliculus Neurons in the Awake Bat Measured With Spike Counts and Latencies

Authors: Riziq Sayegh, Brandon Aubie, Siavosh Fazel-Pour and Paul A. Faure

Publication: Frontiers in Neural Circuits (2012) 6:56

Comments: This manuscript was conceived by RS and PAF. Data were collected by RS, BA, and SFP. RS performed all data analyses and wrote the manuscript under supervision of PAF. RS performed all data analysis and produced all of the figures. Subsequent drafts were edited by RS, BA and PAF. Reprinted with permission.

Chapter 4 - Monaural and Binaural sound-evoked Inhibition Underlying Duration Selectivity in the Inferior Colliculus

Authors: Riziq Sayegh, John H. Casseday, Ellen Covey and Paul A. Faure

Publication: In Preparation

Comments: This project was conceived by PAF, JHC and EC. Data were collected by PAF and RS. RS performed all data analyses and wrote the manuscript under supervision of PAF. Subsequent drafts were edited by RS and PAF. This manuscript will be further edited by all co-authors prior to submission for publication. Project funded by JHC, EC and PAF.

Chapter 5 - Dichotic Sound Localization Properties of Duration-Tuned Neurons in the Inferior Collculus of the Big Brown Bat

Authors: Riziq Sayegh, Brandon Aubie and Paul A. Faure

Publication: In Preparation

Comments: This manuscript was conceived by RS and PAF. Data were collected by RS and BA. RS performed all data analyses and wrote the manuscript under supervision of PAF. Subsequent drafts were edited by RS and PAF. This manuscript will be further edited by all co-authors prior to submission for publication.

Chapter 6 - Discussion

Author: Riziq Sayegh

1 Introduction

The ability to process temporal information in an auditory signal is beneficial and likely a feature of the auditory system of all hearing animals. In humans, for example, temporal processing of auditory signals is important for speech recognition (Denes, 1955; Shannon et al., 1995). Temporal processing also allows humans to communicate with one another at great distances through the use of technology and morse code. In morse code, differences in the duration of tones and the interval between tones represent letters and numbers to form words and sentences (Mauk and Buonomano, 2004). Processing temporal information is also important for sound localization. Neural processing of differences in the time of arrival of sound reaching each ear allows humans, and other animals, to localize the source of the sound (Rayleigh, 1907) as sounds coming from the left of the listener would reach the left ear before the right ear.

Discrimination of temporal parameters of vocalizations can provide reproductive benefits to the animal. Crickets have been shown to be able to identify, and prefer, calling songs that match the songs of their conspecifics over calling songs of other cricket species (Pollack and Hoy, 1979). The female pacific tree frog can also discriminate conspecific calling calls from the calls of other frog species by evaluating temporal cues such as call duration and pulse rate. The female pacific tree frog also appears to prefer conspecific calling songs that are longer in duration, even when total signal energy is taken into account by reducing the duration of individual pulses within the call. These long duration calls are thought to signal the males' fitness as longer duration calls require a greater energy investment on the part of the male (Klump and Gerhardt, 1987).

Echolocating bats are an ideal example of the benefit imparted from the ability to process temporal information in an auditory signal. Echolocation is an active auditory process in which the echolocating animal emits a sound pulse and listens for the returning echoes.

By comparing the time between the outgoing pulse and the returning echoes, bats are able to infer the distance between themselves and the target that caused the echo (Simmons, 1973; O'Neill and Suga, 1979; Dear et al., 1993; Au, 2000). Echolocation is thought to provide a number of benefits to the echolocating bat, including the ability to operate in the absence of light for both hunting and roosting, the ability to compete against other aerial insectivores and even for communication with conspecifics (for review, see Fenton, 1984).

In the auditory midbrain (inferior colliculus; IC) there exists a class of neurons known as duration-tuned neurons (DTNs). Typical auditory neurons respond selectively to the frequency and amplitude of the auditory stimulus. These so-called DTNs response characteristics are set apart from typical auditory neurons by their selective response to the duration of the auditory stimulus, in addition to their selectivity to frequency and amplitude. Duration-tuned neurons are found across vertebrates, including mammals in which they are studied most extensively and provide a potential neural mechanism for temporal processing. The IC is the first auditory nucleus in the auditory pathway where DTNs are found to exist (e.g. Jen and Schlegel, 1982; Pinheiro et al., 1991; Casseday et al., 1994). Duration-tuned neurons have also been observed in ascending auditory nuclei including the auditory thalamus (He, 2002) and the auditory cortex (Galazyuk and Feng, 1997; He et al., 1997). The IC receives excitatory and inhibitory synaptic afferents from almost all descending and ascending auditory nuclei. The underlying neural circuitry involved in duration selectivity is thought to involve an interplay of excitatory and inhibitory synaptic inputs offset in time (Casseday et al., 1994; Covey et al., 1996; Casseday et al., 2000; Faure et al., 2003; Aubie et al., 2009, 2012). *In vivo* extracellular recordings of DTNs combined with inhibitory receptor antagonists (e.g. bicuculline and strychnine; $GABA_A$ and glycine receptor antagonists, respectively) have demonstrated the importance of synaptic inhibition for duration tuning, as a majority of DTNs lose their duration selectivity when inhibition is blocked (Casseday et al., 1994; Jen and Feng, 1999; Casseday et al., 2000). Whole-cell patch-clamp recordings

have also demonstrated that inhibition is important for duration selectivity, with inhibition typically preceding excitation (Covey et al., 1996; Tan and Borst, 2007; Leary et al., 2008). Paired tone presentation combined with *in vivo* extracellular recordings have also provided evidence that DTNs receive excitatory and inhibitory synaptic inputs offset in time with inhibition preceding excitation (Faure et al., 2003).

The majority of research conducted on DTNs has focused primarily on neural responses to monaural (one ear) or free-field (contralateral-biased) stimulation. Dichotic stimulation proper has not been employed on DTNs, with the exception of two reports on the response properties of DTNs in the IC of the mouse (Brand et al., 2000) and bat (Covey and Faure, 2005). Other studies that focus on general characteristics of the IC have demonstrated that neurons in the IC respond to binaural stimulation (e.g. Lu and Jen, 2003). Furthermore, the IC receives afferents from a number of auditory nuclei bilaterally (Zook and Casseday, 1982). It stands to reason, therefore, that DTNs in the IC receive binaural innervation. The extent to which this is the case, and its effect on DTNs, has yet to be characterized. In the real world, as opposed to the laboratory setting, sounds typically stimulate both ears so it is important to understand the response properties of DTNs to both monaural and binaural stimulation.

Although they were discovered almost fifty years ago, the exact function(s) of DTNs to hearing is(are) unknown. This dissertation aims to further our understanding of DTNs found in the auditory midbrain with a primary focus on attempting to elucidate the possible role(s) DTNs play in hearing and a secondary focus on exploring the mechanism underlying duration selectivity. This dissertation relies primarily on single-unit extracellular neural data obtained from the auditory midbrain of the echolocating big brown bat, *Eptesicus fuscus*; however the implications of this work likely extend to non-echolocating animals, including humans.

Chapter 2 reviews the mechanisms underlying, and response properties of, DTNs across

echolocating and non-echolocating vertebrates. This chapter serves to bring the reader up to speed on the duration tuning literature and highlights the various neural mechanisms that are thought to be involved in creating duration-tuned neural responses. Here the hypothesis that DTNs are involved in echolocation in echolocating species and involved in processing communication signals in non-echolocating species is explored by comparing the durations that DTNs respond best to with the durations of species-specific vocalizations.

Chapter 3 quantifies the ability of DTNs and non-DTNs in the IC of the big brown bat to respond to pairs of excitatory pulses. These pairs of excitatory pulses can be thought of as echolocation pulse-echo pairs. By varying the interpulse interval of the two pulses, we are able to measure the minimum time separation required for the neuron to respond to the second pulse at 50% of the spiking response to the first pulse. This minimum time is known as the recovery cycle time. Previous studies have shown that neural recovery cycle times can be shortened by blocking synaptic inhibition and we exploit this fact to indirectly measure inhibition in DTN and non-DTN IC populations through their recovery cycle times. Here we show that a subset of DTNs appear to recruit increased synaptic inhibition, as predicted by mechanisms thought to underlie duration selectivity. We also show that DTNs are able to respond to pairs of pulses at a range of time courses that mimic biologically relevant pulse-echo delays in echolocation. This finding suggests that DTNs in the bat are able to respond to echolocation pulse-echo pairs, strengthening the argument that DTNs might be involved in the processing of echolocation calls.

Chapter 4 measures the relative contribution of sound inputs to each ear in forming duration selectivity in the IC. This is accomplished by presenting an excitatory tone and a non-excitatory suppression tone in a paired tone stimulus paradigm similar to Faure et al. (2003), while varying the ear that is stimulated by the non-excitatory suppression tone. Previous studies on DTNs have shown that inhibition is important in forming duration-selective responses and that the inhibition underlying duration selectivity typically lasts as

long as, or longer than, the duration of the stimulus (Casseday et al., 1994, 2000; Covey et al., 1996; Fuzessery and Hall, 1999; Faure et al., 2003). In the binaural condition, where the excitatory tone and non-excitatory suppression tone were presented to separate ears, we find that about half of DTNs did not exhibit measurable inhibition. For those DTNs that do show measurable inhibition in the binaural condition, the inhibition recruited in the monaural condition is almost always stronger. We also show that the inhibition recruited monaurally always lasts as long as, or longer than, the duration of the stimulus that evokes it, but in the binaural condition the inhibition is almost always shorter than the duration of the inhibitory stimulus. Together, these results provide evidence that the mechanisms underlying the formation of duration selectivity in the IC are monaural in nature. These results also demonstrate that a sub-population of DTNs respond to binaural stimulation and therefore may function in sound localization.

Chapter 5 explores the response of DTNs in the big brown bat to binaural sound localization cues thought to be important for sound localization in echolocation. The ability to localize the source of the echo allows the echolocating animal to identify the position of a target in both azimuth and elevation. Combined with the distance information obtained through a neural analysis that compares the time between the outgoing pulse and returning echo, the echolocating animal is able to precisely locate a target in three-dimensional space. Here we characterize the neural responses of DTNs and non-DTNs to binaural differences in sound pressure level and time of arrival at each ear. We find that responses to differences in sound pressure level are most prominent in the IC and that DTNs are just as likely, if not more so, as non-DTNs to respond selectively to sound localization cues. The fact that DTNs are able to respond selectively to sound localization cues, combined with the ability of DTNs to respond to pairs of pulses, provides evidence for the hypothesis that DTNs play a role in processing echolocation calls in echolocating species.

The final chapter of this dissertation discusses the implications of the findings of the pre-

vious chapters with regards to duration tuning in the auditory midbrain. The potential role that DTNs play in processing echolocation calls in echolocating species is discussed along with other potential roles that DTNs may serve in both echolocating and non-echolocating species.

2 Duration Tuning in the Auditory Midbrain of Echolocating and Non-Echolocating Vertebrates

2.1 Abstract

Neurons tuned for stimulus duration were first discovered in the auditory midbrain of frogs. Duration-tuned neurons (DTNs) have since been reported from the central auditory system of both echolocating and non-echolocating mammals, and from the central visual system of cats. We hypothesize that the functional significance of auditory duration tuning likely varies between species with different evolutionary histories, sensory ecologies, and bioacoustic constraints. For example, in non-echolocating animals such as frogs and mice the temporal filtering properties of auditory DTNs may function to discriminate species-specific communication sounds. In echolocating bats duration tuning may also be used to create cells with highly selective responses for specific rates of frequency modulation (FM) and/or pulse-echo delays. The ability to echolocate appears to have selected for high temporal acuity in the duration tuning curves of inferior colliculus neurons in bats. Our understanding of the neural mechanisms underlying sound duration selectivity has improved substantially since DTNs were first discovered almost 50 years ago, but additional research is required for a comprehensive understanding of the functional role and the behavioural significance that duration tuning plays in sensory systems.

2.2 Introduction

Extracting temporal information from sensory input is vital for acoustic processing. Acoustic communication (Pollack and Hoy, 1979), sound localization (Knudsen and Konishi, 1979; Carr and Konishi, 1990) and speech recognition (Shannon et al., 1995) all rely on the processing of temporal information. Echolocating bats and dolphins are two groups of mammals that rely on exquisite temporal processing of acoustic information for detection, identification, and localization of airborne and underwater targets, respectively (Thomas et al., 2004). Echolocation (biosonar) is an active auditory process in which an animal emits a sound (pulse) and then listens to reflection(s) of that sound (echo) to create neural images of its surrounding. For example, bats and dolphins use the time interval between an outgoing sound pulse and its returning echo to infer distance (range) to a target (Simmons, 1973; O'Neill and Suga, 1979; Dear et al., 1993; Au, 2000).

In both bats and dolphins, the outgoing calls are typically loud, short duration, spectrally complex signals. Figure 2.1 shows example echolocation calls recorded from two species of insectivorous bats that employ different signaling strategies. The big brown bat (*Eptesicus fuscus*, family *Vespertilionidae*; Fig 2.1a) is a temperate North American species that emits downward frequency modulated (FM) signals and uses low duty cycle echolocation (duty cycle = ratio of call duration to interpulse interval). The unidentified mustached/naked-backed bat (*Pteronotus sp.*, family *Mormoopidae*; Fig 2.1b) is a Neotropical species that emits signals containing a combination of constant frequency (CF) tones and FM elements and uses higher duty cycle echolocation. The recording of the *Pterontus sp.* also shows a terminal feeding buzz and nicely illustrates the rapid increase in pulse repetition rate and decrease in signal duration that occurs during an attempted prey capture (Griffin et al., 1960; Kalko and Schnitzler, 1989). The ability to process temporally and spectrally complex signals in rapid succession makes the echolocating bat an ideal animal model for studying

mechanisms of temporal processing in the central auditory system.

Within the auditory midbrain (inferior colliculus) of echolocating bats there exists a class of cells known as duration-tuned neurons (DTNs) whose neurophysiological responses are characterized by selectivity for stimulus duration (Pinheiro et al., 1991; Casseday et al., 1994; Covey et al., 1996; Ehrlich et al., 1997; Fuzessery and Hall, 1999; Casseday et al., 2000; Faure et al., 2003; Mora and Kössl, 2004; Fremouw et al., 2005). Auditory DTNs have also been reported from the inferior colliculus of non-echolocating mammals, including rats (Pérez-González et al., 2006), mice (Brand et al., 2000; Xia et al., 2000), guinea pigs (Wang et al., 2006), and chinchillas (Chen, 1998). Moreover, DTNs have been reported from the auditory thalamus of guinea pigs (He, 2002) and the auditory and visual cortex of cats (Duysens et al., 1996; He et al., 1997). Auditory DTNs also exist in the midbrain of frogs (Gooler and Feng, 1992; Leary et al., 2008) where they were first discovered (Potter, 1965; Narins and Capranica, 1980).

Neurons tuned to the duration of a stimulus are found in more than one class of vertebrate, in multiple sensory modalities, and in both echolocating and non-echolocating mammals. Therefore, the ability to echolocate cannot be a prerequisite for the evolution of duration selectivity in the mammalian central auditory system; however, this does not preclude a functional role for duration tuning in the neural basis of echolocation.

This review synthesizes the known electrophysiological response properties and underlying cellular mechanisms responsible for creating DTNs in the auditory midbrain of frogs (torus semicircularis) and mammals (inferior colliculus; IC), as evidenced by electrophysiological (extracellular and intracellular) recording, application of neuropharmacological agents that block synaptic inhibition combined with extracellular recording, and by computational modeling studies. We then focus and speculate on the potential roles of duration selectivity in hearing and echolocation by bats. Finally, we suggest future studies that we feel will further elucidate the neural mechanisms of duration selectivity and help shape our

understanding of the role(s) DTNs play in temporal and sensory processing by the central nervous system (CNS).

2.3 Electrophysiology of duration tuning

2.3.1 Response classes

Auditory DTNs can be classified into one of three electrophysiological response profiles (Fig. 2.2). A cells classification is determined by the relative number of spikes evoked across all stimulus durations (Jen and Zhou, 1999; Faure et al., 2003). The stimulus duration with the maximum response is defined as best duration. Ideally, the duration tuning response class should be determined with signals at (or near) the cells best excitatory frequency. The names of the response classes (for better or worse) are analogous to the shapes of frequency filters in resonant electrical circuits. (1) Shortpass DTNs (Fig. 2.2a) have spike counts that peak at best duration and drop to $\leq$50% of the peak in response to longer duration signals. (2) Bandpass DTNs (Fig. 2.2b) also show peak spiking in response to best duration sounds but have reduced spike counts that drop to $\leq$50% of the peak at durations both shorter and longer than best duration. (3) Longpass DTNs (Fig. 2.2c) do not have a best duration and respond only when the duration of a best excitatory frequency stimulus exceeds some minimum duration, with little or no spiking in response to shorter duration signals. One in vivo study reported a minority of cells that fell into a fourth category of band-reject (multi-peaked) duration tuning (Mora and Kössl, 2004). Band-reject DTNs have strong spiking at multiple stimulus durations and a minimum (or null) response to a band of signal durations in-between. The existence of plausible biological mechanisms to produce band-reject DTNs has been proposed (Mora and Kössl, 2004; Aubie et al., 2009). Three additional studies have reported band-reject duration tuning. In two cases, the cells responded weakly and prior to signal offset, bringing into question how the cell could de-

termine stimulus duration (Pérez-González et al., 2006; Luo et al., 2008). In the third case, classification of band-reject tuning was dependent on the temporal width of the spike analysis window (Wang et al., 2006).

Computationally, shortpass, bandpass and band-reject DTNs are the most interesting because the specificity of their spiking response cannot be explained by simple integration of stimulus energy. The temporal tuning of shortpass, bandpass and band-reject DTNs must involve a complex interaction of excitatory and inhibitory synaptic inputs and intrinsic cellular properties (see Mechanisms of duration tuning). Although the spiking responses of longpass DTNs can be similar to typical auditory neurons that integrate stimulus energy (e.g. Kiang, 1965), there are important differences. In a longpass DTN proper, the cells first-spike latency and minimum duration necessary to elicit spiking do not continue to decrease as signal energy (amplitude) increases (Brand et al., 2000; Faure et al., 2003; Pérez-González et al., 2006). This is in contrast to the decrease in first-spike latency observed for sounds of increasing stimulus energy that is typical of invertebrate (e.g. Mörchen et al., 1978) and vertebrate auditory neurons (e.g. Rose et al., 1963). Some longpass DTNs require longer minimum durations and have longer first-spike latencies at higher stimulus amplitudes, resulting in a paradoxical latency shift of the spiking response (e.g. Covey et al., 1996; Faure et al., 2003; Pérez-González et al., 2006).

2.3.2 Response properties

Spontaneous firing rates of DTNs are typically low, a feature common to IC neurons in general (bat: Ehrlich et al. 1997; Jen and Feng 1999; mouse: Brand et al. 2000; Xia et al. 2000). Shortpass and bandpass DTNs in bats exhibit phasic spiking, with most cells responding with first-spike latencies that follow stimulus offset (e.g. Casseday et al. 1994; Ehrlich et al. 1997; Fuzessery and Hall 1999; Casseday et al. 2000; Faure et al. 2003; but see Luo et al. 2008). Longpass DTNs typically exhibit tonic or primary-like spiking and

have spikes that occur during the ongoing portion of the stimulus (Chen, 1998; Brand et al., 2000; Faure et al., 2003; Mora and Kössl, 2004; Luo et al., 2008). Faure et al. (2003) reported that first-spike latencies of shortpass and bandpass DTNs in the IC of *E. fuscus* were always longer than best duration, and that different neurons tuned to the same best duration had a wide range of first-spike latencies. Moreover, cells that responded with a burst of two or more spikes had burst durations (last-spike latency minus first-spike latency) that were greater than the cells best duration.

Auditory neurons in the mammalian IC are tonotopically organized (Rose et al., 1963) and DTNs are no exception; the best excitatory frequency of *E. fuscus* DTNs systematically increase with electrode penetration depth in a dorsal-lateral to ventral-medial direction (Pinheiro et al., 1991; Jen and Wu, 2006; Wu and Jen, 2008). Jen and Wu (2006) reported a correlation between neuronal best duration and best excitatory frequency in the IC of *E. fuscus*, with cells tuned to shorter best durations more likely to have lower best excitatory frequencies. This suggests a potential spatial map of duration selectivity running parallel with the tonotopic axis; however, this correlation has not been reported in other studies of DTNs in the bat (Pinheiro et al., 1991; Ehrlich et al., 1997; Faure et al., 2003; Luo et al., 2008).

Although DTNs share similar response profiles across species, the range of neuronal best durations and the width of temporal tuning varies between species with different auditory and signaling constraints. For example, shortpass DTNs in both frogs and mammals are typically tuned to shorter best durations and have narrower duration tuning curves than bandpass DTNs tuned to similar best durations from the same species (e.g. Fuzessery and Hall, 1999; Faure et al., 2003; Mora and Kössl, 2004; Fremouw et al., 2005; Leary et al., 2008; Luo et al., 2008; Wu and Jen, 2008). Longpass duration tuning appears to be more common in non-echolocating mammals such as rodents and cats (He et al., 1997; Chen, 1998; Brand et al., 2000), whereas shortpass and bandpass tuning is frequently observed in

the IC of bats (Faure et al., 2003). Interestingly, the shortpass and bandpass duration tuning curves of echolocating bats tend to be more narrowly tuned than in non-echolocating mammals (Table 2.1). This suggests that the ability to echolocate may have selected for cells with more restricted temporal tuning profiles, perhaps as an evolutionary adaption to facilitate rapid processing of short duration pulses and echoes (Fremouw et al., 2005).

The spiking responses and temporal response specificity of duration tuning are largely tolerant to changes in stimulus amplitude (Zhou and Jen, 2001; Fremouw et al., 2005). Fremouw et al. (2005) reported amplitude tolerance in spike number and temporal tuning profile for stimulus level changes up to 50 dB. First-spike latencies also remained fairly constant across sound pressure levels (SPLs). Figure 2.2 demonstrates amplitude tolerance in spike count across a 20 dB (x10) change in SPL. For each example neuron shown, there was no significant difference in first-spike latency at $+10$ dB and $+30$ dB (re threshold).

2.4 Mechanisms of duration tuning

The auditory midbrain is the first stage in the central auditory pathway where DTNs have been found in both frogs (torus semicircularis) and mammals (IC). To date, DTNs have not been reported from the auditory periphery or from the lower brainstem central nuclei (i.e. cochlear nucleus, medial nucleus of the trapezoid body, olivary complex, nuclei of the lateral lemniscus). This suggests that duration tuning is an emergent electrophysiological response property that is created in the auditory midbrain. Neurons selective for stimulus duration have also been reported from the auditory thalamus (He, 2002) and cortex in mammals (Galazyuk and Feng, 1997; He et al., 1997; Razak and Fuzessery, 2006).

Within the IC, duration selectivity is putatively created through the convergence and temporal interaction of excitatory and inhibitory synaptic inputs that are offset in time (Casseday et al., 1994; Ehrlich et al., 1997; Fuzessery and Hall, 1999; Casseday et al.,

2000; Faure et al., 2003; Mora and Kössl, 2004; Covey and Faure, 2005; Fremouw et al., 2005). The importance of inhibition on duration tuning can be revealed with experiments using pharmacological antagonists that block inhibitory neurotransmitters. When inhibition acting on a DTN is diminished or blocked, a cells duration selectivity is severely reduced (broadened) or abolished (Casseday et al., 1994; Fuzessery and Hall, 1999; Jen and Feng, 1999; Casseday et al., 2000; Jen and Wu, 2005; Yin et al., 2008). These studies combined with limited evidence from intracellular recordings (e.g. Covey et al., 1996) indicate that duration tuning is created de novo in the IC and is not a response property that is inherited (relayed) from lower brainstem auditory nuclei. The mechanisms responsible for DTNs in the auditory thalamus and cortex are still unknown.

In theory, any central auditory neuron could exhibit duration tuning if the relative timing and/or strength of its sound-evoked excitatory and inhibitory synaptic inputs varied as a function of stimulus duration. Evidence obtained from extracellular (Narins and Capranica, 1980; Gooler and Feng, 1992; Casseday et al., 1994; Ehrlich et al., 1997; Chen, 1998; Fuzessery and Hall, 1999; Brand et al., 2000; Casseday et al., 2000; Zhou and Jen, 2001; Faure et al., 2003; Fremouw et al., 2005; Pérez-González et al., 2006; Wang et al., 2006) and intracellular recordings (Covey et al., 1996; Leary et al., 2008) along with computational modeling studies (Singh and Mountain, 1997; Hooper et al., 2002; Aubie et al., 2009) have proposed two basic mechanisms that are theorized to underlie duration-tuned neural circuits. Although the details of the proposed mechanisms differ between animal species and duration tuning response classes, all may be classified as either coincidence detection or anti-coincidence mechanisms.

2.4.1 Coincidence detection mechanisms

Coincidence detection mechanisms rely on the simultaneous occurrence (coincidence) of at least two excitatory (depolarizing) events (Narins and Capranica, 1980). The first excitatory

event is linked to stimulus onset (ON_E) and the second is linked to stimulus offset (OFF_E). On their own, each excitatory event is insufficient to push the membrane potential of the DTN above spike threshold; however, when the ON_E and OFF_E events coincide, excitation is augmented and spikes are evoked from the DTN. The coincidence detection mechanism predicts that first-spike latencies of DTNs will track stimulus offset (i.e. spiking occurs at a constant latency relative to stimulus offset) because spikes can be evoked only on or after the arrival of the OFF_E event. Offset responses are frequently observed from in vivo recordings of DTNs in bats (e.g. Fuzessery and Hall, 1999; Faure et al., 2003).

Different classes of duration tuning can emerge from the coincidence detection mechanism by delaying the latency of the ON_E event relative to stimulus onset. Short delays produce shortpass tuning because the ON_E and OFF_E events will only coincide at the shortest stimulus durations (Fig. 2.3a); however, bandpass duration tuning results when the latency of the ON_E event is delayed such that the OFF_E event occurs before the ON_E event when the stimulus duration is short (Fig. 2.3b). Band-reject duration tuning could arise if the OFF_E event is subthreshold for short stimulus durations and thus requires coincidence with the ON_E event to evoke spikes but then becomes suprathreshold at longer stimulus durations (Aubie et al., 2009). Alternatively, band-reject tuning could result form the coincidence of multiple onset-evoked excitations with different temporal delays (Mora and Kössl, 2004).

Stimulus evoked inhibition acting on the DTN plays an important role in modulating the strength and timing of the coincident excitations and has been observed in vivo via whole-cell recordings of DTNs in the midbrains of frogs (Leary et al., 2008) and bats (Covey et al., 1996). Indeed, sound evoked inhibition may be required for duration selectivity as iontophoretic application of the $GABA_A$ antagonist bicuculline abolishes or broadens duration tuning in 60-80% of DTNs in the bat (Casseday et al., 1994; Fuzessery and Hall, 1999; Jen and Feng, 1999; Casseday et al., 2000; Jen and Wu, 2005). Application of the

glycine antagonist strychnine also diminishes duration selectivity, albeit to a lesser extent (Casseday et al., 2000).

Based on evidence from intracellular whole-cell patch clamp recordings (Covey et al., 1996; Leary et al., 2008) and single-unit extracellular recordings combined with paired-tone stimulation (Faure et al., 2003; Covey and Faure, 2005), we know that inhibition acting on a DTN usually precedes excitation. We also know that the inhibition lasts as long or longer than the duration of the stimulus. Inhibition sharpens duration selectivity by decreasing the temporal window of coincidence, thus ensuring that isolated excitatory events remain subthreshold (Aubie et al., 2009). Inhibitory effects can also accumulate over repeated stimulus presentations. For example, DTNs respond with fewer spikes to successive pulses in rapidly presented pulse trains, resulting in increased temporal selectivity. Application of the $GABA_A$ antagonist bicuculline abolishes both of these effects (Jen and Wu, 2005).

2.4.2 Anti-coincidence mechansisms

An anti-coincidence mechanism was hypothesized to account for the responses of some shortpass DTNs and requires at least one excitatory (depolarizing) and one inhibitory (hyperpolarizing) event (Fuzessery and Hall, 1999). The depolarizing excitatory event may be either onset- or offset-evoked, and the hyperpolarizing event is a sustained onset-evoked inhibition (SUS_I) lasting for at least the duration of the stimulus. The excitation is suprathreshold and is capable of producing spikes on its own, but can be rendered subthreshold when coincident with inhibition.

In one version of the anti-coincidence mechanism, short duration sounds evoke spikes in the DTN when the latency of an ON_E event is delayed so that it occurs after the end of the SUS_I. At longer stimulus durations, the duration of the SUS_I event increases and eventually overlaps with the ON_E event rendering it subthreshold (Fig. 2.3c). This mechanism predicts constant first-spike latencies across stimulus duration (re stimulus onset) be-

cause the ON_E event arrives at the same latency regardless of stimulus duration. Relatively constant first-spike latencies have been observed in some in vivo recordings of shortpass DTNs (Fuzessery and Hall, 1999). Hypothetically, the sustained inhibition could cause small increases in first-spike latency at the longest excitatory durations as the SUS_I event encroaches upon the ON_E event (Aubie et al., 2009).

In an alternative version of the anti-coincidence mechanism, short duration sounds can also evoke spikes in the DTN when the latency of an OFF_E event is shorter than the latency of the SUS_I event. At longer stimulus durations, the OFF_E event arrives later in time and is eventually overlapped and rendered subthreshold by the sustained SUS_I event (Fig. 2.3d). This version of the anti-coincidence model of short-pass duration tuning predicts that first-spike latencies will follow stimulus offset because, like in the coincidence detection model, spikes are evoked by the OFF_E event.

2.4.3 Neural circuit implementations

The CNS could implement coincidence-detection and anti-coincidence mechanisms of duration tuning in a variety of ways. Excitatory inputs to the IC are primarily from glutamatergic neurons (Covey et al., 1996; Ma et al., 2002) whereas inhibitory inputs are from GABAergic and/or glycinergic neurons (Casseday et al., 2000). Transient onset-evoked responses are observed in brainstem nuclei with projections to the IC as early as the cochlear nucleus (Haplea et al., 1994) as well as the medial superior olive (Grothe et al., 1997, 2001) and the nuclei of the lateral lemniscus (Covey and Casseday, 1991; Vater et al., 1997). A transient onset response might be produced by neurons with low- and high-threshold K^+ currents that evoke a single spike per stimulus regardless of amplitude or duration (Sivaramakrishnan and Oliver, 2001) or with excitation that slightly precedes inhibition (Nelson and Erulkar, 1963; Le Beau et al., 1996). Offset responding neurons with excitatory projections to the IC are found in the medial superior olive and could provide the offset-evoked

excitation predicted by the coincidence detection mechanism (Grothe et al., 2001). Alternatively, the DTN could produce offset-evoked excitation intrinsically via post-inhibitory rebound mediated by hyperpolarization-activated currents (Sivaramakrishnan and Oliver, 2001; Hooper et al., 2002; Koch and Grothe, 2003; Sun and Wu, 2008). Because the amplitude of a rebound depolarization increases with the duration of hyperpolarization (Sun and Wu, 2008), neurons with post-inhibitory rebound could plausibly underlie band-reject DTNs if the rebound depolarization is subthreshold at short stimulus durations but becomes suprathreshold at long stimulus durations. Post-inhibitory rebound has the critical ability to mark the offset of temporal events and is thus a probable component of temporal processing in general. Offset components are predicted in both general mechanisms of duration tuning and post-inhibitory rebounds are predicted to mark the offset of preferred duration intervals for interval selective neurons in weakly electric fish (Large and Crawford, 2002). Sources of stimulus evoked sustained inhibition might originate from the nuclei of the lateral lemniscus where both GABAergic and glycinergic neurons project to the IC (Covey and Casseday, 1991; Vater et al., 1997). The arrival of excitation and inhibition to a cell can be delayed relative to stimulus onset through delay lines created by varying axon length and diameter (Carr and Konishi, 1990; Seidl et al., 2010) and/or receptor activation times (e.g. AMPA versus NMDA receptors; Sanchez et al., 2007). Alternatively, currents can be delayed intrinsically by the DTN itself via membrane ion channels that activate slowly over the course of a stimulus (Hooper et al., 2002).

Using computational models of neural circuits, Aubie et al. (2009) confirmed the biological plausibility of several previously proposed conceptual mechanisms of duration tuning. These computational models reproduced a wide range of in vivo response characteristics, including best duration tuning, response classes, spike counts, first-spike latencies, level tolerance to changes in signal amplitude, and the effects of applying antagonists of inhibitory neurotransmitters to DTNs.

It is important to note that the coincidence and anti-coincidence mechanisms are not necessarily mutually exclusive in a duration-tuned neural circuit. For example, a hybrid mechanism could require the coincidence of onset- and offset-evoked excitations as well as anti-coincidence with sustained inhibition to evoke spiking in a DTN. The full gamut of duration tuning mechanisms employed by the CNS is likely composed of a host of such hybrid mechanisms. This variation could account for the wide variability of best durations, spike counts, and first-spike latencies observed both within and across species.

2.5 Duration tuning and echolocation

The echolocation calls of bats are highly diverse and species-specific (Jones and Teeling, 2006). Echolocation works by comparing temporal and spectral differences between outgoing pulses and reflected echoes to infer information about the size, shape, position, texture and velocity of objects in the environment (Simmons, 1973; O'Neill and Suga, 1979; Neuweiler, 1984; Suga and Horikawa, 1986; Neuweiler, 1990; Dear et al., 1993; Veselka et al., 2010). Echolocating bats adjust both their signal structure and calling behaviour to meet the acoustical and perceptual demands associated with detecting targets in different environments and foraging tasks (Simmons and Stein, 1980; Neuweiler, 1984, 1990; Faure and Barclay, 1994). The signals are composed of CF, FM and/or a combination of CF + FM acoustic elements that can vary in duration (Fig. 2.1). Equally diverse is the temporal pattern of call emission when bats are foraging, landing, commuting, and interacting with conspecifics. For example, in free flight *E. fuscus* emit search phase calls up to 20 ms in duration with interpulse intervals ranging from 20 to >100 ms, but during target capture it decreases its call duration and interpulse interval to <1 ms and <10 ms, respectively (Surlykke and Moss, 2000; Petrites et al., 2009).

The contribution of duration tuning to hearing and echolocation by bats is still unknown,

but the available evidence suggests that DTNs play a functional role. The best duration and range of temporal selectivity of DTNs in bats closely mirrors the range of echolocation call durations (Table 2.1). Moreover, a disproportionately high number of DTNs in the IC of *E. fuscus* and *Molossus molossus* have best excitatory frequencies within the range of the fundamental FM acoustic element used in echolocation (Pinheiro et al., 1991; Faure et al., 2003; Mora and Kössl, 2004). In low duty cycle bats like *E. fuscus*, spike counts and first-spike latencies of DTNs at best duration are quite tolerant to large changes in stimulus amplitude (Zhou and Jen, 2001; Fremouw et al., 2005), whereas in high duty cycle species like *M. molossus* and *R. pusillus*, DTNs show more variation in amplitude tolerance (Mora and Kössl, 2004; Luo et al., 2008). This suggests that amplitude tolerance of DTNs in bats may vary between species that emit different echolocation call types and that employ different signaling strategies. If DTNs operated in neural circuits that detected the delay between pulses and echoes, amplitude tolerance ensures that the magnitude and latency of DTN firing would remain stable when responding to loud outgoing vocalizations and weaker returning echoes. Duration-tuned neurons with similar best durations but different first-spike latencies could function as delay lines for higher auditory centers. For example, if the response of a delay-tuned neuron in the auditory thalamus (Olsen and Suga, 1991) or auditory cortex (Tanaka et al., 1992) depended on the coincidence of inputs from DTNs in the IC, then this circuit could detect the delay between two sounds with specific durations (Faure et al., 2003; Covey and Faure, 2005). More specific and complex response properties would emerge by including additional DTNs tuned to similar (different) frequencies and amplitudes.

Integrating temporal information across varying interstimulus intervals is particularly relevant to echolocation because bats naturally experience large variation in the timing of pulses and echoes during target pursuit (Griffin et al., 1960; Simmons, 1973; Kalko and Schnitzler, 1989; Surlykke and Moss, 2000; Moss and Surlykke, 2001). Some bat DTNs

maintain or sharpen their temporal specificity when they are repeatedly stimulated with pairs of best duration tones resembling pulse-echo pairs in echolocation (Jen and Zhou, 1999; Jen and Wu, 2005; Wu and Jen, 2008). This suggests that DTNs might function as a filtering mechanism for isolating specific durations and frequencies in pulses and echoes. Bat DTNs with short best durations have shorter recovery times in response to best duration pulse-echo pairs than cells with longer best durations (Wang et al., 2008, 2010). Such responses might be expected if DTNs play a role in echolocation because both call duration and interpulse interval decrease as the bat moves from the search (long call durations, long pulse-echo delays) to the approach (intermediate call durations and pulse-echo delays) and finally to the terminal phase (short duration calls, short pulse-echo delays) of hunting (Kalko and Schnitzler, 1989). Decreased call durations during insect pursuit are illustrated for the *Pteronotus sp.* in Figure 2.1b.

Preliminary computational studies and single-unit recordings from the IC of *E. fuscus* performed by the authors suggest that DTNs may also contribute to hearing and echolocation when tested with sounds shorter than best duration. Take, for example, a bandpass neuron with a best duration of 5 ms. By definition, the cell responds maximally to 5 ms suprathreshold sounds, but the same cell may show little (or no) response to shorter sounds of the same frequency and energy (e.g. see Fig. 4b in Faure et al., 2003). Presenting the same bandpass cell with pairs of 2 ms signals (i.e. pulse-echo pairs at a non-responsive duration) also results in a weak response; however, the response is stronger when the interpulse interval is shortened so that the combined duration of the pulse+gap+echo is close to the neuronal best duration. We hypothesize that when the interval between the onset of the outgoing echolocation pulse (Signal 1) and the offset of the returning echo (Signal 2) is close to neuronal best duration, and when the pulse-echo interval is shorter than the recovery time of the cell (recovery time defined as the minimum interval for the response to Signal 2 to be $\geq$50% of the response to Signal 1), then the pulse-echo pair would effec-

tively be perceived by the cell as a single, unified stimulus. This mechanism of temporal integration predicts that the DTN will respond at the offset of the echo. It also predicts that cells with longer best durations will respond to longer pulse-echo gaps, and thus be useful in detecting more distant targets than cells with short best durations. Because the pulse-echo gap must be sufficiently short to prevent the DTN from fully recovering, DTNs could be especially useful for detecting pulse-echo delays shorter than 8 to 30 ms, which is the range preferred by delay-tuned neurons in the auditory midbrain of *E. fuscus* (Dear and Suga, 1995).

So far we have emphasized how the responses of DTNs could serve as temporal filters in auditory processing, but it is important to remember that DTNs are also tuned in frequency and have V-shaped, U-shaped, and O-shaped excitatory frequency response curves just like other types of central auditory neurons (e.g. Sutter, 2000). This makes the response of a DTN extremely specific because the neuron will only fire action potentials when it hears a sound that is of the correct frequency, duration, and amplitude. Therefore, midbrain DTNs have the capacity to act as spectrotemporal filters for auditory information processing. Populations of DTNs with different best excitatory frequencies, excitatory frequency response areas, best durations, and temporal tuning response areas could act as inputs to the equivalent of a neural spectrogram and provide the brain with highly specific information about the auditory environment. We speculate that such spectrotemporal filters would be very useful for hearing in general and echolocation by bats.

2.6 Future studies

Considerable effort has been devoted to understanding the neural mechanisms underlying auditory duration selectivity since DTNs were first discovered from the midbrain of frogs (Potter, 1965; Narins and Capranica, 1980) and then later in bats (Casseday et al., 1994).

Although the exact function that DTNs play in hearing is unknown, the general range of neuronal best durations within a species correlates well with the range of vocalization durations. Table 2.1 summarizes the range of best duration tuning exhibited by DTNs in frogs and mammals, and also shows the range of durations for typical species-specific vocalizations. In both echolocating and non-echolocating species, the range of neuronal best duration tuning in DTNs correlates fairly well with the range of vocalization durations of species-specific echolocation and communication / social signals. For example, in FM bats that use low duty cycle echolocation, call durations are typically $<$10 ms and they have shortpass and bandpass DTNs that are typically tuned to $<$10 ms (e.g. *E. fuscus*, *A. pallidus*, *M. lucifugus*). High duty cycle bats that emit a combination of CF-FM acoustic elements usually have call durations $>$10 ms (e.g. *M. molossus* and *R. pusillus*) and possess cells tuned to longer best durations. The concordance between neuronal best durations and echolocation signal duration suggests that DTNs play an active role in echolocation. Frogs with best durations ranging from 4 to 50 ms emit communication sounds in rapid sequence that range from 8 to 17 ms. Mouse DTNs have best durations that typically range from 8 to 80 ms and this correlates well with the durations of typical communication calls that vary from 8 to 100 ms in pups and 8 to 75 ms in adults. Rat DTNs range from 4 to 128 ms in best duration and have social/communication calls with durations ranging from 80 to 140 ms in pups and 20 to 80 ms in adults (with some adult calls lasting $>$300 ms). In the chinchilla, guinea pig and cat, best duration neuronal tuning tends to be shorter than the duration of species-specific vocalizations; however, in these species DTNs may still be used to detect and discriminate specific call elements within the longer duration sounds. It is also possible that duration selectivity is not the primary function of DTNs.

The majority of research on duration tuning has used CF tones to measure responses from DTNs, and this makes sense given how duration tuning as a neurophysiological response type is defined. A few studies have reported midbrain DTNs that respond best to

FM sweeps containing the cells best excitatory frequency response area (Casseday et al., 1994; Ehrlich et al., 1997; Fuzessery and Hall, 1999; Casseday et al., 2000; Fuzessery et al., 2006) or to combinations of CF tones + FM sweeps (Luo et al., 2008); however, it is unclear if duration selectivity for a DTN is as functionally significant as the selectivity for FM sweep rate. As the duration of a constant bandwidth FM signal increases, the duration of specific frequency bands within the signal also lengthen resulting in a slower rate of modulation through a cells excitatory frequency response area. When FM DTNs are stimulated with FM sweeps systematically varied in duration, it is possible that these cells are simply responding to specific rates of FM rather than signal duration per se (Fuzessery et al., 2006).

Complex interactions between subthreshold excitatory and inhibitory synaptic inputs play a major role in determining what signals best stimulate an auditory neuron. While a number of intracellular recordings have been obtained from auditory midbrain neurons (Kuwada et al., 1997; Pedemonte et al., 1997; Voytenko and Galazyuk, 2007; Xie et al., 2007; Peterson et al., 2008; Voytenko and Galazyuk, 2008; Xie et al., 2008; Gittelman et al., 2009; Li et al., 2010) intracellular responses of auditory midbrain neurons to varying durations of pure tones have only once been reported (Covey et al., 1996). Additional intracellular studies are needed to fully characterize the synaptic inputs and intrinsic properties of DTNs to further our understanding of the neural basis of duration selectivity.

The major neuroanatomical projections to and from the IC have been described for a number of mammalian species, including bats (Winer and Schreiner, 2005), but the specific projections that create cells with different electrophysiological response properties in the IC remain unknown. The synaptic inputs to and the projections of midbrain DTNs have yet to be described. Intracellular filling of DTNs with anterograde and retrograde tracers would reveal the auditory nuclei that create duration selective cells in the IC. Cell fill and tracing studies would also yield detailed circuit information. For example, do midbrain DTNs send their projections first to the auditory thalamus or do they project directly to primary auditory

cortex? Are inputs from specific brainstem nuclei necessary to create cells with different classes of duration selectivity? Knowing which cells and auditory nuclei project to DTNs in the IC, and where DTNs send their outputs is vital for deciphering the role that duration tuning plays in hearing and more specifically in echolocation by bats.

Finally, midbrain auditory DTNs in amphibians and mammals share many of the same underlying neural mechanisms even though the cells themselves likely fulfill different processing roles. For example, temporally selective cells in frogs may be tuned to the duration of communication calls or the intervals between repeated pulses in a train (Edwards et al., 2002; Leary et al., 2008), whereas DTNs in bats may respond best to pairs of pulse-echo sounds consisting of multiple acoustic elements (Jen and Wu, 2005). Midbrain neurons in the posterior exterolateral nucleus of mormyrid electric fish likely encode different temporal patterns of electric organ discharges by differences in the dynamics of short-term synaptic plasticity in excitatory and inhibitory input pathways (Carlson, 2009). Additional behavioural, electrophysiological and computational studies comparing duration tuning and other mechanisms of temporal selectivity across species are needed to understand how species-specific constraints have shaped the evolution of temporal processing in echolocating and non-echolocating vertebrates.

References

Au, W. W. (2000). Echolocation in dolphins. In Popper, A. and Fay, R., editors, *Hearing by whales and dolphins*, pages 364–408. Springer New York.

Aubie, B., Becker, S., and Faure, P. A. (2009). Computational models of millisecond level duration tuning in neural circuits. *J Neurosci*, 29(29):9255–9270.

Brand, A., Urban, A., and Grothe, B. (2000). Duration tuning in the mouse auditory midbrain. *J Neurophysiol*, 84(4):1790–1799.

Capranica, R. R. (1968). The vocal repertoire of the bullfrog (*Rana catesbeiana*). *Behaviour*, 31(3-4):302–325.

Carlson, B. A. (2009). Temporal-pattern recognition by single neurons in a sensory pathway devoted to social communication behavior. *J Neurosci*, 29(30):9417–9428.

Carr, C. E. and Konishi, M. (1990). A circuit for detection of interaural time differences in the brain stem of the barn owl. *J Neurosci*, 10(10):3227–3246.

Casseday, J. H., Ehrlich, D., and Covey, E. (1994). Neural tuning for sound duration: role of inhibitory mechanisms in the inferior colliculus. *Science*, 264(5160):847–850.

Casseday, J. H., Ehrlich, D., and Covey, E. (2000). Neural measurement of sound duration: control by excitatory-inhibitory interactions in the inferior colliculus. *J Neurophysiol*, 84(3):1475–1487.

Chen, G.-D. (1998). Effects of stimulus duration on responses of neurons in the chinchilla inferior colliculus. *Hearing Res*, 112:142–150.

Covey, E. and Casseday, J. H. (1991). The monaural nuclei of the lateral lemniscus in an echolocating bat: parallel pathways for analyzing temporal features of sound. *J Neurosci*, 11(11):3456–3470.

Covey, E. and Faure, P. A. (2005). Neural mechanisms for analyzing temporal patterns in echolocating bats. In Pressnitzer, D., Cheveigné, A. d., McAdams, S., and Collet, L., editors, *Auditory signal processing: physiology, psychoacoustics, and models*, pages 251–257. Springer Verlag, New York.

Covey, E., Kauer, J. A., and Casseday, J. H. (1996). Whole-cell patch-clamp recording reveals subthreshold sound-evoked postsynaptic currents in the inferior colliculus of awake bats. *J Neurosci*, 16(9):3009–3018.

Dear, S. and Suga, N. (1995). Delay-tuned neurons in the midbrain of the big brown bat. *J Neurophysiol*, 73(3):1084–1100.

Dear, S. P., Simmons, J. A., and Fritz, J. (1993). A possible neuronal basis for representation of acoustic scenes in auditory cortex of the big brown bat. *Nature*, 364(6438):620–623.

Duysens, J., Schaafsma, S. J., and Orban, G. A. (1996). Cortical off response tuning for stimulus duration. *Vision Res*, 36(20):3243–3251.

Edwards, C. J., Aldter, T. B., and Rose, G. J. (2002). Auditory midbrain neurons that count. *Nat Neurosci*, 5(10):934–936.

Ehrlich, D., Casseday, J. H., and Covey, E. (1997). Neural tuning to sound duration in the inferior colliculus of the big brown bat, *Eptesicus fuscus*. *J Neurophysiol*, 77(5):2360–2372.

Faure, P. and Barclay, R. (1994). Substrate-gleaning versus aerial-hawking: plasticity in

the foraging and echolocation behaviour of the long-eared bat, *Myotis evotis*. *J Comp Physiol A*, 174(5):651–660.

Faure, P. A., Fremouw, T., Casseday, J. H., and Covey, E. (2003). Temporal masking reveals properties of sound-evoked inhibition in duration-tuned neurons of the inferior colliculus. *J Neurosci*, 23(7):3052–3065.

Fremouw, T., Faure, P. A., Casseday, J. H., and Covey, E. (2005). Duration selectivity of neurons in the inferior colliculus of the big brown bat: tolerance to changes in sound level. *J Neurophysiol*, 94(3):1869–1878.

Fuzessery, Z. M., Buttenhoff, P., Andrews, B., and Kennedy, J. M. (1993). Passive sound localization of prey by the pallid bat (*Antrozous p. pallidus*). *J Comp Physiol A*, 171(6):767–777.

Fuzessery, Z. M. and Hall, J. C. (1999). Sound duration selectivity in the pallid bat inferior colliculus. *Hearing Res*, 137(1-2):137–154.

Fuzessery, Z. M., Richardson, M. D., and Coburn, M. S. (2006). Neural mechanisms underlying selectivity for the rate and direction of frequency-modulated sweeps in the inferior colliculus of the pallid bat. *J Neurophysiol*, 96(3):1320–1336.

Galazyuk, A. V. and Feng, A. S. (1997). Encoding of sound duration by neurons in the auditory cortex of the little brown bat, *Myotis lucifugus*. *J Comp Physiol A*, 180(4):301–311.

Gittelman, J. X., Li, N., and Pollak, G. D. (2009). Mechanisms underlying directional selectivity for frequency-modulated sweeps in the inferior colliculus revealed by *in vivo* whole-cell recordings. *J Neurosci*, 29(41):13030–13041.

Gooler, D. M. and Feng, A. S. (1992). Temporal coding in the frog auditory midbrain: the influence of duration and rise-fall time on the processing of complex amplitude-modulated stimuli. *J Neurophysiol*, 67(1):1–22.

Griffin, D. R., Webster, F. A., and Michael, C. R. (1960). The echolocation of flying insects by bats. *Anim. Behav.*, 8(3):141–154.

Grothe, B., Covey, E., and Casseday, J. H. (2001). Medial superior olive of the big brown bat: neuronal responses to pure tones, amplitude modulations, and pulse trains. *J Neurophysiol*, 86(5):2219–2230.

Grothe, B., Park, T. J., and Schuller, G. (1997). Medial superior olive in the free-tailed bat: response to pure tones and amplitude-modulated tones. *J Neurophysiol*, 77(3):1553–1565.

Haplea, S., Covey, E., and Casseday, J. H. (1994). Frequency tuning and response latencies at three levels in the brainstem of the echolocating bat, *Eptesicus fuscus*. *J Comp Physiol A*, 174(6):671–683.

He, J. (2002). OFF responses in the auditory thalamus of the guinea pig. *J Neurophysiol*, 88(5):2377–2386.

He, J., Hashikawa, T., Ojima, H., and Kinouchi, Y. (1997). Temporal integration and duration tuning in the dorsal zone of cat auditory cortex. *J Neurosci*, 17(7):2615–2625.

Hooper, S. L., Buchman, E., and Hobbs, K. H. (2002). A computational role for slow conductances: single-neuron models that measure duration. *Nat Neurosci*, 5(6):552–556.

Hunyady, H. (2008). Vocal sounds of the chinchilla. Master's thesis, Bowling Green State University.

Jen, P. H.-S. and Feng, R. B. (1999). Bicuculline application affects discharge pattern and pulse-duration tuning characteristics of bat inferior collicular neurons. *J Comp Physiol A*, 184:185–194.

Jen, P. H.-S. and Wu, C. H. (2005). The role of GABAergic inhibition in shaping the response size and duration selectivity of bat inferior collicular neurons to sound pulses in rapid sequences. *Hearing Res*, 202:222–234.

Jen, P. H.-S. and Wu, C. H. (2006). Duration selectivity organization in the inferior colliculus of the big brown bat, *Eptesicus fuscus*. *Brain Res.*, 1108(1):76–87.

Jen, P. H.-S. and Zhou, X. M. (1999). Temporally patterned pulse trains affect duration tuning characteristics of bat inferior collicular neurons. *J Comp Physiol A*, 185(5):471–478.

Jones, G. and Teeling, E. C. (2006). The evolution of echolocation in bats. *Trends Ecol. Evol.*, 21(6):149–156.

Kalko, E. K. V. and Schnitzler, H.-U. (1989). The echolocation and hunting behavior of Daubenton's bat, *Myotis daubentoni*. *Behav. Ecol. Sociobiol.*, 24(4):225–238.

Kiang, N. Y.-S. (1965). *Discharge patterns of single fibers in the cat's auditory nerve*. MIT Press, Cambridge, MA.

Knudsen, E. I. and Konishi, M. (1979). Mechanisms of sound localization in the barn owl (*Tyto alba*). *J Comp Physiol A*, 133(1):13–21.

Knutson, B., Burgdorf, J., and Panksepp, J. (2002). Ultrasonic vocalizations as indices of affective states in rats. *Psych. Bull.*, 128(6):961–977.

Koch, U. and Grothe, B. (2003). Hyperpolarization-activated current (I_h) in the inferior colliculus: distribution and contribution to temporal processing. *J Neurophysiol*, 90(6):3679–3687.

Kössl, M., Mora, E., Coro, F., and Vater, M. (1999). Two–toned echolocation calls from *Molossus molossus* in Cuba. *J. Mammal.*, 80(3):929–932.

Kuwada, S., Batra, R., Yin, T. C., Oliver, D. L., Haberly, L. B., and Stanford, T. R. (1997). Intracellular recordings in response to monaural and binaural stimulation of neurons in the inferior colliculus of the cat. *J Neurosci*, 17(19):7565–7581.

Large, E. W. and Crawford, J. D. (2002). Auditory Temporal Computation: Interval Selectivity Based on Post-Inhibitory Rebound. *J. Comp. Neurosci.*, 13:125–142.

Le Beau, F. E., Rees, A., and Malmierca, M. S. (1996). Contribution of GABA- and glycine-mediated inhibition to the monaural temporal response properties of neurons in the inferior colliculus. *J Neurophysiol*, 75(2):902–919.

Leary, C. J., Edwards, C. J., and Rose, G. J. (2008). Midbrain auditory neurons integrate excitation and inhibition to generate duration selectivity: an *in vivo* whole-cell patch study in anurans. *J Neurosci*, 28(21):5481–5493.

Li, N., Gittelman, J. X., and Pollak, G. D. (2010). Intracellular recordings reveal novel features of neurons that code interaural intensity disparities in the inferior colliculus. *J Neurosci*, 30(43):14573–14584.

Liu, R. C., Miller, K. D., Merzenich, M. M., and Schreiner, C. E. (2003). Acoustic variability and distinguishability among mouse ultrasound vocalizations. *J Acoust Soc Am*, 114(6):3412–3422.

Luo, F., Metzner, W., Wu, F., Wu, F. J., Zhang, S., Zhang, S. Y., Chen, Q., and Chen, Q. C. (2008). Duration-sensitive neurons in the inferior colliculus of horseshoe bats: adaptations for using CF-FM echolocation pulses. *J Neurophysiol*, 99(1):284–296.

Ma, C. L., Kelly, J. B., and Wu, S. H. (2002). AMPA and NMDA receptors mediate synaptic excitation in the rat's inferior colliculus. *Hearing Res*, 168:25–34.

Mecham, J. S. (1971). Vocalizations of the leopard frog, *Rana pipiens*, and three related mexican species. *Copeia*, pages 505–516.

Melendez, K. V., Jones, D. L., and Feng, A. S. (2006). Classification of communication signals of the little brown bat. *J Acoust Soc Am*, 120(2):1095.

Mora, E. C. and Kössl, M. (2004). Ambiguities in sound duration selectivity by neurons in the inferior colliculus of the bat *Molossus molossus* from Cuba. *J Neurophysiol*, 91:2215–2226.

Mörchen, A., Rheinlaender, J., and Schwartzkopff, J. (1978). Latency shift in insect auditory nerve fibers. *Naturwissenschaften*, 65(12):656–657.

Moss, C. F. and Surlykke, A. (2001). Auditory scene analysis by echolocation in bats. *J Acoust Soc Am*, 110(4):2207–2226.

Narins, P. M. and Capranica, R. R. (1980). Neural adaptations for processing the two-note call of the Puerto Rican treefrog, *Eleutherodactylus coqui*. *Brain Behav. Evol.*, 17(1):48–66.

Nelson, P. G. and Erulkar, S. D. (1963). Synaptic mechanisms of excitation and inhibition in the central auditory pathway. *J Neurophysiol*, 26:908–923.

Neuweiler, G. (1984). Foraging, Echolocation and Audition in Bats. *Naturwissenschaften*, 71:446–455.

Neuweiler, G. (1990). Auditory adaptations for prey capture in echolocating bats. *Physiol. Rev.*, 70(3):615–641.

Olsen, J. F. and Suga, N. (1991). Combination-sensitive neurons in the medial geniculate body of the mustached bat: encoding of target range information. *J Neurophysiol*, 65(6):1275–1296.

O'Neill, W. E. and Suga, N. (1979). Target range-sensitive neurons in the auditory cortex of the mustache bat. *Science*, 203(4375):69–73.

Pedemonte, M., Torterolo, P., and Velluti, R. A. (1997). In vivo intracellular characteristics of inferior colliculus neurons in guinea pigs. *Brain Res.*, 759:24–31.

Pérez-González, D., Malmierca, M. S., Moore, J. M., Hernández, O., and Covey, E. (2006). Duration selective neurons in the inferior colliculus of the rat: topographic distribution and relation of duration sensitivity to other response properties. *J Neurophysiol*, 95(2):823–836.

Peterson, D. C., Voytenko, S., Gans, D., Galazyuk, A., and Wenstrup, J. (2008). Intracellular recordings from combination-sensitive neurons in the inferior colliculus. *J Neurophysiol*, 100(2):629–645.

Petrites, A. E., Eng, O. S., Mowlds, D. S., Simmons, J. A., and DeLong, C. M. (2009). Interpulse interval modulation by echolocating big brown bats (*Eptesicus fuscus*) in different densities of obstacle clutter. *J Comp Physiol A*, 195:603–617.

Pinheiro, A. D., Wu, M., and Jen, P. H. (1991). Encoding repetition rate and duration in the inferior colliculus of the big brown bat, *Eptesicus fuscus*. *J Comp Physiol A*, 169(1):69–85.

Pollack, G. S. and Hoy, R. R. (1979). Temporal pattern as a cue for species-specific calling song recognition in crickets. *Science*, 204(4391):429–432.

Potter, H. D. (1965). Patterns of acoustically evoked discharges of neurons in the mesencephalon of the bullfrog. *J Neurophysiol*, 28(6):1155–1184.

Razak, K. A. and Fuzessery, Z. M. (2006). Neural mechanisms underlying selectivity for the rate and direction of frequency-modulated sweeps in the auditory Cortex of the pallid bat. *J Neurophysiol*, 96:1303–1319.

Rose, J. E., Greenwood, D. D., Goldberg, J. M., and Hind, J. E. (1963). Some discharge characteristics of single neurons in the inferior colliculus of the cat. I. Tonotopical organization, relation of spike-counts to tone intensity, and firing patterns of single elements. *J Neurophysiol*.

Sanchez, J. T., Gans, D., and Wenstrup, J. J. (2007). Contribution of NMDA and AMPA receptors to temporal patterning of auditory responses in the inferior colliculus. *J Neurosci*, 27(8):1954–1963.

Seidl, A. H., Rubel, E. W., and Harris, D. M. (2010). Mechanisms for adjusting interaural time differences to achieve binaural coincidence detection. *J Neurosci*, 30(1):70–80.

Shannon, R. V., Zeng, F.-G., Kamath, V., Wygonski, J., and Ekelid, M. (1995). Speech recognition with primarily temporal cues. *Science*, 270:303–304.

Simmons, J. A. (1973). The resolution of target range by echolocating bats. *J Acoust Soc Am*, 54(1):157–173.

Simmons, J. A. (1989). A view of the world through the bat's ear: the formation of acoustic images in echolocation. *Cognition*, 33(1-2):155–199.

Simmons, J. A. and Stein, R. A. (1980). Acoustic imaging in bat sonar: echolocation signals and the evolution of echolocation. *J Comp Physiol A.*, 135(1):61–84.

Singh, S. and Mountain, D. C. (1997). A model for duration coding in the inferior colliculus. In Bower, J. M., editor, *Computational neuroscience: trends in research*, pages 497–503. Plenum Press, New York.

Sivaramakrishnan, S. and Oliver, D. L. (2001). Distinct K currents result in physiologically distinct cell types in the inferior colliculus of the rat. *J Neurosci*, 21(8):2861–2877.

Suga, N. and Horikawa, J. (1986). Multiple time axes for representation of echo delays in the auditory cortex of the mustached bat. *J Neurophysiol*, 55(4):776–805.

Sun, H. and Wu, S. H. (2008). Physiological characteristics of postinhibitory rebound depolarization in neurons of the rat's dorsal cortex of the inferior colliculus studied *in vitro*. *Brain Res.*, 1226:70–81.

Surlykke, A. and Moss, C. F. (2000). Echolocation behavior of big brown bats, *Eptesicus fuscus*, in the field and the laboratory. *J Acoust Soc Am*, 108(5):2419–2429.

Sutter, M. L. (2000). Shapes and level tolerances of frequency tuning curves in primary auditory cortex: quantitative measures and population codes. *J Neurophysiol*, 84(2):1012–1025.

Tanaka, H., Wong, D., and Taniguchi, I. (1992). The influence of stimulus duration on the delay tuning of cortical neurons in the FM bat, *Myotis lucifugus*. *J Comp Physiol A*, 171(1):29–40.

Thomas, J. A., Moss, C. F., and Vater, M., editors (2004). *Echolocation in Bats and Dolphins*. The University of Chicago Press, Chicago.

Vater, M., Covey, E., and Casseday, J. H. (1997). The columnar region of the ventral nucleus of the lateral lemniscus in the big brown bat (*Eptesicus fuscus*): synaptic arrangements and structural correlates of feedforward inhibitory function. *Cell Tissue Res*, 289(2):223–233.

Veselka, N., McErlain, D. D., Holdsworth, D. W., Eger, J. L., Chhem, R. K., Mason, M. J., Brain, K. L., Faure, P. A., and Fenton, M. B. (2010). A bony connection signals laryngeal echolocation. *Nature*, 463:939–942.

Voytenko, S. and Galazyuk, A. (2007). Intracellular recording reveals temporal integration in inferior colliculus neurons of awake bats. *J Neurophysiol*, 97(2):1368–1378.

Voytenko, S. and Galazyuk, A. (2008). Timing of sound-evoked potentials and spike responses in the inferior colliculus of awake bats. *Neuroscience*, 155(3):923–936.

Wang, J., van Wijhe, R., Chen, Z., and Yin, S. (2006). Is duration tuning a transient process in the inferior colliculus of guinea pigs? *Brain Res.*, 1114(1):63–74.

Wang, X., Luo, F., Philip, H., and Chen, Q. (2010). Recovery cycle of neurons in the inferior colliculus of the FM bat determined with varied pulse-echo duration and amplitude. *Chinese J. Phys.*, 53(2):119–129.

Wang, X., Luo, F., Wu, F.-J., Chen, Q.-C., and Jen, P. H.-S. (2008). The recovery cycle of bat duration-selective collicular neurons varies with hunting phase. *Neuroreport*, 19(8):861–865.

Winer, J. a. and Schreiner, C. E., editors (2005). *The Inferior Colliculus*. Springer, New York, NY.

Wu, C. H. and Jen, P. H. S. (2008). Echo frequency selectivity of duration-tuned inferior

collicular neurons of the big brown bat, *Eptesicus fuscus*, determined with pulse-echo pairs. *Neuroscience*, 156:1028–1038.

Xia, Y.-F., Qi, Z.-H., and Shen, J.-X. (2000). Neural representation of sound duration in the inferior colliculus of the mouse. *Acta Oto-laryngol.*, 120:638–643.

Xie, R., Gittelman, J. X., Li, N., and Pollak, G. D. (2008). Whole cell recordings of intrinsic properties and sound-evoked responses from the inferior colliculus. *Neuroscience*, 154(1):245–256.

Xie, R., Gittelman, J. X., and Pollak, G. D. (2007). Rethinking tuning: In vivo whole-cell recordings of the inferior colliculus in awake bats. *J Neurosci*, 27(35):9469–9481.

Yin, S., Chen, Z., Yu, D., Feng, Y., and Wang, J. (2008). Local inhibition shapes duration tuning in the inferior colliculus of guinea pigs. *Hearing Res*, 237(1-2):32–48.

Zhou, X. and Jen, P. H. (2001). The effect of sound intensity on duration-tuning characteristics of bat inferior collicular neurons. *J Comp Physiol A*, 187(1):63–73.

Table 2.1: Neuronal best duration tuning in amphibians and mammals compared with typical species-specific acoustic vocalization durations. Neuronal data reported as the range of best durations of shortpass and bandpass DTNs in each species. Because the range of temporal tuning in a DTN is usually larger than its best duration, this would increase overlap between neuronal tuning and vocalization durations.

Species	Brain region	Neuronal best duration	Vocalization duration
Frog			
R. pipiens and *H. regilla*	TS	4-50 ms (PT) (Leary et al., 2008)	8-17 ms at 32-39.9 pulses/s (Mecham 1971; *R. pipiens*)
R. pipiens	TS	25-280 ms (PT) (Gooler and Feng, 1992)	
R. catesbeiana	TS	25-40 ms (PT) (Potter, 1965)	800 ms (Capranica, 1968)
Mouse			
M. musculus	IC	6-80 ms (PT) (Brand et al., 2000)	Adults: ca. 8-75 ms
		3-300 ms (PT) (Xia et al., 2000)	Pups: ca. 8-100 ms (Liu et al., 2003)
Rat			
R. norvegicus	IC	4-128 ms (PT)	Adults ∼20-80 ms and >300 ms
		Respond up to ˜160 ms (Pérez-González et al., 2006)	Pups: ∼80-140 ms (Knutson et al., 2002)
Chinchilla	IC	20-60 ms (PT) (Chen, 1998)	∼15->400 ms (Hunyady, 2008)
Guinea pig	IC	<8-128 ms (PT) (Wang et al., 2006)	∼100+ ms (Wang et al., 2006)
	MGB	200 ms (PT)[a] (He, 2002)	
Cat			
F. domesticus	AC	50-200 ms (PT) (He et al., 1997)	400-1,600 ms (Brown et al. 1978)
Bat			
E. fuscus	IC	1-8 ms (PT) (Faure et al., 2003)	<1-20 ms (echolocation)
	IC	1-7 ms (PT)	Primarily ∼1 ms (Simmons, 1989)
		2-20 ms (FM) (Ehrlich et al., 1997)	
	IC	1-20 ms (PT) (Pinheiro et al., 1991)	
A. pallidus	IC	0.5-7 ms (PT and FM) (Fuzessery and Hall, 1999)	1.5-6 ms (echolocation) (Fuzessery et al., 1993)
M. lucifugus	AC	<10 ms (PT) (Galazyuk and Feng, 1997)	0.5-20 ms (echolocation) (Galazyuk and Feng, 1997)
			40-120 ms (social) (Melendez et al., 2006)
M. molossus	IC	1-25 ms (PT and noise)[b] (Mora and Kössl, 2004)	∼10 ms (echolocation) (Kössl et al., 1999)
R. pusillus	IC	∼5-40 ms (PT)	16.8-58 ms (echolocation) (Luo et al., 2008)
		∼5-60 ms (PT+FM) (Luo et al., 2008)	

AC auditory cortex, FM frequency modulated, IC inferior colliculus, MGB medial geniculate body, PT pure tone, TS torus semicircularis

[a] He (2002) found only 1 DTN (bandpass) out of 20 cells tested for duration selectivity

[b] Mora and Kössl (2004) report offset responding DTNs with two distinct best durations, a feature thus far unique to *M. molossus*

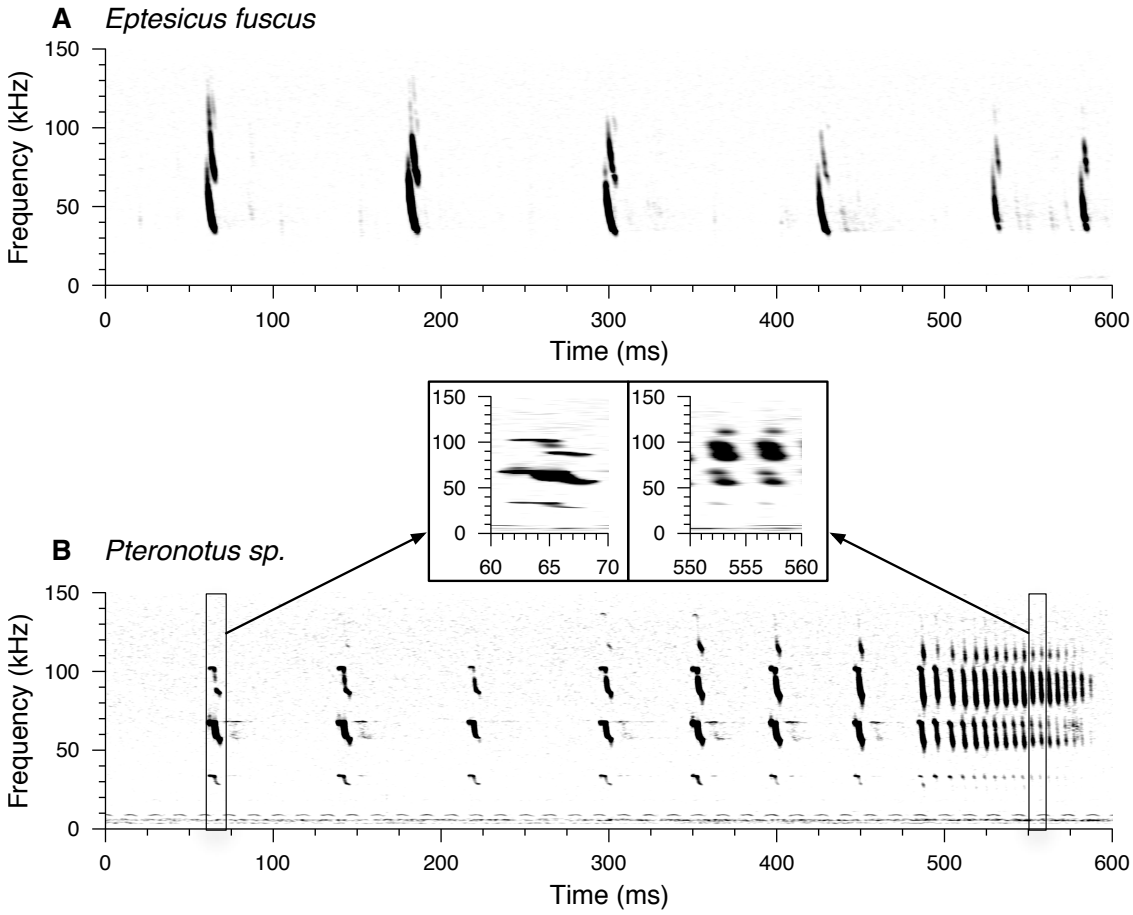

Figure 2.1: Echolocation calling sequences from two species of bats that employ different signaling strategies. (a) The low duty cycle echolocation calls of *Eptesicus fuscus* are downward frequency modulated (FM) sweeps. The calls consist of a fundamental FM element with one harmonic and most of the call energy is contained within the fundamental. The average call duration is 4.68 ms (range = 3.13 to 7.04 ms). (b) The higher duty cycle echolocation calls of *Pteronotus sp.* during insect pursuit consist of an initial constant-frequency (CF) component followed by a downward FM sweep. Unlike *E. fuscus*, most of the energy in the calls of the *Pteronotus sp.* is concentrated in the first or second harmonic. Note the terminal buzz sequence with decreased call duration and shortened interpulse intervals as the bat closes in on an insect target. Inset: magnified 10 ms views comparing the duration of a search phase call with two terminal buzz calls.

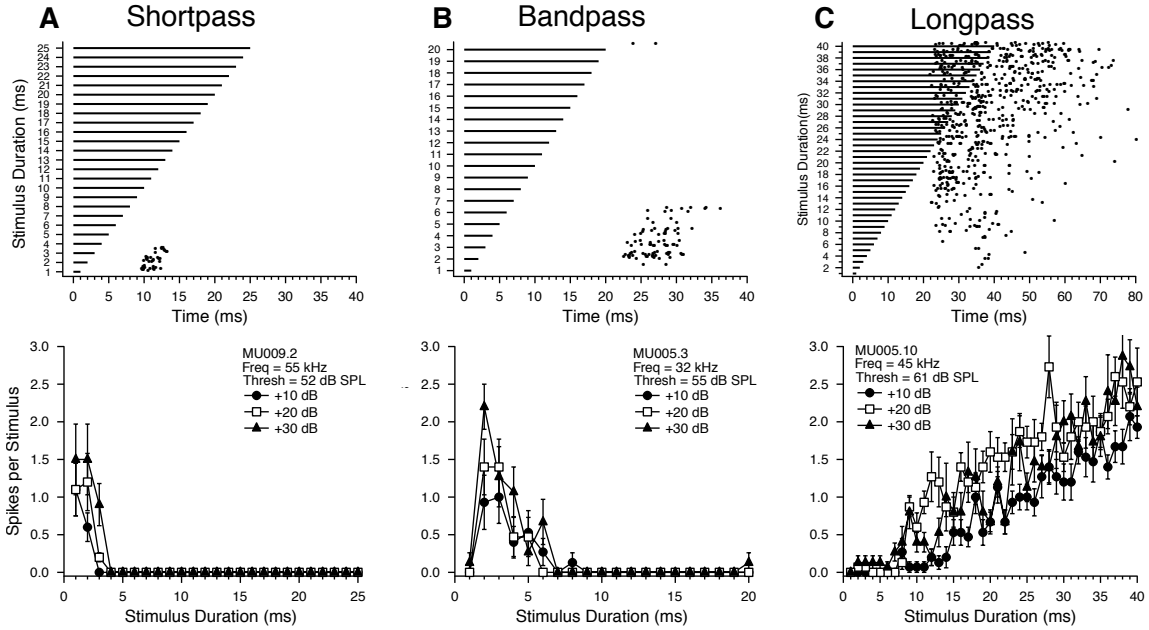

Figure 2.2: Example DTNs in the IC of *E. fuscus*. (a) Shortpass neuron, (b) bandpass neuron, and (c) longpass neuron. Top row; dot raster displays illustrating the timing of action potentials in response to best excitatory frequency tone pulses randomly varied in duration at +30 dB above threshold. Bottom row; mean ± standard error (SE) spikes per stimulus as a function of signal duration for best excitatory frequency tones presented at +10 dB, +20 and +30 dB above threshold. (a) Mean ± standard deviation (SD) first-spike latency at best duration (1 ms) = 9.76±0.25 ms and 9.83±0.25 ms at +10 dB and +30 dB (re threshold), respectively (p = 0.305; t17 = 1.057). (b) Mean ± SD first-spike latency at best duration (2 ms) = 23.52±1.07 ms and 23.62±0.89 ms at +10 dB and +30 dB, respectively (p = 0.836; t16 = 0.210). (c) Mean ± SD first-spike latency at 30 ms = 35.25±4.59 ms and 32.06±5.93 ms at +10 dB and +30 dB, respectively (p = 0.151; t24 = 1.484). (a) 10 trials per stimulus; (b, c) 15 trials per stimulus.

Figure 2.3 *(following page)*: Conceptual models of (a, b) coincidence detection and (c, d) anti-coincidence mechanisms of duration tuning. Each panel contains three traces that illustrate the hypothetical membrane potential of a DTN resulting from the summation of excitatory and inhibitory synaptic inputs to the cell at three different stimulus durations (black bars). Excitatory events are illustrated as positive deflections and inhibitory events as negative deflections relative to the baseline resting potential (solid line with arrow to illustrate time). The all-or-none spiking threshold of the DTN is illustrated as a dotted line. Onset-evoked excitatory events are labelled as ON_E, offset-evoked excitatory events are labeled as OFF_E, and sustained onset-evoked inhibitory events are labeled as SUS_I. (a) Coincidence detection shortpass duration tuning. Spikes are evoked only at the shortest stimulus duration when the subthreshold ON_E and the subthreshold OFF_E events coincide. (b) Coincidence detection bandpass duration tuning. The subthreshold ON_E is delayed so that spikes are evoked only at the intermediate stimulus duration when the subthreshold ON_E and the subthreshold OFF_E events coincide. (c) Anti-coincidence shortpass duration tuning with onset-evoked excitation. Spikes are evoked only at the shortest stimulus duration when the suprathreshold ON_E occurs sufficiently after the offset of SUS_I. (d) Anti-coincidence shortpass duration tuning with offset-evoked excitation. Spikes are evoked only at the shortest stimulus duration when the suprathreshold OFF_E occurs sufficiently before the onset of SUS_I.

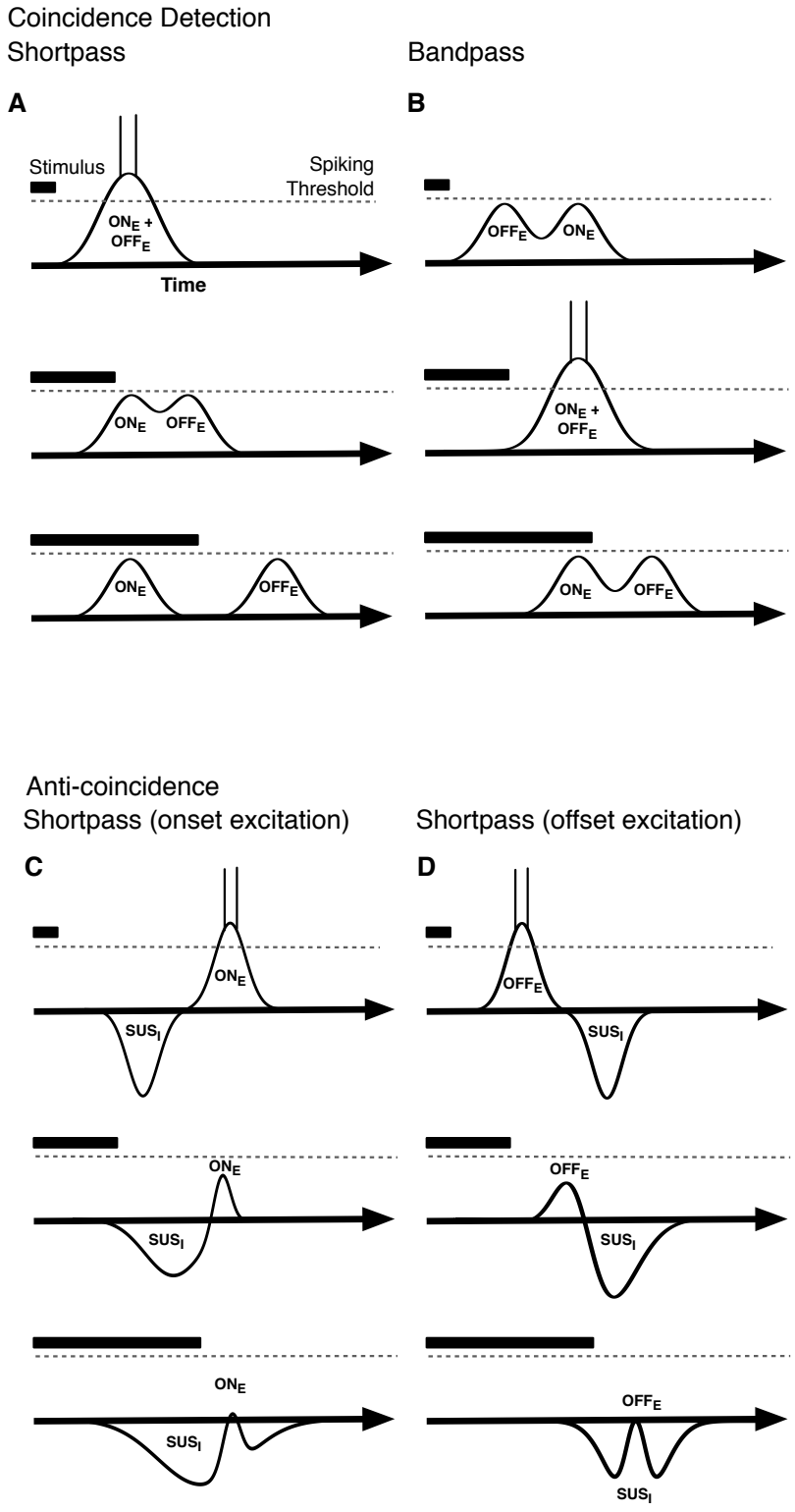
Coincidence Detection
Shortpass
Bandpass
A
B
Stimulus
Spiking Threshold
ONE + OFFE
Time
ONE
OFFE
ONE + OFFE
ONE
OFFE
ONE
OFFE
Anti-coincidence
Shortpass (onset excitation)
Shortpass (offset excitation)
C
D
ONE
SUSI
OFFE
SUSI
ONE
SUSI
OFFE
SUSI
ONE
SUSI
OFFE
SUSI

3 Recovery Cycle Times of Inferior Colliculus Neurons in the Awake Bat Measured With Spike Counts and Latencies

3.1 Abstract

Neural responses in the mammalian auditory midbrain (inferior colliculus; IC) arise from complex interactions of synaptic excitation, inhibition and intrinsic properties of the cell. Temporally selective duration-tuned neurons (DTNs) in the IC are hypothesized to arise through the convergence of excitatory and inhibitory synaptic inputs offset in time. Synaptic inhibition can be inferred from extracellular recordings by presenting pairs of pulses (paired tone stimulation) and comparing the evoked responses of the cell to each pulse. We obtained single unit recordings from the IC of the awake big brown bat (*Eptesicus fuscus*) and used paired tone stimulation to measure the recovery cycle times of DTNs and non-temporally selective auditory neurons. By systematically varying the interpulse interval (IPI) of the paired tone stimulus, we determined the minimum IPI required for a neuron's spike count or its spike latency (first- or last-spike latency) in response to the second tone to recover to within $\geq$50% of the cell's baseline count or to within 1 SD of it's baseline latency in response to the first tone. Recovery times of shortpass DTNs were significantly shorter than those of bandpass DTNs, and recovery times of bandpass DTNs were longer than allpass neurons not selective for stimulus duration. Recovery times measured with spike counts were positively correlated with those measured with spike latencies. Recovery times were also correlated with first-spike latency. These findings, combined with previous studies on duration tuning in the IC, suggest that persistent inhibition is a defining characteristic of DTNs. Herein we discuss measuring recovery times of neurons with spike counts and

latencies. We also highlight how persistent inhibition could determine neural recovery times and serve as a potential mechanism underlying the precedence effect in humans. Finally, we explore implications of recovery times for DTNs in the context of bat hearing and echolocation.

3.2 Introduction

The ability to extract temporal information from an acoustic signal is important for processing human speech (Denes, 1955), discriminating species-specific communication calls (Pollack and Hoy, 1979), localizing sounds (Knudsen and Konishi, 1979; Carr and Konishi, 1990), and echolocation by bats (Simmons, 1971, 1979; Suga and O'Neill, 1979; O'Neill and Suga, 1982). Neurons with spiking responses selective for signal duration, known as duration-tuned neurons (DTNs), provide one neural mechanism for encoding temporal information. Duration-tuned neurons have been observed across a variety of vertebrate species and taxa including frogs (Potter, 1965; Gooler and Feng, 1992; Leary et al., 2008), chinchillas (Chen, 1998), guinea pigs (Wang et al., 2006), mice (Brand et al., 2000; Xia et al., 2000; Tan and Borst, 2007), rats (Pérez-González et al., 2006), cats (He et al., 1997) and bats (Jen and Schlegel, 1982; Pinheiro et al., 1991; Casseday et al., 1994; Ehrlich et al., 1997; Fuzessery and Hall, 1999; Faure et al., 2003; Mora and Kössl, 2004; Luo et al., 2008). Because DTNs have also been found in the visual cortex of cats (Duysens et al., 1996), this suggests that neural mechanisms of duration selectivity may be similar across sensory modalities. The physiological response properties and underlying neural mechanisms of auditory DTNs have been studied most extensively in echolocating bats. The biological function(s) of DTNs to hearing is(are) unknown; however, the range of neural best durations (BD) within a species (BD = stimulus duration that causes maximum spiking) correlates with the range of vocalization durations of species-specific communication sounds in non-echolocating vertebrates and with biosonar pulse durations in echolocating bats (for reviews, see Sayegh et al., 2011; Jen et al., 2012).

Duration tuning in the mammalian inferior colliculus (IC) is hypothesized to arise from the convergence and temporal interaction of excitatory and inhibitory synaptic inputs arriving at the neuron (Casseday et al., 1994; Covey et al., 1996; Casseday et al., 2000; Faure

et al., 2003; Aubie et al., 2009). Biologically plausible computational models of DTNs support the hypothesis that neural mechanisms of duration selectivity may be shared across vertebrates (Aubie et al., 2012). A number of studies have demonstrated that neural inhibition is necessary for creating DTNs in the IC. For example, focal application of $GABA_A$ and/or glycine receptor antagonists have been shown to greatly diminish and/or eliminate the spiking responses of DTNs (Fuzessery and Hall, 1999; Jen and Feng, 1999), with the blocking of $GABA_A$ receptors having the greatest effect on temporal tuning and duration selectivity (Casseday et al., 2000). Whole-cell intracellular patch clamp recordings (Covey et al., 1996; Tan and Borst, 2007; Leary et al., 2008) and/or single-unit extracellular recordings combined with paired tone stimulation (Faure et al., 2003) have revealed that inhibitory inputs to DTNs usually precede excitatory inputs, and that the inhibition lasts from 5 to 150 ms after stimulus offset. Hence, DTNs receive inhibition that leads excitation. This inhibition also persists for as long or longer than the duration of the stimulus that evoked it. We know that inhibition occurs in some types of IC neurons that are not tuned to stimulus duration (Faingold et al., 1991; Pollak and Park, 1993; Torterolo et al., 1995; Kuwada et al., 1997; Pedemonte et al., 1997; Klug et al., 1999), and in these cells inhibition can persist for as long as 100 ms after stimulus offset (Yin, 1994; Covey et al., 1996; Litovsky and Delgutte, 2002). Owing to the importance of inhibition in creating the temporal tuning profile and response properties of DTNs, we hypothesized that the leading and persistent inhibition evoked by each signal in a paired tone stimulus could temporally interact and sum, resulting in DTNs exhibiting longer recovery cycle times than non-DTNs. Herein we test this hypothesis.

The recovery time of an evoked neural response can be measured with paired pulse stimulation (Grinnell, 1963). Often the stimulus is a pair of equal amplitude pure tones set to the cell's characteristic or best excitatory frequency (BEF) and presented at varying interpulse intervals (IPIs). Some studies have used pairs of acoustic clicks presented at

varying interstimulus delays (Fitzpatrick et al., 1995; Litovsky and Yin, 1998a; Litovsky and Delgutte, 2002), while others have used pairs of frequency modulated (FM) sweeps or variable amplitude tones to mimic the loud outgoing vocalizations and faint returning echoes used for echolocation by bats (Grinnell, 1963; Suga, 1964; Friend et al., 1966; Pollak et al., 1977a,b; Lu et al., 1997; Wang et al., 2010). A cell's recovery time is measured by determining the minimum IPI required for the spiking response evoked by the second stimulus (R2) to recover within a specified level of the spiking response evoked by the first stimulus (R1). The most common and unbiased criterion for measuring recovery time is to report the IPI where the R2/R1 ratio is $\geq$0.5. Note that this measure is normally based enitrely on spike counts. To the best of our knowledge, no previous study has measured neural recovery times with a spike latency criterion.

Previous studies in bats reported that spike count recovery cycle times of IC neurons are highly variable, ranging anywhere from 4 to 200 ms (Suga, 1964; Friend et al., 1966; Suga and Schlegel, 1973; Pollak et al., 1977b; Lu et al., 1997; Tang et al., 2011). The recovery cycle times of many DTNs are shortest when the pulse and echo durations are set to the cell's BD and presented at biologically relevant pulse-echo amplitude differences (Wang et al., 2008, 2010). The frequency selectivity of DTNs has also been reported to sharpen when the pulse and echo are presented at BD (Wu and Jen, 2008b). These findings suggest that the responses of DTNs may be specialized for processing loud outgoing echolocation pulses and fainter returning echos. Because DTNs are found in both echolocating and non-echolocating mammals, the ability to echolocate cannot be a prerequisite for the evolution of auditory duration selectivity (Sayegh et al., 2011). Nevertheless, this does not preclude a more specialized functional role for DTNs in hearing and echolocation by bats.

Recovery cycle times also provide a way to observe the effects of synaptic inhibition to a neuron. Application of bicucculine, a $GABA_A$ receptor antagonist, has been shown to shorten the recovery times of IC neurons (Lu et al., 1997; Zhou and Jen, 2003), suggesting

that inhibitory inputs control the minimum time needed for response recovery. In this study, we measured and compared the recovery cycle times of DTNs and non-DTNs using both spike count and spike latency measures as a way to further our understanding about the strength and time course of the leading and persistent inhibition that is responsible for the creation of auditory midbrain microcircuits sensitive to temporal acoustic features.

3.3 Methods

3.3.1 Surgical procedures

Electrophysiological data were obtained from 33 adult big brown bats (*Eptesicus fuscus*) of both sexes that were housed in a husbandry facility where colony temperature and lighting varied according to ambient conditions (Faure et al., 2009). To facilitate multiple recordings and to precisely replicate the position of the bat's head between sessions, a stainless steel post was glued to the skull. Prior to the head-posting surgery, bats were given a subcutaneous injection of buprenorphine (0.03 mL; 1:9 mixture of 0.3 mg/mL Temgesic and sterile water; 0.045 mg/kg). For the surgery, bats were first placed in an anesthesia induction chamber (12 x 10 x 10 cm) where they inhaled a 1 to 5% isofluorane:oxygen gaseous mixture (flow rate: 1 L/min). Anesthetized bats were then placed in a foam-lined body restraint within a stereotaxic alignment system (David Kopf Instruments Model 1900) fitted with a custom mask for gas inhalation. The hair covering the skull was shaved and the underlying skin was swabbed with Betadine® disinfectant. Local anesthetic (0.2 mL bupivicaine; 5 mg/mL) was injected subcutaneously prior to making a midline incision in the scalp. The temporal muscles were reflected, the skull was scraped clean and swabbed with 70% ethanol, and a post was glued to the skull overlying the cortex with cyanoacrylate adhesive (Henkel Loctite Corporation) cured with liquid acrylic hardener (Zipkicker; Pacer Technology®). A chlorided silver wire, attached to the head post, was placed under

the temporal muscles and served as the reference electrode. Recordings began 1 to 4 days after surgery. Each bat was used in 1 to 8 sessions lasting ca. 4 to 8 hrs each on separate days. Recordings were terminated if a bat showed signs of discomfort (e.g. struggling body movements). Between sessions, the electrode penetration site was covered with a piece of contact lens and Gelfoam® coated in Polysporin®. Bats were housed individually in a temperature- and humidity-controlled room and were given *ad libitum* access to food and water. All procedures were approved by the McMaster University Animal Research Ethics Board and were in accordance with the Canadian Council on Animal Care.

3.3.2 Electrophysiological recordings

Recordings were conducted inside a double-walled, sound attenuating booth with electrical shielding (Industrial Acoustics Co., Inc.). Prior to recording, each bat was given a subcutaneous injection of a neuroleptic (0.3 mL; 1:1 mixture of 0.05 mg/mL fentanyl citrate and 2.5 mg/mL Inapsine [droperidol]; 19.1 mg/kg). Bats were then placed in a foam-lined body restraint that was suspended by springs within a small animal stereotaxic frame that was customized for bats (ASI Instruments) and mounted atop of an air vibration table (TMC Migro-g). The bat's head was immobilized by securing the headpost to a stainless steel rod attached to a manipulator (ASI Instruments) mounted on the stereotaxic frame. The dorsal surface of the IC was exposed for recording by making a small hole in the skull and dura mater with a scalpel. Single-unit extracellular recordings were made with thin-wall borosilicate glass microelectrodes with a capillary filament (o.d. = 1.2 mm; A-M Systems, Inc.) and filled with 3M NaCl. Typical electrode resistances ranged from 10 to 30 MΩ. Electrodes were positioned over the dorsal surface of the IC with manual manipulators (ASI Instruments), and advanced into the brain with a stepping hydraulic micropositioner (David Kopf Instruments Model 2650). Action potentials were recorded with a Neuroprobe amplifier (A-M Systems Model 1600) whose 10x output was bandpass filtered and further

amplified (500 to 1000x) by a Tucker Davis Technologies spike pre-conditioner (TDT PC1; lowpass f_c = 7 kHz; high-pass f_c = 300 Hz). Spike times were logged on a computer by passing the PC1 output to a spike discriminator (TDT SD1) and then an event timer (TDT ET1) synchronized to a timing generator (TDT TG6). Electrodes were visually aimed at the dorsal surface of the IC and all recordings are assumed to be from the central nucleus of the inferior colliculus (ICc).

3.3.3 Stimulus generation and data collection

Stimulus generation and on-line data collection were controlled with custom software that displayed spike times as dot raster displays ordered by the acoustic parameter that was randomized during unit testing (see Faure et al., 2003). Briefly, pure tone pulses were digitally generated with a two-channel array processor (TDT Apos II; 357 kHz sampling rate) optically interfaced to two digital-to-analog (D/A) converters (TDT DA3-2) whose individual outputs were fed to a low-pass anti-aliasing filter (TDT FT6-2; f_c = 120 kHz), two programmable attenuators (TDT PA5) and two signal mixers (TDT SM5) with equal weighting. The output of each mixer was fed to a manual attenuator (Leader LAT-45) before final amplification (Krohn-Hite Model 7500). All stimuli were presented monaurally, contralateral to the IC being recorded, using a Brüel & Kjær (B&K) $\frac{1}{4}$ inch condenser microphone (Type 4939; protective grid on) modified for use as a loudspeaker with a transmitting adaptor (B&K Type UA-9020) to correct for nonlinearities in the transfer function (Frederiksen, 1977). The loudspeaker was positioned ca. 1 mm in front of the external auditory meatus. The output of each speaker, measured with a B&K Type 4138 $\frac{1}{8}$ inch condenser microphone (90^o incidence; grid off) connected to a measuring amplifier (B&K Type 2606) and bandpass filter (K-H Model 3500), was quantified with a sound calibrator (B&K Type 4231) and expressed in decibels sound pressure level (dB SPL re 20 μPa) equivalent to the peak amplitude of continuous tones of the same frequency (Stapells et al., 1982). The loudspeaker

transfer functions were flat ±6 dB from 28 to 118 kHz, and there was at least 30 dB attenuation at the ear opposite the source (Ehrlich et al., 1997). All stimuli had rise/fall times of 0.4 or 0.5 ms shaped with a square cosine function and were presented at a trial stimulation rate of 3 Hz.

Single units were found by searching with short duration pure tones and/or downward FM sweeps. Upon unit isolation, we determined the cell's best excitatory frequency (BEF), acoustic threshold, first-spike latency (FSL) and last-spike latency (LSL) re signal onset, and for DTNs we also determined the best duration (BD) and duration-selective response class (i.e. shortpass, bandpass or longpass DTNs; see Faure et al., 2003; Fremouw et al., 2005). In all cases, neural response parameters were determined by systematically varying the frequency, attenuation or duration of the stimulus in blocks, with 10-20 stimulus repetitions per randomized step in each block. Following the paired tone stimulation paradigm of Faure et al. (2003), we presented cells with pairs of BEF tone pulses. The onset of the first pulse (P1) was fixed in time relative to the onset of recording; the onset of the second pulse (P2) was systematically varied. The stimulus IPI was defined as the time between the onset of P1 and the onset of P2. For DTNs the durations of P1 and P2 were set to the cell's BD, whereas for non-DTNs the paired tone duration was randomly chosen from 1 to 9 ms. Because P1 and P2 were matched in stimulus frequency, duration, amplitude and phase at all IPIs presented, whenever the two tones temporally overlapped they summed to form a single composite tone with a +6 dB amplitude pedestal, the duration of which was determined by the amount of overlap.

3.3.4 Measuring recovery times

We tested 73 IC neurons with paired tone stimulation and generated 132 data files: 59 cells were tested at both +10 dB and +20 dB above threshold (118 files), and 14 cells were tested at only +10 dB above threshold. The IPI between P1 and P2 was randomly varied, typically

in 2 ms steps (115 of 132 files; 87%); however, two files used 1 ms steps, 1 file used 2.5 ms steps, 1 file used 4 ms steps, and 13 files used 5 ms steps.

Baseline data and windowing responses For each file, we measured the baseline FSL and baseline LSL in response to tone P1 for the 10 trials with the longest IPIs. We did this to minimize the influence of tone P2 on the measurement of the Baseline Response R1 re P1 (see Fig. 3.1A). We used 20 stimulus repetitions at each IPI to calculate a mean $\pm$ standard deviation (SD) FSL and LSL (re P1). We then averaged the 10 means and 10 SDs to calculate a grand mean $\pm$ average SD baseline FSL and baseline LSL (re P1) for each file. The baseline FSL and baseline LSL were used to define the P1 and P2 analysis windows. The P1 analysis window started at the onset of P1 + baseline FSL $-$ 2 SDs and ended at the onset of P1 + baseline LSL + 2 SDs. The P2 analysis window started at the onset of P2 + baseline FSL $-$ 2 SDs and ended at the onset of P2 + baseline LSL + 2 SDs. Spikes were assumed to be evoked by P1 if they fell into the P1 analysis window, and spikes were assumed to be evoked by P2 if they fell into the P2 analysis window. For trials where the IPI was small and the P1 and P2 analysis windows overlapped—when the onset of P1 + baseline LSL + 2 SDs was $>$ the onset of P2 + baseline FSL $-$ 2 SDs, thus making it difficult to confidently assign spikes as being evoked by either P1 or P2—we used a single, combined analysis window to measure the evoked response. The combined analysis window started from the onset of P1 + baseline FSL $-$ 2 SDs and ended at the onset of P2 + baseline LSL + 2 SDs.

Spike count recovery We used the P1 and P2 analysis windows (described above) to count spikes and measure spike latencies evoked by tones P1 and P2, respectively, and to calculate the response criteria for measuring recovery cycle times. We did this so that evoked responses were compared with equal duration analysis windows. Assuming spike

latencies are normally distributed, then at 2 SDs wide the P1 and P2 analysis windows should capture $\geq$95% of evoked responses. The P1 analysis window was used to measure the Baseline spiking Response R1 evoked by tone P1. The P2 analysis window was used to measure the spiking Response R2 evoked by tone P2 (Fig. 3.1A). At each IPI, we calculated a R2/Baseline R1 ratio of response (Fig. 3.1B). The R2 spike count was defined as having "recovered" when this ratio was $\geq$0.5—that is, when the spike count evoked by P2 recovered to within 50% of the baseline spike count evoked by P1. For trials where the IPI was small and the P1 and P2 analysis windows overlapped, the spike count ratio of response was calculated by first counting the number of spikes that fell into the combined P1 + P2 analysis window and then subtracting the Baseline Response R1 spike count before dividing this value by the Baseline Response R1 spike count, which is similar to the method used by Suga (1964) to deal with response overlap.

Some cells showed variation (ringing) in their spike count ratio of response function, so we developed two algorithms to measure recovery times from the functions. The algorithms assess response recovery starting from different ends of the function (Fig. 3.1B). The *short-to-long method* assesses the function starting from the shortest IPIs on the left and moving toward the longest IPIs on the right. Using this technique, the recovery time of a cell was defined as the smallest IPI where the ratio of response function crossed and remained $\geq$0.5 for at least two consecutive IPIs (see * in Fig. 3.1B). In a small subset of files (9/132, 6.8%), we observed a brief facilitation in the ratio of response function at short IPIs, followed by a decrease below 0.5 at intermediate IPIs, and then an increase above 0.5 at longer IPIs (e.g. Fig. 3.6C,D). For these files, the recovery time was defined as the smallest IPI where the spike count ratio of response function remained $\geq$0.5 for most of the remaining points at longer IPIs (based on visual inspection by 2 observers), which is similar to the method used by Fitzpatrick et al. (1995). The *long-to-short method* assesses the spike count recovery function starting from the longest IPIs on the right and moving toward the shortest IPIs on

the left. With this technique the recovery time of a cell was defined as the largest IPI where the spike count ratio of response function was $\geq$0.5 if at least two consecutive data points at smaller IPIs were $<$0.5 (see † in Fig. 3.1B), or if most data points at shorter IPIs remained below 0.5 (based on visual inspection by 2 observers).

Spike latency recovery In most data files we noticed an increase in the FSL or LSL (or both) of the evoked response (re P2) at short IPIs, and then a return to baseline R1 latencies at longer IPIs (e.g. Fig. 3.1C,D). We used this latency change as an alternative method for determining the recovery times of IC neurons. Using the Baseline Response R1 FSL and LSL data (re P1) for each file, we measured response recovery with spike latencies using a $\pm$1 SD criterion. We then employed similar short-to-long and long-to-short analysis algorithms to measure spike latency recovery times. The *short-to-long method* starts with the shortest IPI on the left where the R2 latency had increased to $>$1 SD above the Baseline Response R1 latency, and moving right it selects the shortest subsequent IPI where the R2 latency returns and remains within 1 SD of baseline for at least two consecutive IPIs (see * in Fig. 3.1C,D). The *long-to-short method* starts from the longest IPI on the right and moving left it determines the shortest subsequent IPI where the R2 latency falls within 1 SD of baseline if at least two consecutive points at shorter IPIs were $>$1 SD of baseline (see † in Fig. 3.1C,D). A number of data files did not show a $\pm$1 SD change in FSL (8/132, 6.1%) or LSL (56/132, 42.4%), and for these cases it was not possible to measure a spike latency recovery time.

3.3.5 Data analysis

Unless stated otherwise, all data are reported as the mean $\pm$ standard error (SE). Parameter correlations were calculated with linear regression in Python (SciPy module) and relationships are reported as the coefficient of determination (R^2 and p-values). Unless explicitly

testing for factor effects, we grouped recovery time values across cell types (bandpass, shortpass, allpass) at both +10 dB and +20 dB (re threshold). We used the linear and non-linear mixed-effects models analysis-of-variance (ANOVA) package written in R to test for effects of cell type, analysis method, and relative amplitude on recovery cycle times, FSLs, and LSLs, with cell type and relative amplitude as fixed factors and cell ID as a random factor (Pinheiro and Bates, 2000).

3.4 Results

3.4.1 Response properties

Duration-tuned neurons can be categorized into one of three response classes based on the shape of the duration tuning function (Sayegh et al., 2011). Bandpass DTNs respond maximally at BD, with spike counts that eventually fall to $\leq$50% of the maximum at durations both longer and shorter than BD. Shortpass DTNs also respond maximally at BD, with spike counts that eventually fall to $\leq$50% of the maximum at durations longer than BD but not shorter. The spiking responses of shortpass and bandpass DTNs are typically transient and offset-evoked, with FSL (re stimulus onset) increasing with stimulus duration (Faure et al., 2003). Longpass DTNs do not have a BD; instead, they respond only when the stimulus duration exceeds some minimum duration (Faure et al., 2003; Aubie et al., 2009; Sayegh et al., 2011). Longpass DTNs differ from typical sensory neurons in that they do not show a decrease in FSL with increasing stimulus amplitude that is typical of neurons that integrate stimulus energy (Brand et al., 2000; Faure et al., 2003; Pérez-González et al., 2006). Longpass DTNs were not used in this report. By definition, allpass neurons are not duration-selective and therefore do not have a BD. Allpass neurons spike in response to all signal durations that contain sufficient stimulus energy. The response pattern of allpass neurons can be transient or sustained, with spikes typically occurring at a constant

(onset-evoked) FSL re stimulus onset.

We obtained single unit extracellular recordings from 73 IC neurons. Of these, 16 (22%) were shortpass DTNs, 18 (25%) were bandpass DTNs, and 39 (53%) were not duration-selective (i.e. allpass neurons). Recovery times were determined at +10 dB for all cells and at +20 dB re threshold for 59 cells (14 shortpass, 13 bandpass, and 32 allpass).

Traveling dorsal to ventral in direction, the BEF of cells systematically increased as the depth of the recording electrode was advanced into the IC (R^2=0.57, $p \ll 0.001$; data not shown). This tonotopic relationship held true within all cell types and response classes (allpass R^2=0.65, $p \ll 0.001$; shortpass R^2=0.56, $p \ll 0.001$; and bandpass R^2=0.41, $p < 0.001$). There was no correlation between neuronal BD and electrode depth (Fig. 3.2A), but there was a significant negative correlation between BD and BEF (Fig. 3.2B). There was also no correlation between BEF and the mean baseline spike count at +10 dB (R^2=0.030, p=0.15), but at +20 dB (re threshold) there was a weak, positive correlation (R^2=0.068, p=0.046).

We measured the average spike latency (re stimulus onset) at each level above threshold (Table 3.1) and found that FSL (F=2.12, p=0.13) and LSL (F=0.17, p=0.84) did not vary as a function of response class. Mean FSLs decreased with a +10 dB increase in stimulus amplitude (F=7.46, p=0.0084), but there was no change in LSL (F=0.0016, p=0.97). Neurons with higher BEFs had shorter FSLs (Fig. 3.3A,B). There was also a negative correlation between BEF and LSL (Fig. 3.3C,D). Neurons with longer FSLs (but not LSLs) were distributed more dorsally in the IC at shallower electrode depths (data not shown).

3.4.2 Recovery cycle times

Figure 3.4 illustrates the response characteristics of a bandpass DTN to presentations of variable duration BEF tones (Fig. 3.4A,B) and to pairs of BEF and BD tones varied in IPI (Fig. 3.4C,D). This cell responded to 24 kHz tone durations between 1 and 8 ms, with a maximum of ca. 2 spikes per stimulus at a BD of 4 ms. Because the cell's FSL increased

with stimulus duration it was characterized as offset responding. When stimulated with pairs of BD tones that were randomly varied in IPI, spike counts in response to tone P2 became suppressed (Fig. 3.4D) and the spike latency (both FSL and LSL) was delayed at short IPIs (Fig. 3.4E,F). Evidence that neural inhibition alters the responses can be seen in Figure 3.4C during and following the period of response overlap. At an IPI of 2 ms, the leading inhibition evoked by each stimulus sums and this appears to lengthen the cell's FSL without drastically altering its spike count. At IPIs from 4 to ca. 36 ms, the persistent inhibition evoked by P1 appears to interact with the leading inhibition evoked by P2 and this suppresses the spike count and delays the FSL of the response evoked by P2. Eventually, the spike count and latencies recover to within baseline values, although subtle effects of persistent inhibition can still be observed at long IPIs because the mean FSL (re P2) does not begin to overlap the mean FSL (re P1) until an IPI of 76 ms. Indeed, for this cell it is clear that FSL takes longer to recover than LSL. The recovery time of the cell, as determined from the spike count ratio of response function, was similar for the short-to-long (42 ms) and long-to-short (38 ms) analysis methods. The recovery time of the cell, as determined from the FSL function (re P2), returned to within 1 SD of baseline at 56 ms using both the short-to-long and long-to-short methods (Fig. 3.4E). The recovery time of the cell, as determined from LSL function (re P2), returned to within 1 SD of baseline at 20 ms using both methods (Fig. 3.4F).

Figure 3.5 illustrates the response characteristics of a shortpass DTN to presentations of variable duration BEF tones (Fig. 3.5A,B) and to pairs of BEF and BD tones varied in IPI (Fig. 3.5C,D). This cell responded to 38 kHz tone durations between 1 and 4 ms, with a maximum of ca. 1.9 spikes per stimulus at a BD of 2 ms. The FSL of the cell also increased with stimulus duration and followed stimulus offset. When stimulated with pairs of BD ms tones that were randomly varied in IPI, the spike count in response to tone P2 became suppressed (Fig. 3.5D) and both the FSL and LSL were delayed at short IPIs (Fig.

3.5E,F). Eventually, the spike count and latencies recovered to within baseline values. The effect of neural inhibition can be seen in Figure 3.5C during and following the period of response overlap. At an IPI of 2 ms, when the paired BD stimulus was effectively a single 4 ms tone with a brief amplitude modulation at its midpoint (caused by the fall-and-rise times of each stimulus), the leading inhibition evoked by each stimulus sums and this appears to decrease the spike count and lengthen the FSL (re P2). At IPIs from 4 to ca. 40 ms, the persistent inhibition evoked by P1 appears to interact with the leading inhibition evoked by P2 and this suppresses the spike count and delays the FSL of the response evoked by P2. The recovery time of the cell, as determined from the spike count ratio of response function, was 46 ms for both the short-to-long and long-to-short analysis methods. The recovery time of the cell, as determined from the FSL function (re P2), returned to within 1 SD of baseline at an IPI of 20 ms for both analysis methods (Fig. 3.5E). The recovery time of the cell, as determined from the LSL function (re P2), returned to within 1 SD of baseline at an IPI of 14 ms with the short-to-long method, and we were unable to measure a recovery time with the long-to-short method because LSL did not deviate by $>$1 SD for two consecutive IPIs (Fig. 3.5F). Notice again that subtle effects of persistent inhibition can be observed in the paired tone responses because the mean FSL and mean LSL (re P2) do not begin to overlap the mean FSL and mean LSL (re P1) until IPIs longer than the measured recovery times. Again, FSL takes longer to recover than LSL.

Figure 3.6 illustrates the response characteristics of an allpass neuron to presentations of 28 kHz BEF tones that were randomly varied in duration (Fig. 3.6A,B) and to pairs of BEF tones varied in IPI (Fig. 3.6C,D). For this cell, spike counts remained within 50% of the maximum response at all durations tested. Because FSL did not change with stimulus duration, the cell was characterized as onset responding. When the cell was stimulated with 3 ms tone pairs that were randomly varied in IPI (Fig. 3.6C), a brief facilitatory response was observed at IPIs from 2-10 ms before the spike count (re P2) became suppressed at

intermediate IPIs (Fig. 3.6D). Paired tone stimulation only slightly delayed FSLs re P2 (Fig. 3.6E), and LSLs re P2 were unaffected (Fig. 3.6F). The recovery time of the cell, as determined from the spike count ratio of response function, was 54 ms using both the short-to-long and long-to-short analysis methods. The recovery time of the cell, as determined from the FSL function (re P2), returned to within 1 SD of baseline at an IPI of 14 ms using the short-to-long method, and at 22 ms using the long-to-short method (Fig. 3.6E). We were unable to measure a recovery time with LSL because it did not deviate by $>$1 SD at any IPI tested (Fig. 3.6F).

3.4.3 Recovery cycles measured with spike counts and latencies

For the majority of cells and data files (92 of 132 files; 70%), recovery cycle times measured with the short-to-long and long-to-short analysis algorithms yielded identical values. Indeed, recovery times determined with the two algorithms were highly correlated at both +10 dB (Fig. 3.7) and +20 dB (data not shown) above threshold for spike counts (Fig. 3.7A), FSL (Fig. 3.7B) and LSL measures (Fig. 3.7C). Of the remaining 40 files that were not in agreement, 15 had recovery times that differed by $\leq$4 ms (absolute value). When the two methods for determining recovery times did not agree, the long-to-short method generally yielded longer values than the short-to-long method, as evidenced by the number of points falling above the unity lines in Figure 3.7.

Table 3.2 lists the mean $\pm$ SE 50% spike count recovery times determined with both analysis algorithms as a function of neural response class and level above threshold. Using the short-to-long method, non-duration-selective neurons and shortpass DTNs had the shortest recovery times, and bandpass DTNs had significantly longer recovery times (short-to-long spike recovery time: F=4.31, p=0.017). When we analyzed the data measured with the long-to-short technique, the differences in recovery cycle times across neural response classes were no longer significant (long-to-short spike recovery time: F=1.68, p=0.1942);

however, a statistically significant difference in recovery cycle times between neural response classes re-emerged when the data were re-analyzed using the average recovery cycle time of the short-to-long and long-to-short algorithms (average spike recovery time: F=3.23, p=0.046). There was no effect of tone amplitude (level above threshold) on recovery times measured with either spike count algorithm (short-to-long: F=0.063, p=0.80; long-to-short: F=0.20 p=0.65).

Tables 3.3 and 3.4 list the mean $\pm$ SE spike latency recovery times as a function of neural response class and level above threshold using the short-to-long and the long-to-short analysis methods. Overall, there was no main effect of response class or tone amplitude on FSL (Table 3.3) or LSL (Table 3.4) recovery times. Bandpass DTNs had significantly longer FSL recovery times with the long-to-short method (long-to-short FSL recovery: F=3.90 p=0.026). For the remainder of this paper, we present recovery times as the average of the short-to-long and long-to-short analysis algorithms for both spike counts and spike latencies unless we were unable to obtain an average, in which case the algorithm that provided a value was used.

Previous studies on the recovery cycle times of auditory neurons have used only spike counts as the dependent measure (Suga, 1964; Friend et al., 1966; Suga and Schlegel, 1973; Pollak et al., 1977b; Lu et al., 1997). In our dataset, we were able to measure recovery times with a 50% change in spike count for all 132 data files at +10 dB and +20 dB (re threshold). And for a majority of cells we were able to measure recovery time with a 1 SD change in FSL (n=124 files) and LSL (n=75 files). Recovery times measured with a spike count criterion were positively correlated with recovery times measured with a FSL (Fig. 3.8A,B) and LSL (Fig. 3.8C,D) criterion at both +10 dB and +20 dB (re threshold). There was also a positive correlation between recovery times measured with a FSL and LSL criterion at +10 dB (Fig. 3.8E) and +20 dB above threshold (Fig. 3.8F). Upon closer inspection, we found no obvious bias for recovery times measured with spike counts and FSLs because similar

numbers of points fell above and below the unity lines at both levels above threshold (Fig. 3.8A,B); however, recovery times measured with spike counts and FSLs tended to be longer than those measured with LSLs, as evidenced by a greater number of points falling below the unity lines in the scatterplots (Fig. 3.8C-E).

In a further analysis we compared recovery times measured with spike counts, FSLs and LSLs but only in cells that provided values for all three measures (Table 3.5). Using this subset of data, the positive correlation between spike count and FSL recovery times remained and became stronger (R^2=0.27, $p<0.001$, n=42). Measuring recovery times with a LSL criterion was a limiting factor for inclusion in this restricted subset of data, hence the correlations between spike count and LSL recovery times and between LSL and FSL recovery times were identical to those in Figure 3.8C-F. Using a repeated measures ANOVA, we found a significant main effect of the response parameter used to measure neural recovery (spike count, FSL, LSL: F=15.02, $p \ll 0.001$). Recovery times determined with a 1 SD change in LSL were significantly shorter than recovery times measured with a 50% change in spike count or with a 1 SD change in FSL (Table 3.5). Moreover, there was now a significant main effect of stimulus amplitude, with recovery times decreasing at the higher stimulus level above threshold (+10 dB and +20 dB: F=5.28, p=0.024). There was no significant interaction between any main effects (analyses not shown).

3.4.4 Recovery cycles and response properties

At +10 dB (re threshold), stimulus duration was not correlated with recovery cycle time, regardless of cell type (data not shown), but at +20 dB there was a positive correlation between stimulus duration and the spike count recovery time (Fig. 3.9A). There was no correlation between stimulus duration and FSL recovery time (Fig. 3.9B) or LSL recovery time (Fig. 3.9C) at either level above threshold. When allpass neurons were removed from the analysis there was still no correlation between BD and the spike count recovery

cycle time at +10 dB (R^2=0.023, p=0.39, n=34), and the positive correlation at +20 dB became stronger (R^2=0.16, p=0.044, n=26). Neural BEFs did not correlate with spike count recovery times at either +10 dB (R^2=0.0019, p=0.72) or +20 dB (R^2=0.0095, p=0.46) above threshold (data not shown). There was also no correlation between the spike count recovery time of a cell and its baseline spike count at both +10 dB (R^2=0.019, p=0.25) and +20 dB (R^2=0.00024, p=0.91) above threshold (data not shown).

Neurons with short FSLs typically had short spike count recovery times, and this result held true at both +10 dB (Fig. 3.10A) and +20 dB above threshold (data not shown). At +10 dB (re threshold), neurons with short FSLs also had short FSL (Fig. 3.10B) and LSL recovery times (Fig. 3.10C), but at +20 dB (re threshold) the correlations were no longer significant (data not shown).

3.5 Discussion

3.5.1 Recovery cycles and spike latencies

Spike counts and latencies are basic response properties commonly reported in electrophysiological papers. And while changes in both can be used to assess response features, such as the onset and duration of synaptic inhibition in DTNs (Faure et al., 2003) or the presence of neuromodulators in midbrain microcircuits (Hurley and Pollak, 2005), often studies report only a change in spike count even though numerous electrophysiological and computational papers have shown that spike latency is as (if not more) important at encoding stimulus specific and related information at all levels of the central auditory system (Middlebrooks et al., 1994; Klug et al., 2000; Brugge et al., 2001; Furukawa and Middlebrooks, 2002; Heil, 2004; Nelken et al., 2005). Fontaine and Peremans (2009) argue that a spike-timing code (as opposed to a spike rate or count code) is more appropriate for processing the short duration echolocation signals emitted by bats. Neural FSLs may also be used as

an alternative to spike counts/rates when rapid responses are required (Grothe and Klump, 2000; VanRullen et al., 2005), and are critical to mechanisms underlying sound localization (Joris et al., 1998).

In this study, we compared recovery cycle times measured with spike counts and spike latencies. We do not know which measures are more pertinent for assessing neural response recovery and/or its relevance to perception because both spike count and timing codes can be used independently to represent stimulus features (VanRullen et al., 2005). The relative importance, if any, will depend on which parameter(s) is(are) most important for encoding and transmitting stimulus specific information in the central nervous system. Because our analyses employed dissimilar criteria for assessing response recovery (50% spike count *versus* 1 SD latency change), the sets of results may not be directly comparable. Despite this caveat, recovery times measured with spike counts were reasonably well correlated with those measured with spike latencies (Fig. 3.8). Nevertheless, some neurons with small spike count recovery times had large spike latency recovery times (and vice versa), suggesting that some factors governing spike count recovery differ from those governing spike latency recovery. When we restricted our analysis and examined only those cells that provided recovery times with spike count, FSL and LSL, the correlations between the recovery times remained (or strengthened). Recovery times measured with LSL were significantly shorter than those measured with spike counts and FSL in the same cells (Table 3.5). Altogether, the results suggest that spike latencies can be employed as an alternative measure of response recovery. We encourage researchers to continue developing additional analyses that exploit changes in spike latency.

Inhibition is thought to play a role in determining FSL and the duration of recovery times of central auditory neurons. Bicucculine ($GABA_A$ receptor antagonist) application shortens the recovery times of most IC neurons (Lu et al., 1997; Zhou and Jen, 2003) and also shorten FSLs (Park and Pollak, 1993; Lu et al., 1997). The effect of inhibition on FSL

has been disputed. It has been suggested that a reduction in FSL can be attributed to offset responding neurons changing to onset responding neurons when inhibition is removed or its effects are blocked because this causes FSL to shorten by the duration of the stimulus (Fuzessery et al., 2003). Intracellular recordings from the IC of the big brown bat reveal the presence of an onset-evoked hyperpolarization in the majority of units studied (Covey et al., 1996; Voytenko and Galazyuk, 2008), suggesting that onset-evoked inhibition plays a role in governing first-spike timing. In this study we found that neurons with shorter FSLs had shorter recovery times, a relationship that also exists for sound localizing neurons in the IC of the awake rabbit (Fitzpatrick et al., 1995). Together, these findings support the hypothesis that factors influencing the duration of recovery cycles and the timing of FSLs are related.

3.5.2 Effect of stimulus amplitude and BEF on FSL and recovery times

As in previous studies, we found that FSLs of DTNs and non-DTNs in the IC of the bat decreased with increasing electrode depth (Park and Pollak, 1993; Fuzessery et al., 2003) and increasing BEFs (Haplea et al., 1994; Fuzessery et al., 2003). Neural FSLs also decreased with increasing stimulus amplitude (Table 3.3; Heil, 2004; Tan et al., 2008). We found no correlation between neuronal BEFs and spike count recovery times at either +10 dB or +20 dB (re threshold). This result differs from a previous study that found a strong negative correlation between these variables in the IC of the bat (Zhou and Jen, 2003). Gross electrode recordings from the bat's auditory brainstem revealed that stimulation with higher acoustic frequencies resulted in faster response recovery (Grinnell, 1963). Given that FSL is also negatively correlated with BEF (Fig. 3.3; Haplea et al., 1994; Fuzessery et al., 2003), if a negative correlation exists between BEF and spike count recovery time then we might expect a similar correlation between FSL and spike count recovery time. In the present study, we were unable to detect a correlation between BEF and the spike count recovery time at

either level above threshold. Therefore, the positive relationship that we observed between spike count recovery time and FSL cannot be explained by a covariance with BEF.

Some studies have used pairs of unequal amplitude tones to determine the recovery cycle characteristics of IC neurons. For example, Friend et al. (1966) found that recovery times shortened as the intensity of stimulus P1 was decreased relative to P2. This result is consistent with the hypothesis that inhibition evoked by P1 was easier to overcome by increased excitation evoked by the relatively higher intensity P2 stimulus. Moreover, the effect of stimulus amplitude on spike count recovery times co-varies with stimulus duration (Wang et al., 2008, 2010). Using gross electrode recordings in the bat brainstem in response to equal amplitude tones, Grinnell (1963) reported more rapid neural recovery for stimuli of reduced intensity—a finding that is opposite to our results. In the present study, recovery times in the population of DTNs and non-DTNs remained stable over a 10 dB change in SPL in response to pairs of equal amplitude tones (Tables 3.2-3.4); however, when we restricted our analysis to look only at those cells with recovery times measured with spike count and latency criteria, recovery times shortened from +10 to +20 dB (re threshold) regardless of the recovery parameter examined (Table 3.5). This suggests that neural excitation may have increased relative to inhibition at higher levels above threshold. Additional studies employing a wider range of stimulus amplitudes are needed to determine if the recovery times of DTNs are tolerant over the same dynamic range (40-50 dB) as the amplitude tolerance of duration tuning (Zhou and Jen, 2001; Fremouw et al., 2005).

3.5.3 Spatial mapping of best duration

We found no correlation between neuronal BD and the depth of the recording electrode in the population of DTNs tested (Fig. 3.2). This result agrees with a number of previous studies that found no spatial organization of DTNs in the ICc of the bat (Pinheiro et al., 1991; Ehrlich et al., 1997; Faure et al., 2003; Luo et al., 2008). In contrast, other studies

have reported a significant positive correlation between BD and BEF (Jen and Wu, 2006; Wu and Jen, 2006, 2008b), suggesting the possibility that the ICc of the bat contains a spatial map of duration tuning. In the present study, we found a significant negative correlation between BD and BEF (Fig. 3.2)—a relationship in the opposite direction of three previous reports. Given the inconsistency of the result within and across laboratories, we conclude there is no strong evidence to support the hypothesis that a spatial map of duration tuning exists in the IC of the bat.

3.5.4 Biological significance of recovery times

Recovery cycle times of IC neurons in the cat (Yin, 1994; Litovsky and Yin, 1998a,b), rabbit (Fitzpatrick et al., 1995, 1999) and barn owl (Keller and Takahashi, 1996) have been suggested as a potential neural mechanism underlying the precedence effect for humans listening in reverberant environments (for review, see Litovsky et al., 1999). The precedence effect is a binaural psychoacoustical phenomenon that describes the sound localization performance of participants listening to pairs of sounds separated by an interval (e.g. pulse and reflected echo). When two sounds have a brief IPI ($<$1 ms; Wallach et al., 1949), participants detect a single sound located in a position midway between the sources (i.e., summing localization). When two sounds are presented with a longer delay (1-5 ms IPI for single clicks; $\leq$35-70 ms IPI for other complex sounds; Wallach et al., 1949), participants localize the source in the direction of the first sound. Because the first arriving wavefront takes precedence in sound localization, the precedence effect is also known as the law of the first wavefront. Recovery cycle times measured from auditory neurons in the ICc of the bat (Tables 3.2-3.4) broadly correlate with the range of IPIs over which the precedence effect occurs in humans. A behavioural correlate of the precedence effect has been studied in cats (3-16 ms; Cranford and Oberholtzer, 1976), rats (0.25-16 ms; Kelly, 1974), and crickets (4-75 ms; Wyttenbach and Hoy, 1993). While it seems reasonable to assume that

echolocating bats also experience a precedence effect during acoustic orientation and prey detection, psychoacoustical experiments on two species of gleaning bats suggest they may not (Schuchmann et al., 2006).

Our results demonstrate that recovery cycle times of midbrain auditory neurons in the bat, which have been explored mainly in the context of echolocation (for review, see Jen et al., 2012), are quite similar to those measured from the IC of other vertebrates (Yin, 1994; Fitzpatrick et al., 1995; Keller and Takahashi, 1996). This suggests that factors governing the recovery cycle times of central auditory neurons are similar in echolocating and non-echolocating species. It also reinforces the utility of bats as an animal model for understanding general principles of mammalian hearing and auditory physiology despite the fact that bats echolocate and are "hearing specialists". The function(s) of DTNs to hearing and echolocation is(are) still unknown; however, the range of neural BDs and the temporal bandwidth of duration tuning are generally matched to the range of vocalization durations in echolocating bats (Sayegh et al., 2011). If DTNs play a direct role in echolocation, then one might predict they should exhibit short recovery times so that the same neuron could respond to both loud outgoing vocalizations and later returning echoes. Alternatively, owing to the importance of leading and persistent inhibition in creating temporally selective neural responses, one could also predict that the inhibition evoked by each pulse in a paired tone stimulus would temporally interact and sum, resulting in DTNs exhibiting longer recovery cycle times than non-DTNs. Our results support the latter prediction: bandpass DTNs had significantly longer recovery times than shortpass DTNs and allpass neurons. In contrast, a recent study examining auditory neurons in the IC of the echolocating bat *Pipistrellus abramus* found no significant difference in the recovery times of DTNs and allpass neurons (Wang et al., 2010).

If DTNs function in echo ranging, then the recovery cycle time would play an important role in determining the minimum target distance over which a neuron could respond. The

recovery time can be viewed as equivalent to the two-way travel time of the bat's outgoing sound and returning echo. Assuming a recovery cycle time for a DTN of 36 ms, this would be equivalent to a one-way travel time of 18 ms (speed of sound in air = 344 mm/ms) and would correspond to a target distance of 6.19 m (344 mm/ms*18 ms). Neurons with shorter (longer) recovery cycles would have shorter (longer) minimum target detection distances because these cells could respond more rapidly (slowly) to successive sound presentations such as pulse-echo pairs. For example, a neuron with a recovery time of 2 ms could fire action potentials in response to both the pulse and echo at a minimum distance of 34.4 cm (344 mm/ms*1 ms), whereas a neuron with a recovery time of 100 ms could encode a minimum target distance of 17.2 m (344 mm/ms*50 ms).

In theory, the recovery time of a DTN, in combination with BD, could determine perceptual integration time and cause a cell to be tuned to detect small pulse-echo delays and short target distances. For example, assume a bandpass DTN with a BD of 5 ms is stimulated with pulse and echo biosonar sounds lasting 2 ms each. Although the cell may not spike in response to either the pulse (P1) or the echo (P2) when presented alone, simply because the durations of both signals are shorter than the cell's BD, the neuron might respond to the stimulus pair if presented at a short IPI of 1 ms representing a target at 17.2 cm (344 mm/ms*0.5 ms). In this case, the DTN may respond to the pulse-echo pair as a single, unified (i.e. fused) stimulus because the combined 2 ms pulse + 1 ms gap + 2 ms echo duration is close to the neuronal BD (Sayegh et al., 2011). By extending this line of reasoning we would predict that neurons with short BDs would be tuned to short target distances, and neurons with longer BDs would be tuned to longer target distances. This is because cells with long BDs may be able to tolerate a wider range of silence between pulse-echo pairs at sub-optimal durations. In support of this novel hypothesis, which is distinct but not mutually exclusive from the idea that DTNs are tuned to the duration of single relevant sounds, we found a weak but positive correlation between stimulus duration and

spike count recovery time at +20 dB above threshold (Fig. 3.9B), but there was no correlation between stimulus duration and spike latency recovery times. Grinnell (1963) observed an increase in recovery time as the duration of the P1 (but not P2) stimulus increased. Jen et al. (2012) reported that spike count recovery times of DTNs increased with the duration of the pulse-echo stimulus; however, this effect does not hold for equal amplitude stimulus pairs and occurs only in some neurons at specific pulse-echo amplitude differences (Wang et al., 2008). In contrast, Pollak et al. (1977a) found recovery times of IC auditory neurons increased at short (<2 ms) stimulus durations. These conflicting reports point to the need for future studies to test the hypothesis that DTNs can respond to pairs of tones presented at sub-optimal durations (i.e. not at BD) and separated by relatively short gaps of silence.

In a small subset of cells we observed a brief facilitation in the spike count ratio of recovery function at short IPIs (Fig. 3.6C,D). These neurons could be delay-tuned combination-sensitive cells that respond best at short echo delays (O'Neill and Suga, 1982; Portfors and Wenstrup, 1999). The range of recovery times that we observed for both DTNs and non-DTNs in the ICc of *E. fuscus* nicely corresponds to the range of pulse-to-pulse intervals (repetition rates) used by foraging bats during the search (50-100 ms), approach (10-50 ms) and terminal feeding buzz (4-7 ms) phases of hunting (Griffin et al., 1960). The subset of DTNs with facilitatory responses at short IPIs may be especially well-suited for echolocation at short target distances.

3.5.5 Recovery cycles and neural inhibition

Faure et al. (2003) used paired tone stimulation to measure the onset and duration of the leading and persistent inhibition that creates DTNs in the IC of the bat. In that study, P1 was set to the neuron's BD and P2 was set to a longer, non-excitatory duration. In the present study, we used pairs of excitatory tones to measure and compare the recovery cycle times of DTNs with non-DTNs, and found that bandpass DTNs had significantly longer

recovery times than non-DTNs using spike count recovery and one measure of spike latency recovery. These results also highlight the importance of neural inhibition to duration tuning. Previous studies have suggested that the strength and time course of GABAergic inhibition can account for some variation in the recovery cycles of DTNs. Blocking GABAergic inhibition with bicucculine shortened recovery times in a majority of IC cells (Lu et al., 1997; Zhou and Jen, 2003). Presenting stimuli that mimicked pulse-echo pairs at short IPIs also sharpened duration-selectivity (Wu and Jen, 2006; Jen and Wu, 2008) and frequency-selectivity (Wu and Jen, 2008a,b); in the latter two examples, the sharpening of the response evoked by the "echo" was thought to have arisen from the recruitment and persistence of inhibition evoked by the "pulse".

During paired tone stimulation, if the inhibition evoked by stimulus P1 encroaches upon the excitation evoked by stimulus P2 then recovery times of cells with persistent inhibition are expected to be longer than in cells with less or no persistent inhibition. We might also expect FSLs (re signal onset) to increase because spikes evoked by P2 could be delayed by persistent inhibition evoked by P1. Meanwhile, neuronal LSLs (re P2) may largely be unaffected. In general, our results support the hypothesis that recovery cycle times are determined, at least in part, by the inhibition evoked by tone P1 that persists and influences the spiking responses evoked by tone P2. We also found that FSLs (re P2) were more likely to deviate by >1 SD from baseline than LSLs (re P2), a finding that is consistent with the effects of persistent inhibition.

Recovery times measured in IC neurons are on the order of tens of milliseconds and therefore cannot be due to a neuron's absolute and/or relative refractory periods caused by post-spiking increases in potassium permeability and inactivation of sodium channels because these effects typically last only a few milliseconds (Hodgkin, 1951; Hodgkin and Huxley, 1952). Stimulus repetition rate can also affect the measurement of recovery times. In the ICc of the bat, increasing stimulus repetition rate increases the observed FSL and

minimum threshold (Jen and Chen, 1998), increases directional selectivity (Zhou and Jen, 2004), and alters duration selectivity (Jen and Zhou, 1999; Jen and Wu, 2005; Zhou and Jen, 2006). In theory, increasing the stimulus repetition rate increases the recovery cycle time of a neuron because persistent inhibition evoked by one stimulus trial influences responses evoked on the subsequent trial. In our study, stimulus repetition rate cannot explain differences in the recovery cycle times between DTNs and non-DTNs because all of the data were collected at the same rate (3 Hz). We believe that differences in the recovery times between DTNs and non-DTNs were caused, in part, by inhibition lasting longer than the duration of the P1 tone that evoked it. This persistent inhibition would sum with the leading inhibition evoked by tone P2, resulting in DTNs exhibiting longer recovery times than a random selection of other types of IC neurons not tuned to stimulus duration. Other factors can also affect neural recovery times, including the length of the axons that provide synaptic input (axonal delay; Smith et al., 1993), the time course of temporal facilitation and depression of excitatory and inhibitory synapses (e.g. neurotransmitter depletion; Zucker and Regehr, 2002), receptor desensitization (Raman and Trussell, 1992; Raman et al., 1994), presynaptic modulation of inhibition via intracellular calcium accumulation (Lu and Trussell, 2000) and/or $GABA_B$ receptors (Ma et al., 2002), and intrinsic cellular properties such as subthreshold sound-evoked oscillations (Hechavarría et al., 2011). Additional studies are needed to shed light on the mechanisms that shape and govern the recovery cycle times of mammalian central auditory neurons.

3.6 Summary

1. Spike counts are traditionally used to measure the recovery cycle times of neurons. Herein we demonstrate that spike latencies may also be used to measure response recovery. In general, recovery times measured with spike counts were positively cor-

related with recovery times measured with spike latencies, although recovery times measured with a 1 SD change in LSL (re baseline latency) were significantly shorter than recovery times measured with a 50% change in spike count (re baseline count) or with a 1 SD change in FSL (re baseline latency).

2. Previous studies have shown that neural inhibition is necessary for creating DTNs in the IC of the bat. Because DTNs are known to have inhibition that persists for as long or longer than the duration of the stimulus evoking the inhibition, we predicted that DTNs would have longer recovery times than non-DTNs. Recovery times of bandpass DTNs obtained with spike counts and one measure of FSL recovery were longer than recovery times of shortpass DTNs and non-DTNs.

3. Increasing the amplitude of the paired tone stimulus from +10 to +20 dB (re threshold) did not shorten recovery times in the population of cells tested, indicating that recovery kinetics of IC neurons in the bat are tolerant to a +10 dB change in stimulus amplitude. When we restricted our analysis to the subset of neurons that provided recovery time values measured with spike counts, FSLs, and LSLs, we found that increasing stimulus amplitude shortened recovery times in the same cells. Additional studies employing a wider range of stimulus levels are needed to fully characterize the effect of stimulus amplitude on the recovery times of IC neurons.

4. Neurons with short FSLs had shorter recovery times than cells with longer FSLs. Inhibition is an important determinant of the recovery cycle time and FSL of DTNs and non-DTNs. Our results demonstrate that the neural mechanisms controlling FSL and recovery cycle kinetics may be related.

References

Aubie, B., Becker, S., and Faure, P. A. (2009). Computational models of millisecond level duration tuning in neural circuits. *J. Neurosci.* 29, 9255–9270.

Aubie, B., Sayegh, R., and Faure, P. A. (2012). Duration tuning across vertebrates. *J. Neurosci.* 32, 6373–6390.

Brand, A., Urban, A., and Grothe, B. (2000). Duration tuning in the mouse auditory midbrain. *J. Neurophysiol.* 84, 1790–1799.

Brugge, J. F., Reale, R. A., Jenison, R. L., and Schnupp, J. (2001). Auditory cortical spatial receptive fields. *Audiol. Neurootol.* 6, 173–177.

Carr, C. E., and Konishi, M. (1990). A circuit for detection of interaural time differences in the brain stem of the barn owl. *J. Neurosci.* 10, 3227–3246.

Casseday, J. H., Ehrlich, D., and Covey, E. (1994). Neural tuning for sound duration: role of inhibitory mechanisms in the inferior colliculus. *Science* 264, 847–850.

Casseday, J. H., Ehrlich, D., and Covey, E. (2000). Neural measurement of sound duration: control by excitatory-inhibitory interactions in the inferior colliculus. *J. Neurophysiol.* 84, 1475–1487.

Chen, G-D. (1998). Effects of stimulus duration on responses of neurons in the chinchilla inferior colliculus. *Hearing Res.* 112, 142–150.

Covey, E., Kauer, J. A., and Casseday, J. H. (1996). Whole-cell patch-clamp recording reveals subthreshold sound-evoked postsynaptic currents in the inferior colliculus of awake bats. *J. Neurosci.* 16, 3009–3018.

Cranford, J. L., and Oberholtzer, M. (1976). Role of neocortex in binaural hearing in the cat. II. The 'precedence effect' in sound localization. *Brain Res.* 111, 225–239.

Denes, P. (1955). Effect of duration on the perception of voicing. *J. Acoust. Soc. Am.* 27, 761–764.

Duysens, J., Schaafsma, S. J., and Orban, G. A. (1996). Cortical off response tuning for stimulus duration. *Vision Res.* 36, 3243–3251.

Ehrlich, D., Casseday, J. H., and Covey, E. (1997). Neural tuning to sound duration in the inferior colliculus of the big brown bat, *Eptesicus fuscus*. *J. Neurophysiol.* 77, 2360–2372.

Faingold, C. L., Boersma Anderson, C. A., and Caspary, D. M. (1991) Involvement of GABA in acoustically-evoked inhibition in inferior colliculus neurons. *Hearing Res.* 52, 201–216.

Faure, P. A., Fremouw, T., Casseday, J. H., and Covey, E. (2003). Temporal masking reveals properties of sound-evoked inhibition in duration-tuned neurons of the inferior colliculus. *J. Neurosci.* 23, 3052–3065.

Faure, P. A., Re, D. E., and Clare, E. L. (2009). Wound healing in the flight membranes of big brown bats. *J. Mammal.* 90, 1148–1156.

Fitzpatrick, D. C., Kuwada, S., Batra, R., and Trahiotis, C. (1995). Neural responses to simple simulated echoes in the auditory brain stem of the unanesthetized rabbit. *J. Neurophysiol.* 74, 2469–2486.

Fitzpatrick, D. C., Kuwada, S., Kim, D. O., Parham, K., and Batra, R. (1999). Responses of neurons to click-pairs as simulated echoes: auditory nerve to auditory cortex. *J. Acoust. Soc. Am.* 106, 3460–3472.

Fontaine, B., and Peremans, H. (2009). Bat echolocation processing using first-spike latency coding. *Neural Networks* 22, 1372–1382.

Frederiksen, E. (1977). Condenser microphones used as sound sources. *Brüel & Kjær Tech. Rev.* 3, 3–23.

Fremouw, T., Faure, P. A., Casseday, J. H., and Covey, E. (2005). Duration selectivity of neurons in the inferior colliculus of the big brown bat: tolerance to changes in sound level. *J. Neurophysiol.* 94, 1869–1878.

Friend, J. H., Suga, N., and Suthers, R. A. (1966). Neural responses in the inferior colliculus of echolocating bats to artificial orientation sounds and echoes. *J. Cell. Physiol.* 67, 319–332.

Furukawa, S., and Middlebrooks, J. C. (2002). Cortical representation of auditory space: information-bearing features of spike patterns. *J. Neurophysiol.* 87, 1749–1762.

Fuzessery, Z. M., and Hall, J. C. (1999). Sound duration selectivity in the pallid bat inferior colliculus. *Hearing Res.* 137, 137–154.

Fuzessery, Z. M., Wenstrup, J. J., Hall, J. C., and Leroy, S. (2003). Inhibition has little effect on response latencies in the inferior colliculus. *JARO* 4, 60–73.

Gooler, D. M., and Feng, A. S. (1992). Temporal coding in the frog auditory midbrain: the influence of duration and rise-fall time on the processing of complex amplitude-modulated stimuli. *J. Neurophysiol.* 67, 1–22.

Griffin, D. R., Webster, F. A., and Michael, C. R. (1960). The echolocation of flying insects by bats. *Anim. Behav.* 8, 141–154.

Grinnell, A. D. (1963). The neurophysiology of audition in bats: temporal parameters. *J. Physiol.* 167, 67–96.

Grothe, B., and Klump, G. M. (2000). Temporal processing in sensory systems. *Curr. Opin. Neurobiol.* 10, 467–473.

Haplea, S., Covey, E., and Casseday, J. H. (1994). Frequency tuning and response latencies at three levels in the brainstem of the echolocating bat, *Eptesicus fuscus*. *J. Comp. Physiol., A* 174, 671–683.

He, J., Hashikawa, T., Ojima, H., and Kinouchi, Y. (1997). Temporal integration and duration tuning in the dorsal zone of cat auditory cortex. *J. Neurosci.* 17, 2615–2625.

Hechavarría, J. C., Cobo, A. T., Fernández, Y., Macías, S., Kössl, M., and Mora, E. C. (2011). Sound-evoked oscillation and paradoxical latency shift in the inferior colliculus of the big fruit-eating bat, *Artibeus jamaicensis*. *J. Comp. Physiol., A* 197, 1159–1172.

Heil, P. (2004). First-spike latency of auditory neurons revisited. *Curr. Opin. Neurobiol.* 14, 461–467.

Hodgkin, A. L. (1951). The ionic basis of electrical activity in nerve and muscle. *Biol. Rev.* 26, 339–409.

Hodgkin, A. L., and Huxley, A. F. (1952). A quantitative description of membrane current and its application to conduction and excitation in nerve. *J. Physiol.* 117, 500–544.

Hurley, L. M., and Pollak, G. D. (2005). Serotonin shifts first-spike latencies of inferior colliculus neurons. *J. Neurosci.* 25, 7876–7886.

Jen, P. H.-S., and Chen, Q.-C. (1998). The effect of pulse repetition rate, pulse intensity, and bicuculline on the minimum threshold and latency of bat inferior collicular neurons. *J. Comp. Physiol., A* 182, 455–465.

Jen, P. H.-S., and Feng, R. B. (1999). Bicuculline application affects discharge pattern and pulse-duration tuning characteristics of bat inferior collicular neurons. *J. Comp. Physiol., A* 184, 185–194.

Jen, P. H.-S., and Schlegel, P. A. (1982). Auditory physiological properties of the neurones in the inferior colliculus of the big brown bat, *Eptesicus fuscus*. *J. Comp. Physiol., A* 147, 351–363.

Jen, P. H.-S., and Wu, C. H. (2005). The role of GABAergic inhibition in shaping the response size and duration selectivity of bat inferior collicular neurons to sound pulses in rapid sequences. *Hearing Res.* 202, 222–234.

Jen, P. H.-S., and Wu, C. H. (2006). Duration selectivity organization in the inferior colliculus of the big brown bat, *Eptesicus fuscus*. *Brain Res.* 1108, 76–87.

Jen, P. H.-S., and Wu, C. H. (2008). Echo duration selectivity of the bat varies with pulse-echo amplitude difference. *Neuroreport* 19, 373–377.

Jen, P. H.-S., Wu, C. H., and Wang, X. (2012). Dynamic temporal signal processing in the inferior colliculus of echolocating bats. *Front. Neural Circuits* 6, 27.

Jen, P. H.-S., and Zhou, X. M. (1999). Temporally patterned pulse trains affect duration tuning characteristics of bat inferior collicular neurons. *J. Comp. Physiol., A* 185, 471–478.

Joris P. X., Smith, P. H., and Yin, T. C. T. (1998). Coincidence detection in the auditory system: 50 years after Jeffress. *Neuron* 21, 1235–1238.

Keller, C. H., and Takahashi, T. T. (1996). Responses to simulated echoes by neurons in the barn owl's auditory space map. *J. Comp. Physiol., A* 178, 499–512.

Kelly, J. B. (1974) Localization of paired sound sources in the rat: small time differences. *J. Acoust. Soc. Am.* 55, 1277–1284.

Klug, A., Bauer, E. E., and Pollak, G. D. (1999). Multiple components of ipsilaterally evoked inhibition in the inferior colliculus. *J. Neurophysiol.* 82, 593–610.

Klug, A., Khan, A., Burger, R. M., Bauer, E. E., Hurley, L. M., Yang, L., Grothe, B., Halvorsen, M. B., and Park, T. J. (2000). Latency as a function of intensity in auditory neurons: influences of central processing. *Hearing Res.* 148, 107–123.

Knudsen, E. I., and Konishi, M. (1979). Mechanisms of sound localization in the barn owl (*Tyto alba*). *J. Comp. Physiol., A* 133, 13–21.

Kuwada, S., Batra, R., Yin T. C. T., Oliver, D. L., Haberly, L. B., and Stanford T. R. (1997). Intracellular recordings in response to monaural and binaural stimulation of neurons in the inferior colliculus of the cat. *J. Neurosci.* 17, 7565–7581.

Leary, C. J., Edwards, C. J., and Rose, G. J. (2008). Midbrain auditory neurons integrate excitation and inhibition to generate duration selectivity: an *in vivo* whole-cell patch study in anurans. *J. Neurosci.* 28, 5481–5493.

Litovsky, R. Y., Colburn, H. S., Yost, W. A., and Guzman S. J. (1999). The precedence effect. *J. Acoust. Soc. Am.* 106, 1633–1654.

Litovsky, R. Y., and Delgutte, B. (2002). Neural correlates of the precedence effect in the inferior colliculus: effect of localization cues. *J. Neurophysiol.* 87, 976–994.

Litovsky, R. Y., and Yin, T. C. T. (1998a). Physiological studies of the precedence effect in the inferior colliculus of the cat. I. Correlates of psychophysics. *J. Neurophysiol.* 80, 1285–1301.

Litovsky, R. Y., and Yin, T. C. T. (1998b). Physiological studies of the precedence effect in the inferior colliculus of the cat. II. Neural mechanisms. *J. Neurophysiol.* 80, 1302–1316.

Lu, T., and Trussell, L. O. (2000). Inhibitory transmission mediated by asynchronous transmitter release. *Neuron* 26, 683–694.

Lu, Y., Jen, P. H.-S., and Zheng, Q.-Y. (1997). GABAergic disinhibition changes the recovery cycle of bat inferior collicular neurons. *J. Comp. Physiol., A* 181, 331–341.

Luo, F., Metzner, W., Wu, F. J., Zhang, S. Y., and Chen, Q. C. (2008). Duration-sensitive neurons in the inferior colliculus of horseshoe bats: adaptations for using CF-FM echolocation pulses. *J. Neurophysiol.* 99, 284–296.

Ma, C. L., Kelly, J. B., and Wu, S. H. (2002). Presynaptic modulation of GABAergic inhibition by $GABA_B$ receptors in the rat's inferior colliculus. *Neuroscience* 114, 207–215.

Middlebrooks, J. C., Clock, A. E., Xu, L., and Green, D. M. (1994). A panoramic code for sound location by cortical neurons. *Science* 264, 842–844.

Mora, E. C., and Kössl, M. (2004). Ambiguities in sound duration selectivity by neurons in the inferior colliculus of the bat *Molossus molossus* from Cuba. *J. Neurophysiol.* 91, 2215–2226.

Nelken, I., Chechik, G., Mrsic-Flogel, T. D., King, A. J., and Schnupp, J. W. H. (2005). Encoding stimulus information by spike numbers and mean response time in primary auditory cortex *J. Comput. Neurosci.* 19, 199–221.

O'Neill, W. E., and Suga, N. (1982). Encoding of target range and its representation in the auditory cortex of the mustached bat. *J. Neurosci.* 2, 17–31.

Park, T. J., and Pollak, G. D. (1993). GABA shapes a topographic organization of response latency in the mustache bat's inferior colliculus. *J. Neurosci.* 13, 5172–5187.

Pedemonte, M., Torterolo, P., and Velluti, R. A. (1997). In vivo intracellular characteristics of inferior colliculus neurons in guinea pigs. *Brain Res.* 759, 24–31.

Pérez-González, D., Malmierca, M. S., Moore, J. M., Hernández, O., and Covey, E. (2006). Duration selective neurons in the inferior colliculus of the rat: topographic distribution and relation of duration sensitivity to other response properties. *J. Neurophysiol.* 95, 823–836.

Pinheiro, A. D., Wu, M., and Jen, P. H.-S. (1991). Encoding repetition rate and duration in the inferior colliculus of the big brown bat, *Eptesicus fuscus*. *J. Comp. Physiol., A* 169, 69–85.

Pinheiro, J. C., and Bates, D. M. (2000). *Mixed-effects models in S and S-PLUS*. Springer Verlag.

Pollack, G. S., and Hoy, R. R. (1979). Temporal pattern as a cue for species-specific calling song recognition in crickets. *Science* 204, 429–432.

Pollak, G. D., Bodenhamer, R., Marsh, D. S., and Souther, A. (1977a). Recovery cycles of single neurons in the inferior colliculus of unanesthetized bats obtained with frequency-modulated and constant-frequency sounds. *J. Comp. Physiol., A* 120, 215–250.

Pollak, G. D., Marsh, D. S., Bodenhamer, R., Souther, A. (1977b). Characteristics of phasic on neurons in inferior colliculus of unanesthetized bats with observations relating to mechanisms for echo ranging. *J. Neurophysiol.* 40, 926–942.

Pollak, G. D., and Park, T. J. (1993). The effects of GABAergic inhibition on monaural

response properties of neurons in the mustache bat's inferior colliculus. *Hearing Res.* 65, 99–117.

Portfors, C. V., and Wenstrup, J. J. (1999). Delay-tuned neurons in the inferior colliculus of the mustached bat: implications for analyses of target distance. *J. Neurophysiol.* 82, 1326–1338.

Potter, H. D. (1965). Patterns of acoustically evoked discharges of neurons in the mesencephalon of the bullfrog. *J. Neurophysiol.* 28, 1155–1184.

Raman, I. M., and Trussell, L. O. (1992). The kinetics of the response to glutamate and kainate in neurons of the avian cochlear nucleus. *Neuron* 9, 173–186.

Raman, I. M., Zhang, S., and Trussell, L. O. (1994). Pathway-specific variants of AMPA receptors and their contribution to neuronal signaling. *J. Neurosci.* 14, 4998–5010.

Sayegh, R., Aubie, B., and Faure, P. A. (2011). Duration tuning in the auditory midbrain of echolocating and non-echolocating vertebrates. *J. Comp. Physiol., A* 197, 571–583.

Schuchmann, M., Hübner, M., and Wiegrebe, L. (2006). The absence of spatial echo suppression in the echolocating bats *Megaderma lyra* and *Phyllostomus discolor*. *J. Exp. Biol.* 209, 152–157.

Simmons, J. A. (1971). Echolocation in bats: signal processing of echoes for target range. *Science* 171, 925–928.

Simmons, J. A. (1979). Perception of echo phase information in bat sonar. *Science* 204, 1336–1338.

Smith, P. H., Joris, P. X., and Yin, T. C. T. (1993). Projections of physiologically characterized spherical bushy cell axons from the cochlear nucleus of the cat: evidence for delay lines to the medial superior olive. *J. Comp. Neurol.* 331, 245–260.

Stapells, D. R., Picton, T. W., Smith, A. D. (1982). Normal hearing thresholds for clicks. *J. Acoust. Soc. Am.* 72, 74–79.

Suga, N. (1964). Recovery cycles and responses to frequency modulated tone pulses in auditory neurones of echo-locating bats. *J. Physiol.* 175, 50–80.

Suga, N., and O'Neill, W. E. (1979). Neural axis representing target range in the auditory cortex of the mustache bat. *Science* 206, 351–353.

Suga, N., and Schlegel, P. (1973). Coding and processing in the auditory systems of FM-signal-producing bats. *J. Acoust. Soc. Am.* 54, 174–190.

Tan, M. L., and Borst, J. G. G. (2007). Comparison of responses of neurons in the mouse inferior colliculus to current injections, tones of different durations, and sinusoidal amplitude-modulated tones. *J. Neurophysiol.* 98, 454–466.

Tan, X., Wang, X., Yang, W., and Xiao, Z. (2008). First spike latency and spike count as functions of tone amplitude and frequency in the inferior colliculus of mice. *Hearing Res.* 235, 90–104.

Tang, J., Fu, Z.-Y., Jen, P. H.-S., Chen, Q.-C. (2011). Recovery cycles of single-on and double-on neurons in the inferior colliculus of the leaf-nosed bat, *Hipposideros armiger*. *Brain Res.* 1385, 114–126.

Torterolo, P., Pedemonte, M., and Velluti, R. A. (1995). Intracellular *in vivo* recording of inferior colliculus auditory neurons from awake guinea-pigs. *Arch. Ital. Biol.* 134, 57–64.

VanRullen, R., Guyonneau, R., and Thorpe, S. J. (2005). Spike times make sense. *Trends Neurosci.* 28, 1–4.

Voytenko, S. V., and Galazyuk, A. V. (2008). Timing of sound-evoked potentials and spike responses in the inferior colliculus of awake bats. *Neuroscience* 155, 923–936.

Wallach, H., Newman, E. B., and Rosenzweig M. R. (1949). The precedence effect in sound localization. *Am. J. Psychol.* 62, 315–336.

Wang, J., van Wijhe, R., Chen, Z., and Yin, S. (2006). Is duration tuning a transient process in the inferior colliculus of guinea pigs? *Brain Res.* 1114, 63–74.

Wang, X., Luo, F., Jen, P. H.-S., and Chen, Q.-C. (2010). Recovery cycle of neurons in the inferior colliculus of the FM bat determined with varied pulse-echo duration and amplitude. *Chinese J. Physiol.* 53, 119–129.

Wang, X., Luo, F., Wu, F.-J., Chen, Q.-C., and Jen, P. H. S. (2008). The recovery cycle of bat duration-selective collicular neurons varies with hunting phase. *Neuroreport* 19, 861–865.

Wu, C. H., and Jen, P. H.S. (2006). GABA-mediated echo duration selectivity of inferior collicular neurons of *Eptesicus fuscus*, determined with single pulses and pulse-echo pairs. *J. Comp. Physiol., A* 192, 985–1002.

Wu, C. H., and Jen, P. H.-S. (2008a). Auditory frequency selectivity is better for expected than for unexpected sound duration. *Neuroreport* 19, 127–131.

Wu, C. H., and Jen, P. H.-S. (2008b). Echo frequency selectivity of duration-tuned inferior collicular neurons of the big brown bat, *Eptesicus fuscus*, determined with pulse-echo pairs. *Neuroscience* 156, 1028–1038.

Wyttenbach, R. A., and Hoy, R. R. (1993). Demonstration of the precedence effect in an insect. *J. Acoust. Soc. Am.* 94, 777–784.

Xia, Y.-F., Qi, Z.-H., and Shen, J.-X. (2000). Neural representation of sound duration in the inferior colliculus of the mouse. *Acta Otolaryngol.* 120, 638–643.

Yin, T. C. T. (1994). Physiological correlates of the precedence effect and summing localization in the inferior colliculus of the cat. *J. Neurosci.* 14, 5170–5186.

Zhou, X., and Jen, P. H.-S. (2001). The effect of sound intensity on duration-tuning characteristics of bat inferior collicular neurons. *J. Comp. Physiol., A* 187, 63–73.

Zhou, X., and Jen, P. H.-S. (2003). The effect of bicuculline application on azimuth-dependent recovery cycle of inferior collicular neurons of the big brown bat, *Eptesicus fuscus*. *Brain Res.* 973, 131–141.

Zhou, X., and Jen, P. H.-S. (2004). Azimuth-dependent recovery cycle affects directional selectivity of bat inferior collicular neurons determined with sound pulses within a pulse train. *Brain Res.* 1019, 281–288.

Zhou, X., and Jen, P. H.-S. (2006). Duration selectivity of bat inferior collicular neurons improves with increasing pulse repetition rate. *Chinese J. Physiol.* 49, 46–55.

Zucker, R. S., and Regehr, W. G. (2002). Short-term synaptic plasticity. *Annu. Rev. Physiol.* 64, 355–405.

Table 3.1: Mean ± SE first- and last-spike latency as a function of cell type and level above threshold. The average baseline R1 latency at +10 and +20 dB (re threshold) was used as the input for each cell.

Cell Type	n	Spike Latency (ms) +10 dB	n	Spike Latency (ms) +20 dB
First-spike Latency				
Allpass	39	15.42 ± 0.98	32	13.20 ± 0.96
Bandpass	18	18.33 ± 1.30	13	16.86 ± 1.28
Shortpass	16	14.32 ± 1.57	14	12.76 ± 1.24
Last-spike Latency				
Allpass	39	20.37 ± 1.43	32	18.42 ± 1.58
Bandpass	18	21.34 ± 1.75	13	20.71 ± 1.79
Shortpass	16	19.57 ± 2.49	14	16.00 ± 2.08

Table 3.2: Mean ± SE spike count recovery time (and range) as a function of cell type and level above threshold measured with the short-to-long and long-to-short analysis methods. Recovery measured as the IPI where the spike count in response to P2 was ≥50% of the baseline spike count (re P1).

Cell Type	n	Recovery Time (ms) +10 dB	n	Recovery Time (ms) +20 dB
Short-to-Long Method				
Allpass	39	20.13 ± 2.93 (2-100)	32	17.50 ± 2.14 (0-54)
Bandpass	18	34.83 ± 5.82 (10-105)	13	23.54 ± 3.23 (6-42)
Shortpass	16	23.00 ± 3.81 (2-54)	14	18.79 ± 3.87 (2-54)
Long-to-Short Method				
Allpass	39	25.97 ± 4.05 (0-148)	32	20.91 ± 3.17 (0-76)
Bandpass	18	36.94 ± 5.64 (10-105)	13	26.15 ± 3.70 (6-44)
Shortpass	16	25.75 ± 4.49 (2-68)	14	20.21 ± 4.00 (2-50)

Table 3.3: Mean ± SE first-spike latency (FSL) recovery time (and range) as a function of cell type and level above threshold, measured with the short-to-long and long-to-short analysis methods. Recovery time measured as the IPI where the FSL in response to P2 returned to within 1 SD of the baseline FSL (re P1).

Cell Type	n	Recovery Time (ms) +10 dB	n	Recovery Time (ms) +20 dB
Short-to-Long Method				
Allpass	36	20.64 ± 2.35 (4-58)	28	17.50 ± 2.05 (5-42)
Bandpass	17	23.65 ± 4.26 (2-66)	13	23.08 ± 5.36 (4-68)
Shortpass	16	21.56 ± 3.85 (4-50)	14	26.71 ± 6.40 (4-80)
Long-to-Short Method				
Allpass	29	23.52 ± 2.76 (8-60)	21	23.48 ± 2.52 (8-52)
Bandpass	14	41.14 ± 7.35 (10-110)	11	26.00 ± 5.67 (8-64)
Shortpass	14	34.50 ± 5.62 (10-70)	12	33.83 ± 6.76 (6-72)

Table 3.4: Mean ± SE last-spike latency (LSL) recovery time (and range) as a function of cell type and level above threshold, measured with the short-to-long and long-to-short analysis methods. Recovery time measured as the IPI where the LSL in response to P2 returned to within 1 SD of the baseline LSL (re P1).

Cell Type	n	Recovery Time (ms) +10 dB	n	Recovery Time (ms) +20 dB
Short-to-Long Method				
Allpass	20	13.65 ± 1.90 (4-45)	15	11.33 ± 2.09 (2-34)
Bandpass	13	18.08 ± 3.29 (2-45)	9	17.33 ± 3.46 (4-40)
Shortpass	9	15.33 ± 3.74 (4-42)	9	13.11 ± 1.74 (6-20)
Long-to-Short Method				
Allpass	15	18.40 ± 4.29 (6-58)	7	21.29 ± 5.45 (10-52)
Bandpass	6	42.67 ± 14.82 (12-110)	7	20.57 ± 4.31 (4-40)
Shortpass	9	16.44 ± 3.75 (6-42)	7	14.29 ± 4.52 (6-40)

Table 3.5: Mean ± SE recovery times as a function of the measured recovery parameter and level above threshold. Only cells with recovery times measured with all three parameters were included (n = 42: +10 dB; n = 34: +20 dB).

Recovery Parameter	Recovery Time (ms) + 10 dB	Recovery Time (ms) + 20 dB
Spike Count	33.38 ± 3.83	22.88 ± 2.30
FSL	25.14 ± 2.64	21.74 ± 2.82
LSL	17.99 ± 2.05	13.91 ± 1.61

Figure 3.1 *(following page)*: Measuring recovery cycle times of IC neurons. (A) Dot raster display of an *in vivo* shortpass DTN in response to paired tone stimulation at varying IPIs. The *red bars* represent the onset, duration, and offset of the first tone pulse (P1), and the *blue bars* represent the onset, duration, and offset of the second tone pulse (P2). Stimuli P1 and P2 were set to the cell's BEF and, if duration-tuned, BD. The timing of action potentials are illustrated as *black dots*. We calculated the mean $\pm$ SD baseline FSL and baseline LSL in response to P1 over the 10 longest IPIs from the onset of P1 to the onset of P2. Baseline latencies were used to define the P1 and P2 analysis windows (*grey regions*) used for assigning spikes as being evoked by stimulus P1 or P2, and for calculating the Baseline Response R1. The P1 analysis window began at the onset of P1 + baseline FSL $-$ 2 SDs and ended at the onset of P1 + mean LSL + 2 SDs (re P1). The P2 analysis window began at the onset of P2 + baseline FSL $-$ 2 SDs and ended at the onset of P2 + mean LSL + 2 SDs (re P2), and was used to measure the responses evoked by P2 (Response R2). For trials where the P1 and P2 analysis windows overlapped, a single analysis window was defined starting from the onset of P1 + baseline FSL $-$ 2 SDs and ending at the onset of P2 + baseline LSL + 2 SDs. (B) Recovery times measured with spike count. The ordinate shows the spike count ratio of response (R2/Baseline R1) as a function of stimulus IPI. The *dotted line* at 0.5 represents the 50% spike count recovery threshold. The asterisk (*) at 12 ms illustrates the recovery time of the cell determined with the short-to-long method, and the dagger (†) at 40 ms represents the recovery time of the same cell determined with the long-to-short method. (C,D) Recovery times measured with spike latency. The *red line with closed symbols* represents spike latency (re P1), and the *blue line with open symbols* represents spike latency (re P2). The *dotted lines* represent $\pm$ 1 SD relative to the mean baseline FSL or baseline LSL (see A). (C) Mean FSL (re P1 and P2) as a function of IPI. The asterisk (*) at 70 ms illustrates the FSL recovery time measured with the short-to-long method, and the dagger (†) at 70 ms represents the FSL recovery time of the same cell determined with the long-to-short method. (D) Mean LSL (re P1 and P2) as a function of IPI. The asterisk (*) at 16 ms illustrates the LSL recovery time of the cell measured with the short-to-long method, and the dagger (†) at 40 ms represents the LSL recovery time of the same cell determined with the long-to-short method. In this example, FSL took longer to recover than LSL. MU044.04.09: BEF, 47 kHz; BD, 2 ms; threshold, 33.5 dB SPL; amplitude +20 dB re threshold; 20 repetitions per IPI step.

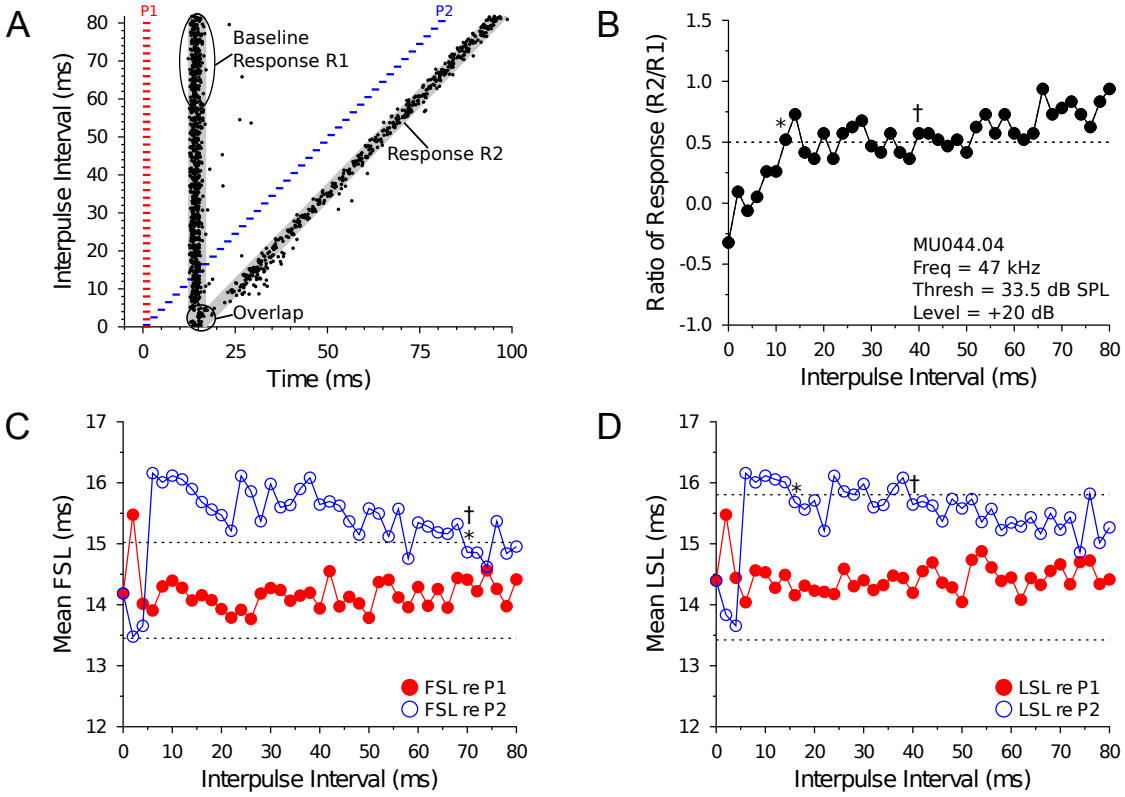
A
P1
P2
Baseline
Response R1
Response R2
Overlap
Interpulse Interval (ms)
Time (ms)
B
Ratio of Response (R2/R1)
MU044.04
Freq = 47 kHz
Thresh = 33.5 dB SPL
Level = +20 dB
Interpulse Interval (ms)
C
Mean FSL (ms)
FSL re P1
FSL re P2
Interpulse Interval (ms)
D
Mean LSL (ms)
LSL re P1
LSL re P2
Interpulse Interval (ms)

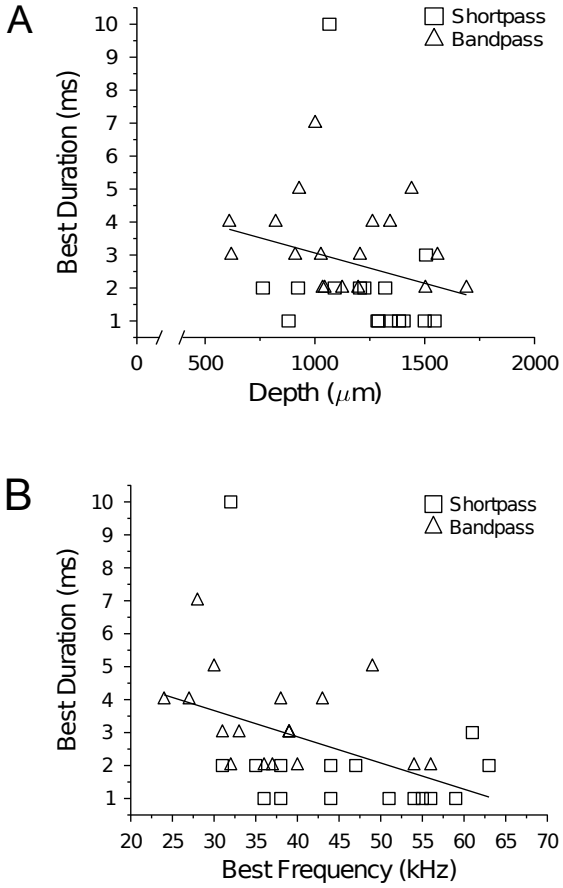

Figure 3.2: Temporal tuning and spatial topography or tonotopy in the IC. (A) There was no correlation between neuronal BD and the depth of the recording electrode (R^2=0.070, p=0.13). Note the broken abscissa. (B) There was a negative correlation between neuronal BD and BEF (R^2=0.20, p=0.0081).

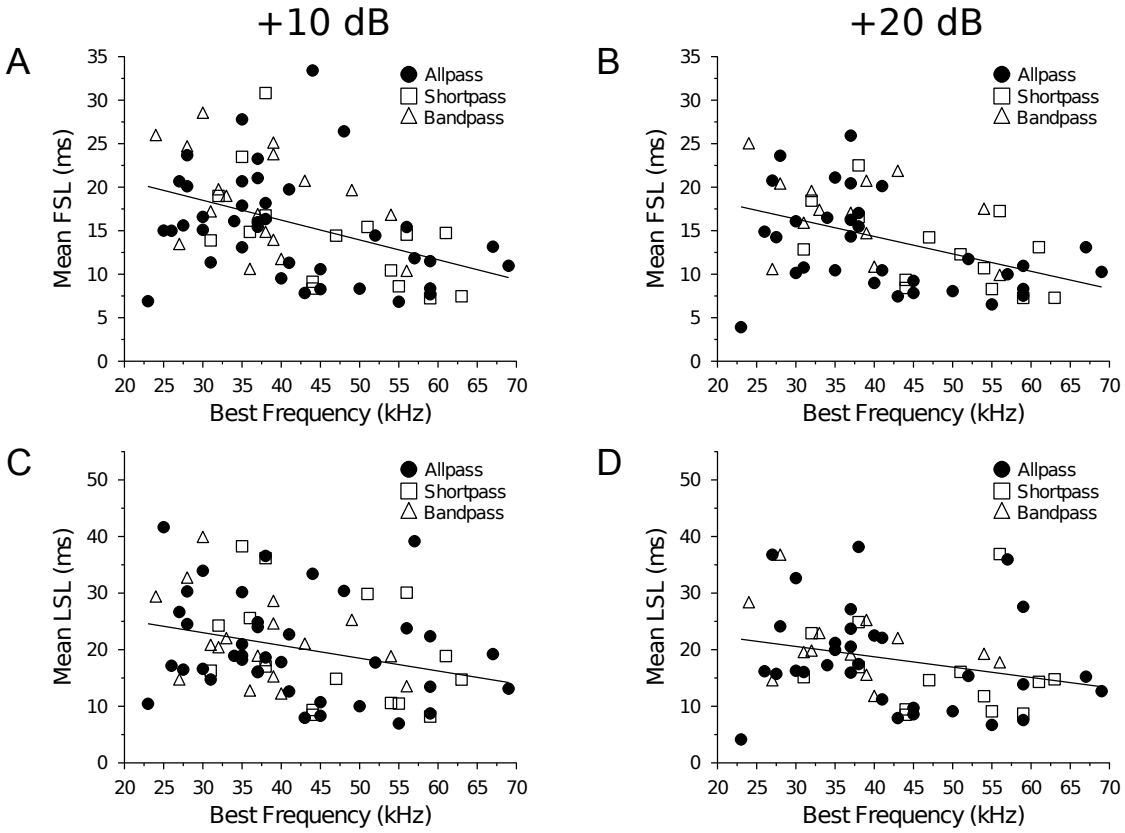

Figure 3.3: Spike latency and tonotopy in the IC. (A,B) First-spike latency as a function of BEF. Neurons with lower BEFs had longer average FSLs at both (A) +10 dB (R^2=0.18, p=0.00019) and (B) +20 dB (R^2=0.21, p=0.00031) re threshold. (C,D) Last-spike latency as a function of BEF. Neurons with lower BEFs had longer average LSLs at both (C) +10 dB (R^2=0.087, p=0.011) and (D) +20 dB (R^2=0.070, p=0.044) re threshold.

Figure 3.4 *(following page)*: Response and recovery in a bandpass DTN. (A) Dot raster display of spiking in a bandpass DTN in response to variable duration BEF tones. (B) Mean ± SE spikes per stimulus as a function of stimulus duration. This cell had a BD of 4 ms. (C) Dot raster display illustrating spiking in response to pairs of BD tones presented at variable IPIs. The *shaded gray regions* illustrate the customized P1 and P2 analysis windows bounded by ±2 SDs from the baseline FSL and baseline LSL of the cell (see Fig. 3.1). (D) Spike count ratio of response as a function of IPI. Evoked spiking in response to P2 recovers to within 50% of baseline (*dotted line*) in response to P1 at 42 ms using the short-to-long method (*), and at 38 ms using the long-to-short method (†). (E) Mean FSL and (F) mean LSL as a function of IPI for responses evoked by P1 *(*red closed symbols) and P2 *(*blue open symbols). (E) The cell's FSL (re P2) returns to within 1 SD of baseline at 56 ms using both the short-to-long and long-to-short methods, whereas (F) the LSL (re P2) returns to within 1 SD of baseline at 20 ms using both the short-to-long and long-to-short methods. Latencies determined after windowing responses with the cell-specific P1 and P2 analysis windows. *Dotted lines* represent ±1 SD relative to baseline latency (re P1). Missing values represent IPIs where no spikes fell into the analysis window. (A,B) MU036.01.06: BEF, 24 kHz; threshold, 27 dB SPL; amplitude +20 dB re threshold; 15 repetitions per stimulus. (C-F) MU036.01.31: BEF, 24 kHz; threshold, 27 dB SPL; amplitude +20 dB re threshold; 20 repetitions per IPI step.

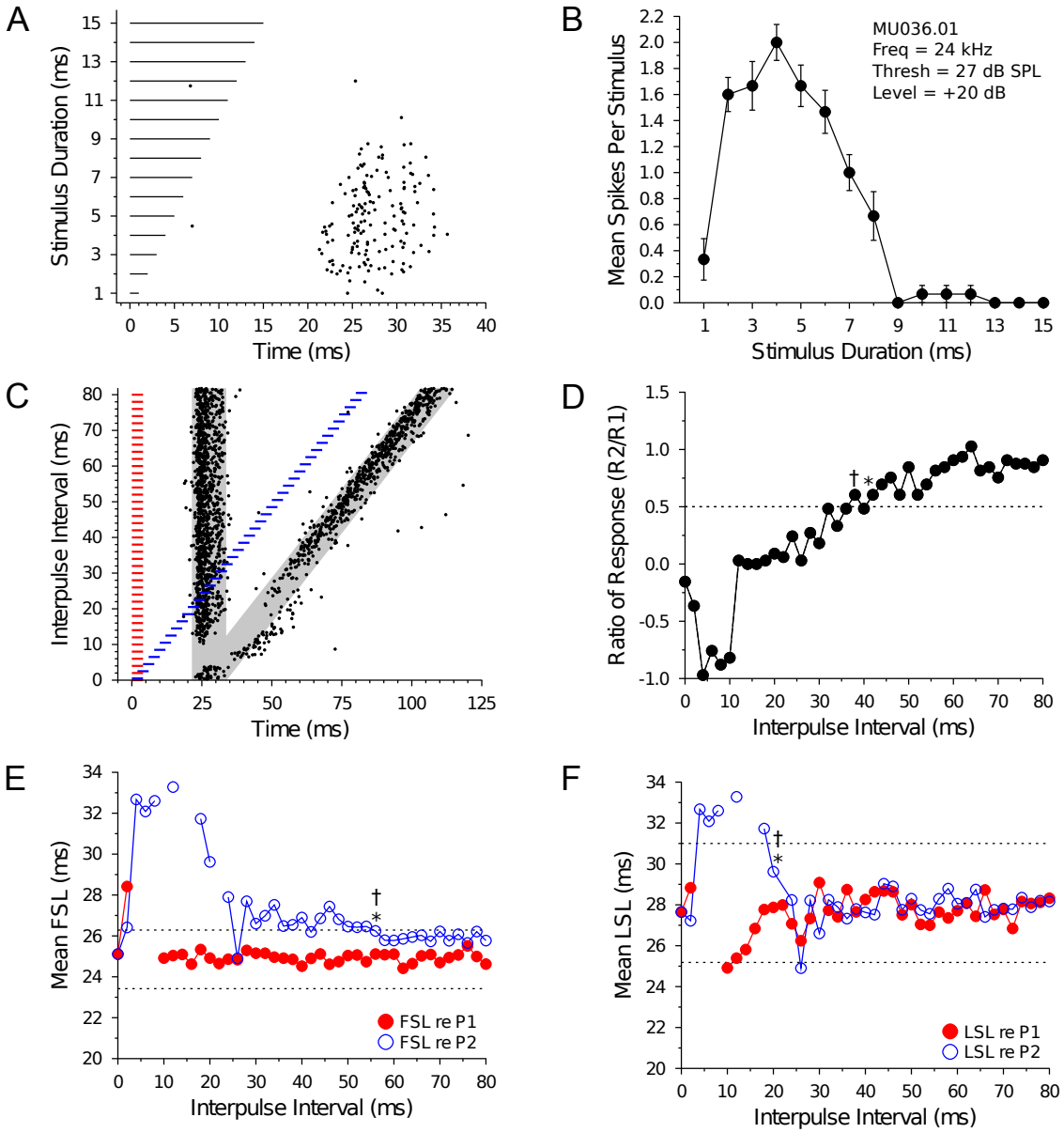
A
Stimulus Duration (ms)
Time (ms)
B
Mean Spikes Per Stimulus
Stimulus Duration (ms)
MU036.01
Freq = 24 kHz
Thresh = 27 dB SPL
Level = +20 dB
C
Interpulse Interval (ms)
Time (ms)
D
Ratio of Response (R2/R1)
Interpulse Interval (ms)
E
Mean FSL (ms)
Interpulse Interval (ms)
FSL re P1
FSL re P2
F
Mean LSL (ms)
Interpulse Interval (ms)
LSL re P1
LSL re P2

Figure 3.5 *(following page)*: Response and recovery in a shortpass DTN. (A) Dot raster display of spiking in a shortpass DTN in response to variable duration BEF tones. (B) Mean $\pm$ SE spikes per stimulus as a function of stimulus duration. This cell had a BD of 2 ms. (C) Dot raster display illustrating spiking in response to pairs of BD tones presented at variable IPIs. The *shaded gray regions* illustrate the customized P1 and P2 analysis windows bounded by $\pm$2 SDs from the baseline FSL and baseline LSL of the cell (see Fig. 3.1). (D) Spike count ratio of response as a function of IPI. Spiking in response to tone P2 recovers to within 50% of baseline (*dotted line*) in response to P1 at 46 ms using both the short-to-long (*) and long-to-short (†) method. (E) Mean FSL and (F) mean LSL as a function of IPI for responses evoked by tone P1 *(*red closed symbols) and tone P2 *(*blue open symbols). (E) The cell's FSL (re P2) returns to within 1 SD of baseline at 20 ms using both the short-to-long and long-to-short methods, whereas (F) the LSL (re P2) returns to within 1 SD of baseline at 14 ms using the short-to-long method. No recovery time value was obtained with the long-to-short method because there was not two consecutive IPIs where the function deviated by $>$1 SD from the baseline LSL. Latencies determined after windowing spikes with the cell-specific P1 and P2 analysis windows. *Dotted lines* represent $\pm$1 SD relative to baseline latency (re P1). Missing values represent IPIs where no spikes fell into the analysis window. (A,B) MU036.02.06: BEF, 38 kHz; threshold, 48 dB SPL; amplitude +20 dB re threshold; 15 repetitions per stimulus. (C-F) MU036.02.12: BEF, 38 kHz; threshold, 48 dB SPL; amplitude +20 dB re threshold; 20 repetitions per IPI step.

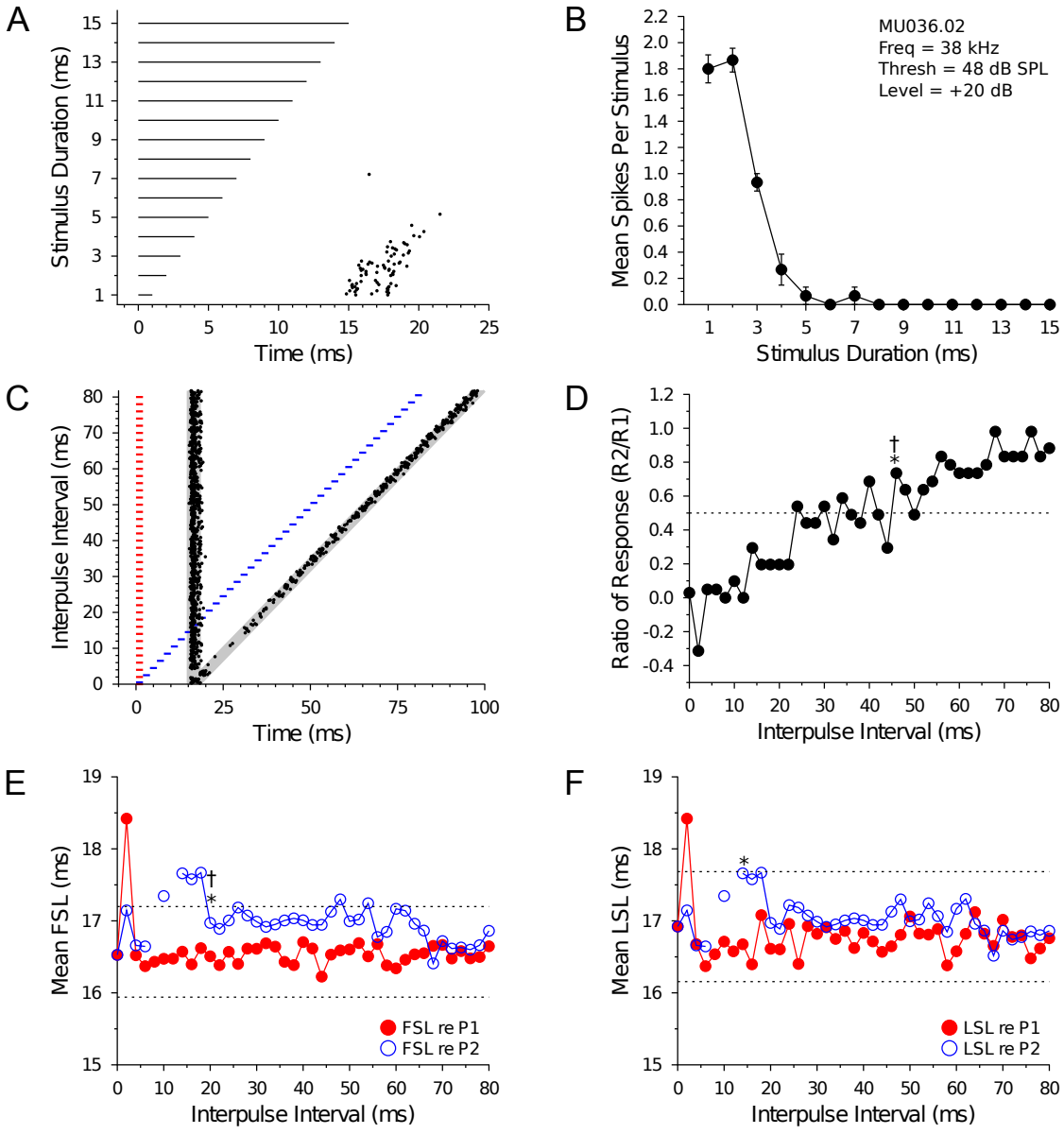
A
Stimulus Duration (ms)
Time (ms)
B
MU036.02
Freq = 38 kHz
Thresh = 48 dB SPL
Level = +20 dB
Mean Spikes Per Stimulus
Stimulus Duration (ms)
C
Interpulse Interval (ms)
Time (ms)
D
Ratio of Response (R2/R1)
Interpulse Interval (ms)
E
Mean FSL (ms)
FSL re P1
FSL re P2
Interpulse Interval (ms)
F
Mean LSL (ms)
LSL re P1
LSL re P2
Interpulse Interval (ms)

Figure 3.6 *(following page)*: Response and recovery in a non-DTN. (A) Dot raster display of spiking in an allpass neuron in response to variable duration BEF tones. (B) Mean $\pm$ SE spikes per stimulus as a function of stimulus duration. By definition, allpass neurons do not have a BD. (C) Dot raster display illustrating spiking in response to pairs of 3 ms tones presented at variable IPIs. The *shaded gray regions* illustrate the customized P1 and P2 analysis windows bounded by $\pm$2 SDs from the baseline FSL and baseline LSL of the cell (see Fig. 3.1). (D) Spike count ratio of response as a function of IPI. Spiking in response to tone P2 recovers to within 50% of baseline (*dotted line*) in response to P1 at 54 ms using both the short-to-long (*) and long-to-short (†) method. (E) Mean FSL and (F) mean LSL as a function of IPI for responses evoked by tone P1 *(*red closed symbols) and tone P2 *(*blue open symbols). (E) The cell's FSL (re P2) returns to within 1 SD of baseline at 14 ms using the short-to-long method and at 22 ms using the long-to-short method, whereas (F) the LSL (re P2) function did not deviate by $>$1 SD from baseline at any IPI, hence no recovery time value was obtained. Latencies determined after windowing spikes with the cell-specific P1 and P2 analysis windows. *Dotted lines* represent $\pm$1 SD relative to baseline latency (re P1). (A,B) MU036.02.06: BEF, 38 kHz; threshold, 48 dB SPL; amplitude +20 dB re threshold; 15 repetitions per stimulus. (C-F) MU036.02.12: BEF, 38 kHz; threshold, 48 dB SPL; amplitude +20 dB re threshold; 20 repetitions per IPI step.

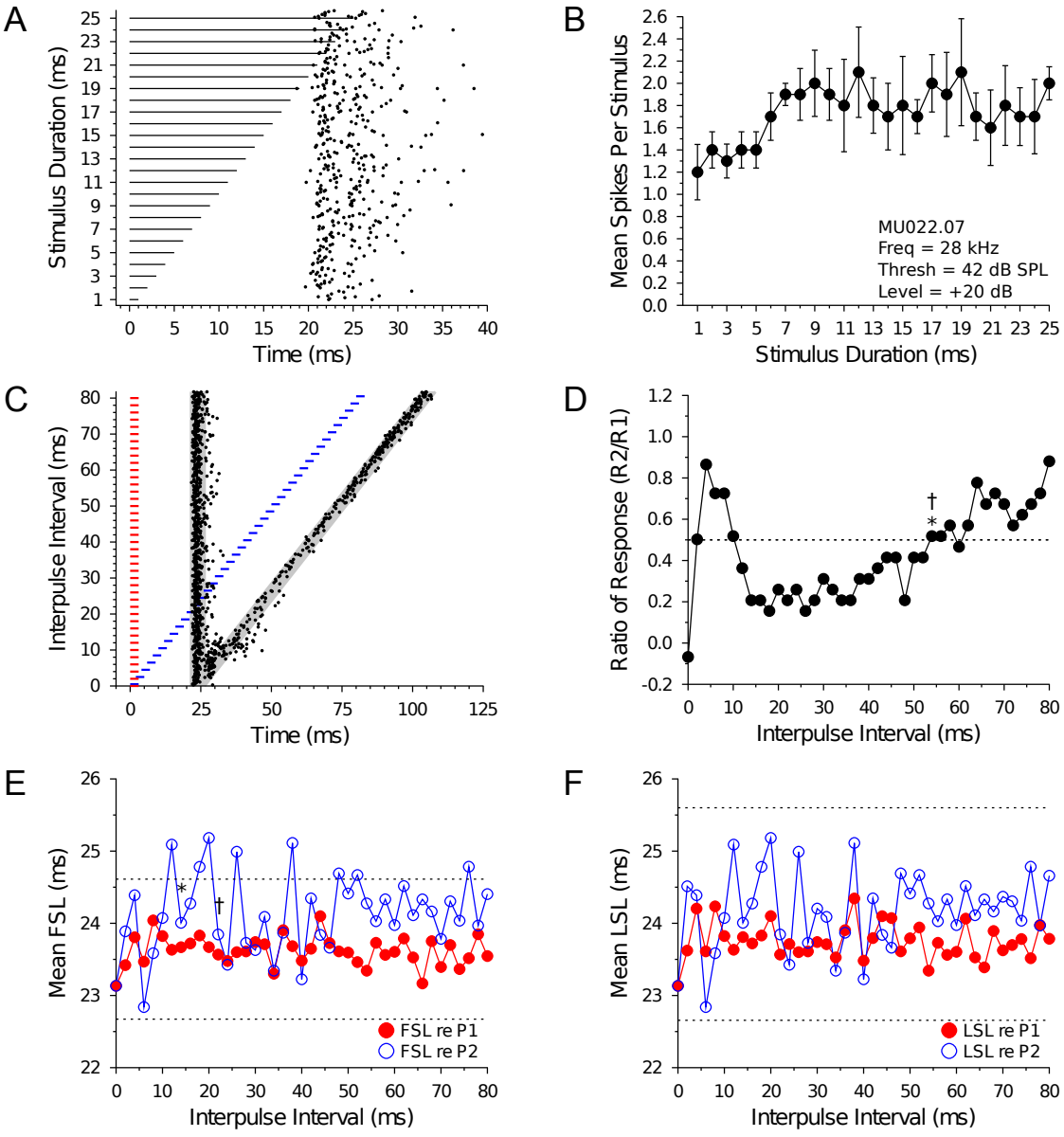
A
Stimulus Duration (ms)
Time (ms)
B
Mean Spikes Per Stimulus
MU022.07
Freq = 28 kHz
Thresh = 42 dB SPL
Level = +20 dB
Stimulus Duration (ms)
C
Interpulse Interval (ms)
Time (ms)
D
Ratio of Response (R2/R1)
Interpulse Interval (ms)
E
Mean FSL (ms)
FSL re P1
FSL re P2
Interpulse Interval (ms)
F
Mean LSL (ms)
LSL re P1
LSL re P2
Interpulse Interval (ms)

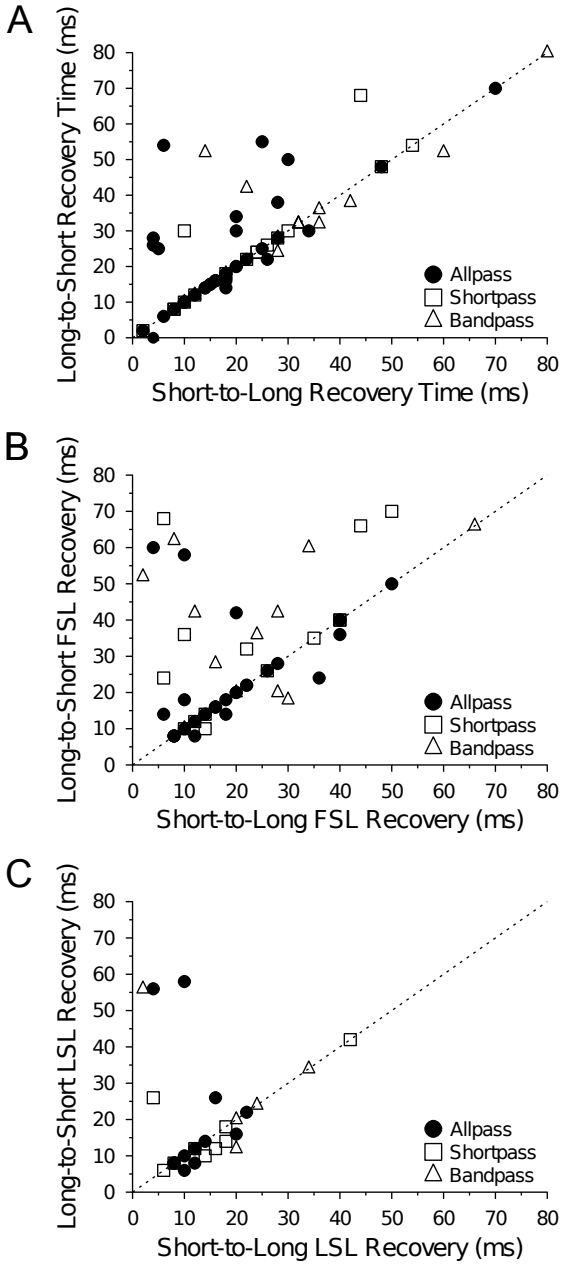

Figure 3.7: Comparison of recovery time measures. Each panel shows recovery times of IC neurons at +10 dB (re threshold) measured with the short-to-long (abscissa) and long-to-short (ordinate) analysis methods based on (A) spike count, (B) FSL and (C) LSL criteria. The two methods are in agreement when points fall along the *dotted unity line* $y = x$. Recovery times were positively correlated at +10 dB (A: R^2=0.77, $p \ll 0.001$; B: R^2=0.30, $p \ll 0.001$; C: R^2=0.22, p=0.0089) and at +20 dB (data not shown) above threshold. The sample size (n) and number of points that fall above, below (but not on) the unity line are: (A) n=73, 14 above, 9 below; (B) n=57, 19 above, 7 below; and (C) n=30, 6 above, 7 below.

Figure 3.8 *(following page)*: Comparison of mean recovery times measured with spike counts and spike latencies. Each panel shows the average recovery times of IC neurons at +10 dB (left) and +20 dB (right) re threshold. Recovery times are in agreement when points fall along the *dotted unity line* $y = x$. (A,B) There was a positive correlation between the mean 50% spike count and mean FSL recovery time in DTNs and non-DTNs at (A) +10 dB (R^2=0.17, $p<0.001$) and (B) +20 dB (R^2=0.21, $p<0.001$) re threshold. (C,D) There was a positive correlation between the mean spike count and mean LSL recovery time at (C) +10 dB (R^2=0.28, $p<0.001$) and (D) +20 dB (R^2=0.35, $p<0.001$) re threshold. (E,F) There was a positive correlation between FSL and LSL recovery times at (E) +10 dB (R^2=0.32, $p\ll0.001$) and (F) +20 dB (R^2=0.41, $p\ll0.001$) re threshold. The sample size (n) and number of points that fall above, below (but not on) the unity line are: (A) n=69, 28 above, 39 below; (B) n=55, 26 above, 24 below; (C) n=42, 6 above, 35 below; (D) n=34, 8 above, 25 below; (E) n=42, 4 above, 25 below; and (F) n=34, 4 above, 17 below.

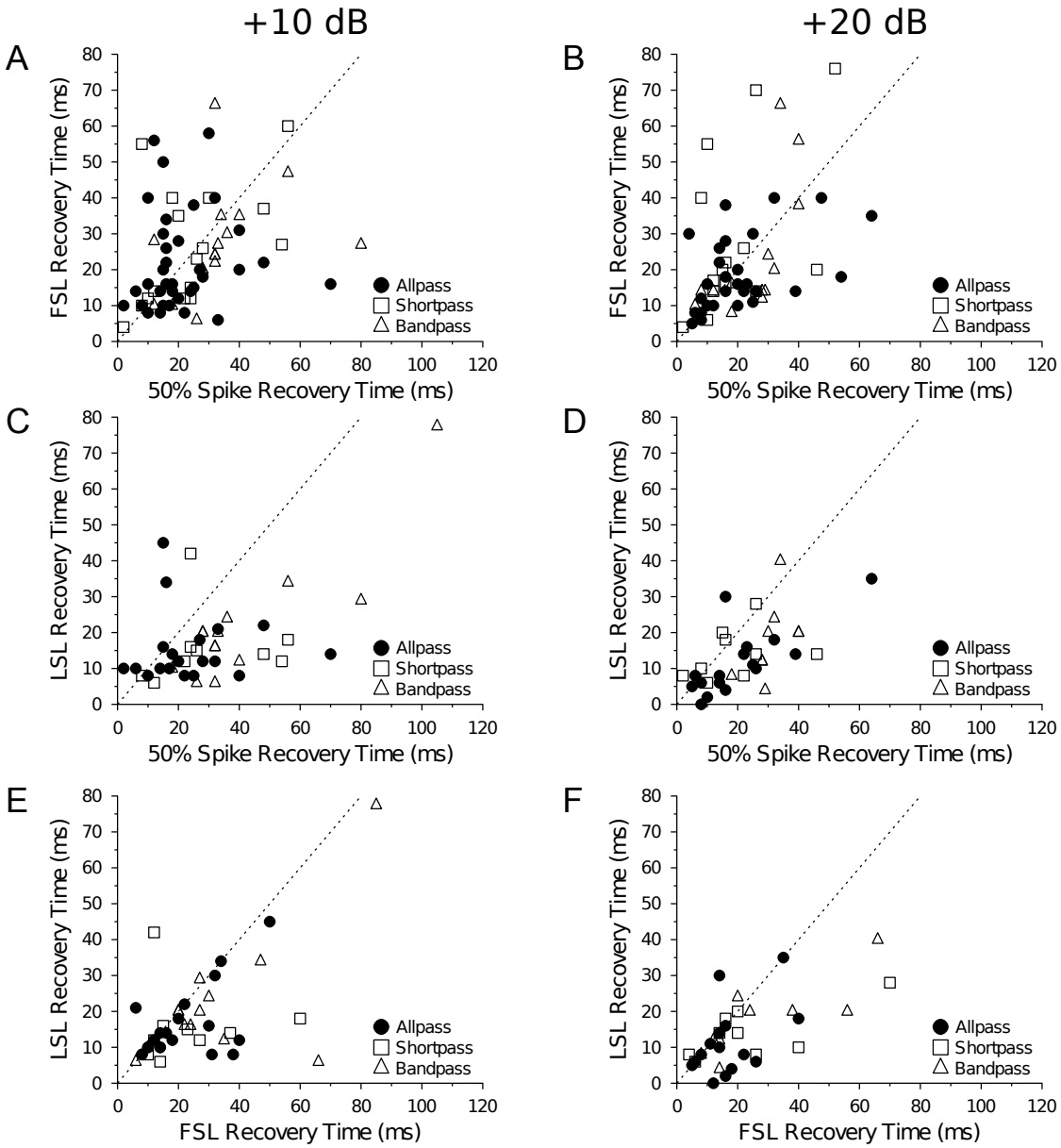
+10 dB
+20 dB
A
B
C
D
E
F
FSL Recovery Time (ms)
LSL Recovery Time (ms)
50% Spike Recovery Time (ms)
FSL Recovery Time (ms)
Allpass
Shortpass
Bandpass

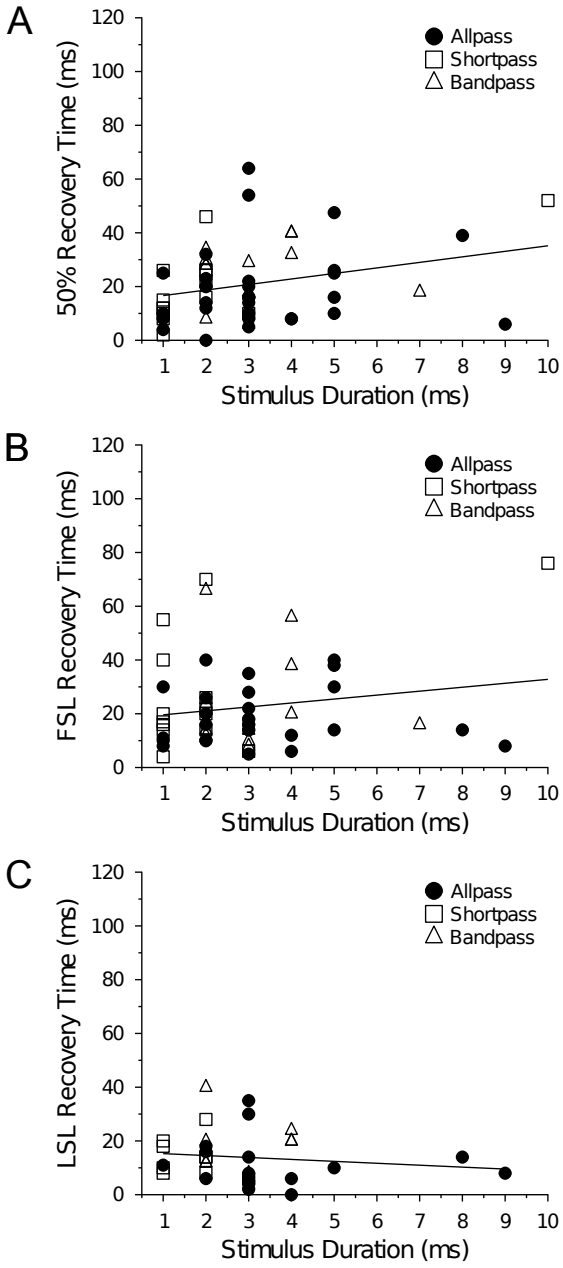

Figure 3.9: Mean recovery time as a function of stimulus duration at +20 dB above threshold. (A) Average 50% spike count recovery times as a function of paired tone stimulus duration. Spike count recovery times were positively correlated with stimulus duration (R^2=0.081, p=0.029). (B) Average FSL and (C) average LSL recovery times as a function of paired tone stimulus duration. Stimulus duration was not correlated with FSL (R^2=0.030, p=0.20) or LSL recovery times (R^2=0.012, p=0.54). Spike count, FSL and LSL recovery times were also not correlated with stimulus duration at +10 dB (re threshold). For DTNs stimulus duration was set to BD, whereas for allpass neurons stimulus duration was randomly chosen between 1 and 9 ms.

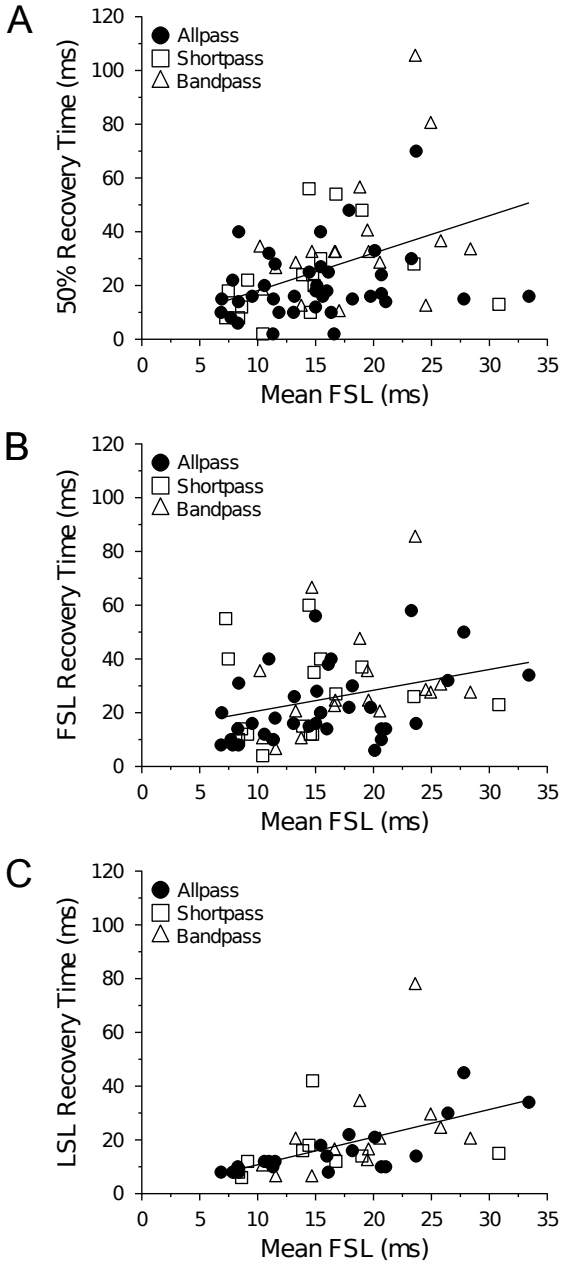

Figure 3.10: Mean recovery time as a function of FSL at +10 dB above threshold. (A) Average 50% spike count recovery times as a function of FSL. Neurons with longer FSLs had longer spike count recovery times (R^2=0.16, p<0.001, n=73). (B) Average FSL and (C) average LSL recovery times as a function of FSL. Neurons with longer FSLs had longer FSL (R^2=0.089, p=0.013, n=69) and LSL recovery times (R^2=0.28, p<0.001, n=42). Spike count recovery times were also correlated with mean FSL at +20 dB (re threshold), but there was no correlation with FSL or LSL recovery times and mean FSL at +20 dB (re threshold).

4 Monaural and Binaural Neural Inhibition Underlying Duration-Selective Responses in the Inferior Colliculus

4.1 Abstract

Duration-tuned neurons (DTNs) from the auditory midbrain of amphibians and mammals are known to arise from the temporal interplay of excitatory and inhibitory synaptic inputs. Previous studies have shown that the neural inhibition that is responsible for creating DTNs precedes excitation (i.e. leading inhibition), and that this inhibition lasts as long or longer than the duration of the stimulus (i.e. persistent inhibition); however, the relative contribution of each ear in creating duration-tuned circuits is unknown. Previous studies have used either monotic or binaural free-field acoustic stimulation (contralateral hemifield) to record the electrophysiological responses of DTNs. Here we used monotic and dichotic stimulation to present DTNs from the inferior colliculus (IC) of the big brown bat with pairs of characteristic frequency tones—a short best duration (BD) excitatory tone and a longer duration non-excitatory (NE) tone—that were varied in interstimulus interval. In both conditions, the BD tone was presented to the contralateral ear. In the monotic condition the NE tone was also presented to the contralateral ear, whereas in the dichotic condition the NE tone was presented to the ipsilateral ear. In the monotic condition when the BD and NE tones were presented sufficiently close in time, the NE tone always suppressed spiking evoked by the BD tone. In contrast, in the dichotic condition about half of DTNs tested did not show spike suppression in response to the ipsilateral NE tone. Of those DTNs with spike suppression in both the monotic and dichotic condition, we found that the latency of the inhibition evoked by NE tone was shorter and the duration of the inhibition was longer for monotic stimulation. In other words, during monotic stimulation of the contralateral

ear we found clear evidence that DTNs receive an inhibitory synaptic input that precedes an excitatory synaptic input to the same neuron, whereas during dichotic stimulation inhibitory inputs to the DTN recruited by the ipsilateral ear were slower, weaker and shorter in duration than the inhibitory inputs recruited from the contralateral ear. These findings indicate that the neural mechanism(s) and circuits that create DTNs in the IC are monaural.

4.2 Introduction

The auditory midbrain or inferior colliculus (IC) is the first nucleus in the central auditory pathway that contains neurons with responses that are selective for the duration of an auditory stimulus. These duration-tuned neurons (DTNs) have been found in the IC of a variety of vertebrates. Although DTNs are primarily studied in bats and are likely important for echolocation, they have also been reported from the auditory midbrain of non-echolocating amphibians and mammals (for review see Sayegh et al., 2011). Therefore, the role DTNs serve in normal hearing cannot be exclusive to echolocation. Although their exact function(s) remain unclear, DTNs provide a potential neural mechanism for processing temporal features of sound in human speech (Denes, 1955) and species-specific communication sounds (Pollack and Hoy, 1979; Bohn et al., 2008; Gadziola et al., 2012).

From a neural circuit standpoint, DTNs are interesting because their temporally selective responses do not simply represent the integration of stimulus energy like auditory afferents and other sensory neurons (Kiang, 1965). For example, shortpass and bandpass DTNs decrease their spiking as stimulus duration is lengthened beyond the cell's best duration (BD) even though increasing signal duration increases stimulus energy ($energy = power * time$; Yost 2007). Previous intracellular (Covey et al., 1996; Tan and Borst, 2007; Leary et al., 2008) and extracellular (Casseday et al., 1994, 2000; Ehrlich et al., 1997; Chen, 1998; Faure et al., 2003) recordings from DTNs have led to the hypothesis that the neural mechanism(s) responsible for duration selectivity involve the interaction of excitatory and inhibitory synaptic inputs that are offset in time, and various mechanisms that exploit the temporal interaction of excitatory and inhibitory synaptic inputs have been proposed (Casseday et al., 1994, 2000; Fuzessery and Hall, 1999; Aubie et al., 2009; Sayegh et al., 2011). Indeed, computational models of the mechanisms can reproduce the *in vivo* spiking responses of DTNs in both echolocating bats and non-echolocating vertebrates (Aubie

et al., 2009, 2012).

Paired tone stimulation combined with single-unit extracellular recordings has previously been employed to characterize the strength and timecourse of inhibitory inputs to DTNs (Faure et al., 2003). These experiments were conducted using monotic stimuli presented to the contralateral ear. To characterize the relative contributions that each ear plays in forming and modifying duration selective responses, we employed both monotic and dichotic paired tone stimulation, with one tone set to the neuron's best duration (BD) and the other tone set to a longer, non-excitatory duration (NE). In both conditions the BD tone was presented to the contralateral ear. In the monotic condition, the NE tone was also presented to the contralateral (excitatory) ear, whereas in the dichotic condition the NE tone was presented to the ipsilateral (inhibitory) ear. Using this stimulus paradigm we found that monotic paired tone stimulation always results in DTNs showing spike suppression via inhibition recruited by the NE tone, whereas during dichotic paired tone stimulation about half of the DTNs did not show spike suppression in response to the NE tone. These results support the conclusion that the underlying neural mechanisms that create DTNs in the mammalian IC are primarily monaural. For the remaining half of DTNs with spike suppression in the dichotic condition caused by the presentation of the NE tone, the evoked inhibition was weaker in strength, shorter in duration and delayed relative to the inhibition evoked during monotic stimulation. These findings suggest that DTNs can receive two distinct types of synaptic inhibition. The first type is monaural in nature, recruited from the contralateral ear, and is responsible for creating the temporally-selective responses characteristic of DTNs. The second type of inhibition is recruited from the ipsilateral ear and is likely similar to the binaural inhibition evoked in other type of IC neurons that aid in sound localization.

4.3 Materials and Methods

4.3.1 Surgical procedures

Methods for surgical procedures and electrophysiological recordings have been described previously (Aubie et al., 2012; Sayegh et al., 2012). Briefly, electrophysiological recordings were obtained from 15 big brown bats (*Eptesicus fuscus*) of both sexes at the University of Washington and McMaster University. To facilitate multiple recordings from individual animals and to precisely replicate the position of the bat's head between recording sessions, a stainless steel post was glued to the skull. Prior to the head-posting surgery, bats were given a subcutaneous injection of buprenorphine (0.03 mL; 0.025 mg/kg). For surgery, bats were first placed in an anesthesia induction chamber (12 x 10 x 10 cm) where they inhaled a 1 to 5% isofluorane:oxygen mixture (1 L/min). Anesthetized bats were then placed in a foam-lined body restraint within a model 1900 stereotaxic alignment system with a custom bite bar or gas mask (David Kopf Instruments) for continuous isofluorane inhalation. The hair covering the skull was cropped and the skin disinfected with Betadine® surgical scrub. Local anesthetic (0.2 mL bupivicaine; 5 mg/mL) was injected subcutaneously prior to making a midline incision in the scalp. The temporal muscles were reflected, the skull was scraped clean and swabbed with 70-100% ethanol, and the post was glued to the skull overlying the cortex with cyanoacrylate superglue (Henkel Loctite Corporation) cured with liquid acrylic hardener (Zipkicker; Pacer Technology). A chlorided silver wire attached to the head post was placed under the temporal muscles and served as the reference electrode. Recordings began 1 to 4 days after surgery. Each bat was used in 1 to 8 sessions lasting 6 to 8 hrs each. Recordings were terminated if a bat showed signs of discomfort. Between sessions, the electrode penetration site was covered with a piece of contact lens and Gelfoam coated in Polysporin®. Bats were housed individually in a temperature- and humidity-controlled room. All procedures were approved by the University of Washington Laboratory Animal

Care and Use Committee or the McMaster University Animal Research Ethics Board and were in accordance with guidelines published by the Canadian Council on Animal Care.

4.3.2 Electrophysiological recordings

Electrophysiological recordings were conducted inside a double-walled, sound attenuating booth with electrical shielding (Industrial Acoustics Co., Inc.). Prior to recording, each bat was given a subcutaneous injection of neuroleptic (0.3 mL; 1:1 mixture of 0.05 mg/mL fentanyl citrate and 2.5 mg/mL droperidol; 19.1 mg/kg). Bats were then placed in a foam-lined body restraint that was suspended by springs within a small animal stereotaxic frame customized for bats (ASI Instruments) mounted atop an air vibration table (TMC Micro-g). The bat's head was immobilized by securing the headpost to a stainless steel rod attached to a micromanipulator (ASI Instruments) mounted on the stereotaxic frame. The dorsal surface of the IC was exposed for recording by making a small hole in the skull and dura mater with a scalpel. Single-unit extracellular recordings were made with thin-wall borosilicate glass microelectrodes with a capillary filament (o.d. = 1.2 mm; A-M Systems, Inc.) and filled with 3M NaCl. Typical electrodes resistances ranged from 10 to 30 MΩ. Electrodes were manually positioned over the dorsal surface of the IC with a manipulator (ASI Instruments) and advanced into the brain with a stepping hydraulic micropositioner (Kopf Model 2650). Action potentials were recorded with a Neuroprobe amplifier (A-M Systems Model 1600) whose 10x output was bandpass filtered and further amplified (500 to 1000x) by a Tucker Davis Technologies spike pre-conditioner (TDT PC1; lowpass f_c = 7 kHz; high-pass f_c = 300 Hz). Spike times were logged on a computer by passing the PC1 output to a spike discriminator (TDT SD1) and then an event timer (TDT ET1) synchronized to a timing generator (TDT TG6).

4.3.3 Stimulus generation and data collection

Stimulus generation and on-line data collection were controlled with custom software that displayed spike-times as peristimulus dot raster displays (rastergrams) ordered by the acoustic parameter that was varied (see Faure et al., 2003). Sound pulses were digitally generated with a two-channel array processor (TDT Apos II; 357 kHz sampling rate) optically interfaced to two digital-to-analog (D/A) converters (TDT DA3-2) whose individual outputs were fed to a low-pass anti-aliasing filter (TDT FT6-2; f_c = 120 kHz), two programmable attenuators (TDT PA5) and two signal mixers (TDT SM5) with equal weighting. The output of each mixer was fed to a manual attenuator (Leader LAT-45) before final amplification (Krohn-Hite Model 7500). Auditory stimuli were presented with a pair of Brüel & Kjær $\frac{1}{4}$ inch condenser microphones (Type 4939; protective grid on), modified for use as loudspeakers with a transmitting adaptor (B&K Type UA-9020) to correct for nonlinearities in the transfer function (Frederiksen, 1977). Each loudspeaker was positioned ca. 1 mm in front of the external auditory meatus. The output of each speaker, measured with a B&K Type 4138 $\frac{1}{8}$ inch condenser microphone (90^o incidence; grid off) connected to a measuring amplifier (B&K Type 2606) and bandpass filter (K-H Model 3500), was quantified with a sound calibrator (B&K Type 4231) and expressed in decibels sound pressure level (dB SPL re 20 μPa) equivalent to the peak amplitude of continuous tones of the same carrier frequency. The loudspeaker transfer function was flat $\pm$6 dB from 28 to 118 kHz, and there was ca. 30 dB attenuation at the ear opposite the source (Ehrlich et al., 1997). All stimuli had rise/fall times of 0.4 ms shaped with a square cosine function and were presented at a rate of 3 Hz. Search stimuli were presented monaurally, contralateral to the IC being recorded. Single units were found by presenting short duration pure tones and/or downward frequency modulated sweeps. Upon unit isolation, we determined each cell's characteristic frequency, minimum threshold, first-spike latency (re signal onset), and for DTNs we

also determined the cell's best duration and duration filter response class (i.e. shortpass, bandpass or longpass DTN; for definitions see Faure et al., 2003; Fremouw et al., 2005).

Following the paired tone stimulation paradigm of Faure et al. (2003), we presented DTNs with pairs of characteristic frequency tones that differed in their duration and inter-stimulus interval (ISI). One tone in the pair was set to the cell's best duration (BD tone; D_{BD}) and the other tone was set to a longer, non-excitatory duration (NE tone; D_{NE}). The onset time of the NE tone was fixed between trials, whereas the onset time of the roving BD tone was randomly varied in 2 ms steps. Because the BD and NE tones were matched in frequency and phase at all ISIs, whenever the two tones overlapped they summed to form a single composite tone with a +6 dB amplitude pedestal, the duration of which was determined by the amount of temporal overlap.

For each cell, we measured the latency and duration of the inhibition evoked by the NE tone during monotic and dichotic paired tone stimulation. In both conditions, the BD tone was presented to the contralateral (excitatory) ear. In the monotic condition, the NE tone was electronically mixed and also presented to the contralateral ear, whereas in the dichotic condition the NE tone was split and presented to the ipsilateral (inhibitory) ear while the BD tone was presented to the contralateral (excitatory) ear. In this way we were able to measure and compare the strength of inhibition evoked by the NE tone through monaural and binaural central auditory pathways. Unless stated otherwise, the BD and NE tones were matched in frequency, amplitude and phase at all ISIs. The frequency of the BD and NE tones was set to the cell's characteristic frequency. The duration of the NE tone was typically 10x the duration of the BD tone duration. The amplitude of the BD tone was typically set to +10 dB (re threshold) and the amplitude of the NE tone was set to +0, +10 or +20 dB (re BD tone).

4.3.4 Data analysis

Unless stated otherwise, all data are reported as the mean $\pm$ standard error (SE) of the mean. Data were tested for normality and homogeneity of variances with a Shapiro-Wilk and Levene's test before further statistical testing. Parametric tests were employed when data were normally distributed with equal variances; otherwise, an equivalent non-parametric test was used. The proportion of DTNs with inhibition in the monotic and dichotic condition were compared with a Fisher's exact test. Comparisons of the onset, offset and relative timing of inhibition were conducted with a two-sample t-test or a Mann-Whitney U test. Comparisons of the latency and timecourse of inhibition evoked in the monotic and dichotic conditions, as well as the durations of inhibition measured with spike counts and latencies, were conducted with a paired t-test or a Wilcoxon signed-rank test. Linear regressions were calculated to evaluate the relationship of BD, first spike latency and leading inhibition. The effect of increasing the amplitude of the NE tone in the dichotic condition was evaluated with a Friedman test. All statistical analyses were performed in SPSS or Python (SciPy) and employed an experiment-wise error rate of α = 0.05.

4.4 Results

4.4.1 Determining the timecourse of inhibition

Example spiking responses from a bandpass DTN tested with monotic paired tone stimulation using equal amplitude BD and NE tones are shown in Figure 4.1, along with details of how the onset (T_1) and offset (T_2) of spike suppression was measured using changes in the cell's spike count, first spike latency (FSL) and/or last spike latency (LSL). Note the gap in the cell's response when the BD and NE tones were presented at sufficiently small ISIs. The circled responses represent the 10 trials with the largest ISIs, when the BD tone preceded

the NE tone, that were used to calculate the mean $\pm$ standard deviation (SD) baseline spike count and baseline spike latencies (Figure 4.1A). For the example cell shown, the baseline spike count was 1.70 $\pm$ 1.02 spikes per stimulus, the baseline FSL (L_{first}) was 13.85 $\pm$ 1.19 ms (re BD tone onset) and the baseline LSL (L_{last}) was 16.09 $\pm$ 1.40 ms (re BD tone onset).

For each cell we plotted the average spike count, FSL and LSL as a function of the gap between the offset of the BD tone and the onset of the NE tone (e.g. Figure 4.1B-D), and then used changes in the evoked response to measure the onset (latency) and time-course (duration) of the spike suppression caused by the sustained inhibition evoked by the stationary NE tone. Using mean spikes per stimulus, the onset (T_1) of spike suppression was determined as the first data point where spiking decreased to $\leq$50% of the baseline spike count as long as the consecutive data point was also $\leq$50% of the baseline count (see Sayegh et al., 2012). The offset (T_2) of spike suppression was determined to be the longest ISI, starting from T_1, where the spike count remained $\leq$50% of baseline if the two next consecutive data points were $>$50% of the baseline count. Using these spike count criteria, T_1 = -3 ms and T_2 = 37 ms (Figure 4.1B). Using mean spike latencies, the onset (T_1) of spike suppression was determined as the first data point where the latency increased or decreased by $>$1 SD from the baseline latency as long as the next data point had also deviated by $>$1 SD (re baseline latency). The offset (T_2) of spike suppression was determined as the longest ISI, starting from T_1, where the spike latency had increased or decreased by $>$1 SD from the baseline latency if the two next consecutive data points were within $\pm$1 SD of baseline. Using these criteria on the cell's FSL, T_1 = 25 ms and T_2 = 37 ms (Figure 4.1C). Using the same criteria for assessing changes in LSL, T_1 = -5 ms and T_2 = 37 ms (Figure 4.1D).

For the bandpass DTN shown in Figure 4.1, the final value for T_1 was -5 ms and was chosen from the LSL measure, and the final value for T_2 was -37 ms because there was

consensus across the spike count and latency measures (see *Comparing the timecourse of inhibition measured with spike counts and latencies*). Upon selecting the final values for T_1 and T_2, the effective start (T_{start}) and end (T_{end}) times of the inhibition evoked by the NE tone were calculated as

$$T_{start} = T_1 + L_{last} - D_{BD} \tag{4.1}$$

and

$$T_{end} = T_2 + L_{first} - D_{BD}, \tag{4.2}$$

where L_{last} is the baseline last spike latency, L_{first} is the baseline first spike latency, and D_{BD} is the duration of the BD tone. The duration of inhibition was calculated as T_{end} - T_{start}. A neuron was said to have leading inhibition when the latency of NE tone evoked inhibition was shorter than the cell's excitatory first spike latency (i.e. $T_{start} < L_{first}$). A neuron was said to have persistent inhibition when the duration of the NE tone evoked inhibition was longer than the duration of the NE tone (i.e. T_{end} - $T_{start} > D_{NE}$). For the bandpass neuron in Figure 4.1, T_{start} = 8.09 ms and T_{end} = 47.85 ms, resulting in an effective duration of inhibition of 39.76 ms. The cell has 5.76 ms of leading inhibition because the latency of the inhibition evoked by the NE tone (T_{start} = 8.09 ms) was shorter than the cell's excitatory baseline FSL (L_{first} = 13.85 ms). The cell also has 9.76 ms of persistent inhibition because the duration of inhibition (T_{end} - T_{start} = 39.76 ms) was longer than the duration of the NE tone (D_{NE} = 30 ms).

4.4.2 Comparing the timecourse of inhibition measured with spike counts and latencies

The final values for T_1 and T_2 were selected using the criterion that best reflected the time course of the inhibition evoked by the NE tone. In this way, T_1 and T_2 could be chosen from a combination of spike count and/or spike latency measures. Doing so permitted us to more accurately quantify the suppressive effects of the NE tone on the spiking responses evoked by the BD tone (Faure et al., 2003). In cases where cells responded with only a single spike per stimulus (i.e. $L_{first} = L_{last}$), or in instances where the spike count of the cell was clearly suppressed even though L_{first} or L_{last} (or both) remained within ± 1 SD of baseline, a change in spike count was typically used for selecting T_1 and T_2 because this criterion more accurately reflected the time course of spike suppression. For cells that responded with more than one spike per stimulus, or in instances where the spike count of the cell had recovered to within 50% of baseline even though L_{first} or L_{last} (or both) were still clearly deviated by >1 SD from baseline, a change in spike latency was typically used for selecting T_1 and T_2 because a latency criterion more accurately reflected the time course of spike suppression. In cases where the mean spike count or latency had not returned to within 50% or ± 1 SD of baseline, respectively, over the range of ISIs presented (monotic condition: n = 10 cells; dichotic condition: n = 0 cells), T_2 was conservatively estimated as the longest ISI tested Faure et al. (2003).

We tested 42 DTNs from the IC of the big brown bat with monotic and dichotic paired tone stimulation. In the monotic condition, there was consensus for the final T_1 value between spike count and latency measures in 17 of 42 cells (40.4%). In the remaining 25 cells, spike counts were used in 17 cases and spike latencies were used in 8 cases (7 with LSL; 1 with FSL). The mean $\pm$ SD spike count for the 17 cells that employed a spike count criterion for T_1 was 1.17 $\pm$ 0.42 spikes per stimulus and for the 8 cells that employed a

spike latency criterion it was 1.88 $\pm$ 0.63 spikes per stimulus, and the spike counts in these two groups were significantly different (Mann-Whitney U = 120.00, p = 0.01). For the final value of T_2, spike count and latency measures were in agreement in only 5 of 42 cells (11.9%). For the remaining 37 cells, spike counts were used in 20 cases and spike latencies were used in 17 cases (14 with FSL; 3 with LSL). The mean $\pm$ SD spike count for the 20 cells that employed a spike count criterion for T_2 was 1.14 $\pm$ 0.39 spikes per stimulus and for the 17 cells that employed a spike latency criterion it was 1.84 $\pm$ 0.58 spikes per stimulus, and the spike counts in these two groups were also significantly different (t(35) = -4.319, p $\ll$ 0.001).

In the dichotic condition, there was consensus for the final T_1 value using spike count and latency measures in only 3 of 20 cells (15.0%). In the remaining 17 cells, spike counts were used in 9 cases and spike latencies were used in 8 cases (3 with LSL; 4 with FSL; 1 consensus). The mean $\pm$ SD spike count for the 9 cells that employed a spike count criterion for T_1 was 1.29 $\pm$ 0.51 spikes per stimulus and for the 8 cells that used a spike latency criterion it was 2.27 $\pm$ 0.69 spikes per stimulus, and the spike counts in these two groups were significantly different (Mann-Whitney U = 62.00, p = 0.011). For the final value of T_2, spike count and latency measures were in agreement for 5 of 20 cells (25.0%). In the remaining 15 cells, spike counts were used in 5 cases and spike latencies were used in 10 cases (8 with FSL; 1 with LSL; 1 consensus). The mean $\pm$ SD spike count for the 5 cells that employed a spike count criterion was 1.44 $\pm$ 0.65 spikes per stimulus and for the 10 cells that employed a spike latency criterion it was 1.63 $\pm$ 0.76 spikes per stimulus; however, the spike counts in these two groups of cells were not significantly different (Mann-Whitney U = 27.00, p = 1.00).

To verify the validity of using changes in spike latency to quantify the timecourse of the inhibition evoked by the NE tone, we compared the duration of inhibition (T_{end} - T_{start}) measured with spike counts and spike latencies for monotic and dichotic paired tone stim-

ulation. Of 42 DTNs tested in the monotic condition, we obtained a duration of inhibition measure with both spike counts and latencies in 37 cells (88.1%). For these neurons, the mean $\pm$ SD duration of inhibition measured with spike counts was 37.32 $\pm$ 15.51 ms and it was 35.75 $\pm$ 15.35 ms when measured with spike latencies, and the difference between the measures was not statistically significant (t(36) = 0.644, p = 0.524). Moreover, our main effect that monotic paired tone stimulation results in significantly longer durations of inhibition compared to dichotic paired tone stimulation held true when we reanalyzed the data using only changes in spike count (t(18) = 7.055, p $\ll$ 0.001).

4.4.3 Inhibition evoked with monotic and dichotic paired tone stimulation

Figure 4.2 shows example responses from a shortpass DTN tested with monotic and dichotic paired tone stimulation using equal amplitude BD and NE tones. Spike suppression was observed in this cell for monotic paired tone stimulation but was absent for dichotic paired tone stimulation. In the monotic condition when the 1 ms BD tone and the 10 ms NE tone were broadcast to the contralateral ear (Figure 4.2A) there was a pronounced suppression in the response that reduced the spike count (Figure 4.2B) and caused a significant change in both the FSL and LSL of the cell (Figure 4.2C,D). The final value for T_1 = 1 ms and was derived from a change in spike count; the final value for T_2 = 49 ms and was derived from a change in FSL. The effective duration of spike suppression was calculated to be 47.21 ms. Note that this neuron did not have leading inhibition because L_{first} = 8.81 ms and T_{start} = 9.60 ms, thus inhibition lagged excitation by 0.79 ms; however, the excitatory and inhibitory inputs to the cell may also have been coincident because the difference in latency between excitation and inhibition was within the measurement resolution (2 ms) of the paired tone stimulus. The cell did have strong persistent inhibition, revealed by changes in both its spike count (Figure 4.2B) and FSL (Figure 4.2C), because the duration of spike suppression lasted 37.21 ms longer than the 10 ms NE tone.

In the dichotic condition, when the BD tone was presented to the contralateral ear and the NE tone was presented to the ipsilateral ear, the NE tone failed to cause spike suppression in the neuron (Figure 4.2E). At all ISIs tested, the spike count remained well above 50% of the baseline count (Figure 4.2F), and both the FSL and LSL did not deviate by >1 SD from the cell's baseline latencies over two consecutive ISIs (Figure 4.2G,H).

In the overall population of cells tested, 42 of 42 DTNs (100%) exhibited spike suppression during monotic paired tone stimulation, whereas only 20 of 42 cells (47.6%) exhibited spike suppression during dichotic paired tone stimulation. This difference was highly significant (Fisher's exact test, $p < 0.0001$). These data support the hypothesis that the inhibition and neural circuits that are responsible for creating the temporally selective responses of DTNs are purely monaural in nature because half of the DTNs we tested showed no evidence of inhibition recruited by stimulation of the ipsilateral ear.

We measured the baseline FSL (L_{first} re BD tone onset) and latency of inhibition evoked by the NE tone (T_{start} re NE tone onset) for each DTN tested with monotic and dichotic paired tone stimulation, and calculated the difference in latency (L_{first} - T_{start}) to determine if the onset of inhibition preceded, was simultaneous with, or followed excitation. A positive difference indicates inhibition leads excitation; a negative difference indicates inhibition lags excitation. The histograms in Figure 4.3 show the number of DTNs with leading and lagging inhibition for monotic and dichotic paired tone stimulation when the BD and NE tones were equal in amplitude (but not in energy). Leading inhibition was observed in 34 of 42 (80.95%) cells in the monotic condition (Figure 4.3A), whereas only 4 of 20 (20%) cells showed leading inhibition in the dichotic condition (Figure 4.3B). The difference in the proportion of DTNs with leading inhibition in the monotic and dichotic conditions was highly significant (Fisher's exact test, $p < 0.0001$) because the majority of cells in the dichotic condition exhibited lagging inhibition. That is, the FSL of the cell was shorter than the latency of inhibition evoked by the NE tone. The mean $\pm$ SD latency dif-

ference of L_{first} minus T_{start} for cells tested in the monotic condition was 3.55 $\pm$ 3.92 ms, whereas it was -1.52 $\pm$ 2.91 ms for cells tested in the dichotic condition, and the difference between the two distributions was statistically significant (Figure 4.3). These data reveal that the inhibitory inputs recruited by stimulation of the contralateral ear during monotic stimulation have a shorter latency to the DTN than the inhibitory inputs recruited by the ipsilateral ear during dichotic stimulation.

The histograms in Figure 4.4 illustrate the timecourse of the inhibition evoked by the NE tone during monotic and dichotic paired tone stimulation. The plots show the duration of inhibition minus the duration of the NE tone that evoked the inhibition (i.e. T_{end} - T_{start} - D_{NE}). A positive difference indicates persistent inhibition because the duration of inhibition evoked by the NE tone was longer than the duration of the NE tone; a negative difference indicates that the inhibition evoked by the NE tone was shorter than the duration of the NE tone. We observed persistent inhibition in 100% (42 of 42) of DTNs tested in the monotic condition. In some cells spike suppression lasted >50 ms after the offset of the NE tone (Figure 4.4A). In the dichotic condition, only 20 of 42 neurons exhibited inhibition evoked by the NE tone, and the total duration of inhibition was usually shorter than the duration of the NE tone that evoked it (Figure 4.4B). Indeed, persistent inhibition was only observed in 5 of 20 DTNs in the dichotic condition, and the difference in the proportion of cells with persistent inhibition in the monotic and dichotic conditions was highly significant (Fisher's exact test, $p < 0.0001$). These data reveal that the timecourse of the inhibition recruited by the contralateral ear during monotic stimulation was longer than the duration of inhibition recruited by the ipsilateral ear during dichotic stimulation.

4.4.4 Comparing monotic and dichotic inhibitory responses

To highlight the differences that monotic and dichotic paired tone stimulation had on the latency and timecourse of the inhibition evoked by the NE tone, we conducted a detailed

paired analysis on the responses of 20 DTNs with inhibition measured in both conditions. The latency of inhibition (T_{start}) evoked during monotic stimulation was significantly shorter than the latency of inhibition evoked during dichotic stimulation in the same cell (Figure 4.5A). Moreover, the duration of inhibition (T_{end} - T_{start}) evoked in the monotic condition was significantly longer than the duration of inhibition evoked in the dichotic condition in the same cell (Figure 4.5B). When we subtracted the latency of inhibition from the baseline FSL, most DTNs showed leading inhibition in the monotic condition but showed lagging inhibition in the dichotic condition (Figure 4.5C). We also compared the duration of inhibition relative to the duration of the NE tone that evoked the inhibition (T_{end} - T_{start} - D_{NE}) and found that all DTNs had persistent inhibition in the monotic condition whereas few cells had persistent inhibition in the dichotic condition (Figure 4.5D). Altogether, these data suggest that DTNs can receive two distinct types of inhibitory inputs: one that is fast and long-lasting, evoked by stimulation of the contralateral ear, and is responsible for creating the temporally selective responses characteristic of DTNs, and another that is slower and shorter-lasting, evoked by stimulation of the ipsilateral ear, and that modifies the spiking response of the cells.

4.4.5 Relation of leading/lagging inhibition to BD, FSL and duration filter characteristic

Conceptual and computational models of DTNs predict that the BD and range of duration selectivity will depend, in part, on the amount of time that inhibition leads excitation (Casseday et al., 1994, 2000; Aubie et al., 2009, 2012). A previous study reported a positive relation between the amount of leading inhibition and BD in a sample of DTNs tested with monotic paired tone stimulation. That same study also reported a positive relation between the amount of leading inhibition and FSL (Faure et al., 2003).

We measured the latency of inhibition evoked by the NE tone during monotic and di-

chotic paired tone stimulation and subtracted this time from the baseline FSL of each cell to evaluate the relationship of leading/lagging inhibition to the BD, FSL and duration filter characteristic in the monotic and dichotic conditions (Figure 4.6). In the monotic condition, the amount of leading inhibition increased significantly in DTNs tuned to longer BDs (Figure 4.6A). Leading inhibition was also significantly larger in bandpass DTNs than shortpass DTNs (bandpass = 4.60 $\pm$ 0.94 ms; shortpass = 1.60 $\pm$ 0.89 ms; Mann-Whitney U = 81.00, $p \ll 0.001$). These findings replicate the results of Faure et al. (2003). In contrast, there was no relation between leading/lagging inhibition and BD when the latency of the NE tone evoked inhibition was measured in the dichotic condition (Figure 4.6B). Moreover, there was no significant difference in the amount of leading/lagging inhibition between bandpass and shortpass DTNs (bandpass = -1.92 $\pm$ 1.08 ms; shortpass = 1.60 $\pm$ 0.89 ms; t(18) = 0.443, $p = 0.663$).

In the monotic condition, there was a significant positive relation between leading inhibition and the baseline FSL of DTNs; cells with short FSLs had smaller durations of leading inhibition and cells with long FSLs had longer durations of leading inhibition (Figure 4.6C). This finding was also reported by Faure et al. (2003); however, there was no significant difference in FSL between bandpass and shortpass DTNs (bandpass = 14.39 $\pm$ 1.05 ms; shortpass = 13.45 $\pm$ 1.15 ms; Mann-Whitney U = 174.00, p = 0.247). In the dichotic condition, there was no relation between leading/lagging inhibition and the baseline FSL (Figure 4.6D). There was also no difference in FSL between bandpass and shortpass DTNs (bandpass = 13.74 $\pm$ 1.05 ms; shortpass = 13.33 $\pm$ 1.39 ms; Mann-Whitney U = 172.00, p = 0.227). Taken together, these data support the hypothesis that the inhibitory inputs responsible for shaping the BD, FSL and duration filter characteristic of DTNs are evoked monaurally through stimulation of the contralateral ear, whereas the inhibitory inputs evoked through stimulation of the ipsilateral ear, when present, are not a major determinant of BD, FSL and duration tuning response class.

4.4.6 Effect of increasing NE tone amplitude in the dichotic condition

Finally, we explored the effect of increasing the amplitude of the NE tone during dichotic paired tone stimulation. In this experiment, the amplitude of the BD tone in the contralateral ear was fixed, typically at +10 to +20 dB above threshold, while the amplitude of the NE tone in the ipsilateral ear was varied from +0, +10 or +20 dB re BD tone (Figure 4.7A). We limited the dichotic amplitude difference of the NE tone to +20 dB (re BD tone) to reduce the likelihood of suppressing BD tone evoked spikes via stimulation of the contralateral ear through acoustic crosstalk (Ehrlich et al., 1997). Of 21 DTNs tested, only 4 exhibited spike suppression in the dichotic condition when the BD and NE tones were equal in amplitude. When the amplitude of the NE tone was increased to +10 dB (re BD tone), 9 of 21 cells showed spike suppression. When the amplitude of the NE tone was increased to +20 dB (re BD tone), 16 of 21 neurons showed suppression. Figure 4.7B shows example spiking responses from a shortpass DTN as the amplitude of the NE tone was increased during dichotic stimulation. This cell did not show ipsilateral evoked inhibition until the amplitude of the NE tone was +20 dB (re BD tone). In this example response suppression was evaluated with a change in spike count, but similar suppressive effects were observed when we examined changes in the cell's FSL and LSL (latency data not shown). Figure 4.7C shows example spiking responses from a bandpass DTN as the amplitude of the NE tone was increased during dichotic stimulation. This cell did not show ipsilateral evoked inhibition at any amplitude of the NE tone as the mean spikes per stimulus, FSL and LSL all remained relatively constant (latency data not shown). We measured the duration of inhibition for each cell at each NE tone amplitude; cells with no suppression were assigned a duration of inhibition of 0 ms. A non-parametric equivalent to a repeated measures ANOVA (Friedman test) revealed there was a significant increase in the duration of inhibition evoked by the NE tone as the amplitude of the NE tone was increased in the ipsilateral ear (Figure 4.7D).

4.5 Discussion

4.5.1 Inhibitory inputs that create duration-tuned neurons are monaural

A number of neural circuit models, backed by electrophysiological studies, have proposed potential biological mechanisms to explain the creation of duration-selective responses in the vertebrate central auditory system. Although there are variations to the models, most rely on the interaction of excitatory and inhibitory synaptic inputs (Casseday et al., 1994, 2000; Covey et al., 1996; Fuzessery and Hall, 1999; Faure et al., 2003; Aubie et al., 2009; Sayegh et al., 2012). One key feature of these models is that DTNs receive a sustained inhibitory input that lasts as long or longer than the duration of the stimulus evoking the inhibition. Additionally, the models combined with limited evidence from whole-cell patch clamp recordings (Covey et al., 1996; Leary et al., 2008), reveal that DTNs have inhibitory inputs that precede their excitatory inputs.

Extracellular electrophysiology typically only allows researchers to observe the expression and/or suppression of excitatory action potentials. In this study we used paired tone stimulation, combined with single unit recordings, to directly infer about the latency and duration of the inhibition acting on DTNs. This technique works for DTNs because the stimulus paradigm uses an excitatory BD tone that reliably evokes spiking, and a second NE tone that reliably suppresses action potentials evoked by the BD tone (Figure 4.1). Here we report that all DTNs exhibited spike suppression during monotic paired tone stimulation when the BD and NE tones were presented to the contralateral ear, whereas half of DTNs showed no spike suppression during dichotic paired tone stimulation when the BD tone was presented to the contralateral ear and the NE tone was presented to the ipsilateral ear (Figures 4.2-4.4). In the monotic condition, the latency of inhibition evoked by the NE tone was shorter than the cell's FSL, a finding that supports the hypothesis that inhibitory inputs to DTNs precede excitatory inputs. Only half of DTNs tested showed spike suppression in

the dichotic condition, and of those most had latencies of inhibition evoked by the NE tone that were longer than the cell's excitatory FSL, revealing that inhibition typically lagged excitation in the dichotic condition (Figure 4.5). All DTNs had sustained inhibition in the monotic condition that lasted as long or longer than the duration of the NE tone, whereas in the dichotic condition the duration of inhibition was almost always shorter than the duration of the NE tone that evoked the inhibition (Figures 4.4,4.5). These findings indicate that the neural circuits and mechanism(s) that create duration-selective cells in the auditory midbrain are primarily monaural. When ipsilateral inhibition was evoked, it was weaker, slower and shorter in duration than the contralateral inhibition to the same cell (Figure 4.5). Taken together, these results indicate that the synaptic inhibition that is recruited through monaural, contralateral auditory pathways is responsible for creating DTNs in the mammalian IC.

4.5.2 Effect of increasing NE tone amplitude in the dichotic condition

The inferior colliculus receives converging bilateral inputs from a number of auditory nuclei (Adams, 1979; Zook and Casseday, 1982), so it is natural to expect that neural inputs evoked from each ear play a role in the response characteristics of IC neurons. In a previous report on the binaural interaction of IC neurons in the big brown bat, approximately 60% of cells showed evidence that the contralateral ear provided an excitatory input and the ipsilateral ear provided an inhibitory input (Lu and Jen, 2003). In the present study, 52% of DTNs received an inhibitory input responsible for creating the duration-tuned response via stimulation of the contralateral ear but were not influenced by stimulation of the ipsilateral ear, whereas 48% of DTNs received inhibitory inputs via stimulation of both the contralateral and ipsilateral ears. Using dichotic paired tone stimulation we were able to recruit an ipsilaterally-evoked inhibition in some cells by increasing the amplitude of the ipsilateral NE tone relative to the contralateral BD tone (Figure 4.7). Increasing the

amplitude of the NE tone up to +20 dB (re BD tone) induced spike suppression in 12 of 17 neurons that previously had not shown spike suppression when the amplitude of the ipsilateral NE tone was equal to the amplitude of the contralateral BD tone. One possible explanation is that increasing the amplitude of the ipsilateral NE tone induced spike suppression via stimulation of the contralateral ear through acoustic crosstalk; however, this seems unlikely as another study using identical loudspeakers reported $>$30 dB of attenuation between the ears (Ehrlich et al., 1997), which is well above the +20 dB interaural level difference that we employed with our dichotic stimuli. The potential for acoustic crosstalk actually strengthens our hypothesis that the circuitry underlying the formation of DTNs is monaural in nature. This is because inadvertent stimulation of the contralateral ear through acoustic crosstalk should have recruited additional inhibition in response to the NE tone in the dichotic condition. This did not occur.

4.5.3 Role of inhibition recruited by the ipsilateral ear

A known function of ipsilaterally-evoked inhibition to binaural hearing is for sound localization (Faure and Hoy, 2000). One way to compute the location of a sound source is to compare the difference in sound pressure level at each ear—the interaural level difference (ILD). Localization with ILD cues is especially important at high frequencies because sounds with short wavelengths more easily reflect off a listener's head and this causes the formation of a sound shadow, with the signal being louder in the near ear and attenuated in the far ear (Rayleigh, 1907). For echolocating bats, ILD cues are important for localizing targets in the azimuth (Shimozawa et al., 1974; Simmons et al., 1983). The lateral superior olive (LSO) is the first nucleus in the mammalian central auditory pathway that contains binaural neurons sensitive to ILD cues. Principal cells of the LSO receive an excitatory input from the cochlear nucleus of the ipsilateral ear and an inhibitory input from the cochlear nucleus of the contralateral ear (via the ipsilateral medial nucleus of the trapezoid body),

and the strength of these inputs varies with the sound level at each ear (Boudreau and Tsuchitani, 1968; Goldberg and Brown, 1968; Tollin and Yin, 2002,b). Because LSO afferents project to the IC (Zook and Casseday, 1982), binaural inhibition observed at the level of the midbrain reflect processing that has occurred in the LSO; however, there is growing evidence that ILD sensitivity is recalculated in the IC in a subset of cells (Kuwada et al., 1997; Li et al., 2010; Pollak, 2012).

Our results clearly demonstrate that the inhibition responsible for creating the temporally-selective responses of DTNs originates from monaural central auditory pathways. This inhibition is recruited by stimulating the contralateral ear, is strong and onset-evoked, is fast and precedes excitation to the DTN, and it is sustained for as long or longer than the duration of the stimulus (Faure et al., 2003). When inhibition was recruited via stimulation of the ipsilateral ear, for the majority of DTNs this onset-evoked inhibition was weaker and longer in latency than either the contralaterally-evoked inhibition or excitation (Figure 4.5). These findings immediately raise two important questions. Why do monaural neurons exist at the level of the auditory midbrain, and what role do DTNs serve in normal hearing? The fact that nearly half of DTNs tested with dichotic paired tone stimulation did not show spike suppression when the ipsilateral ear was stimulated strongly suggests that these cells have large spatial receptive fields with poor acuity for localizing sources in the contralateral hemifield. The remaining half of DTNs showed spike suppression, mainly when the ipsilateral NE tone was +10 to +20 dB louder than the contralateral BD tone (Figure 4.7), and we predict that these cells will have smaller receptive fields with a sharper spatial acuity for localizing sound sources in the contralateral hemifield.

Altogether, our results demonstrate that DTNs in the mammalian IC can receive at least two distinct types of inhibitory inputs. The first type is present in every cell, is evoked by stimulation of the contralateral ear, and is responsible for creating the temporally-selective responses characteristic of DTNs. The second type of inhibition occurs in approximately

half of DTNs, is evoked by stimulation of the ipsilateral ear, and its biological function is unknown. We speculate that this ipsilaterally-evoked inhibition could modulate the strength and timing of contralaterally-evoked spikes and hence these cells may play a role in sound localization. If true, then DTNs could act as spatio-spectro-temporal filters in normal hearing. In the IC of bats, DTNs are known to receive two types of inhibitory neurotransmitters, GABA and glycine (Casseday et al., 2000). While it is tempting to speculate that the two types of inhibitory inputs to DTNs reported in this study are using different neurotransmitters, for now this hypothesis awaits further investigation.

4.5.4 Monotic and dichotic temporal masking

The paired tone stimulation paradigm we employed on DTNs in the IC of the bat mirrors the design of auditory temporal masking experiments in human psychophysics (Faure et al., 2003). The reduction in spiking that occurred when the BD tone preceded the NE tone is the neural equivalent to backward masking and was caused by the leading inhibition evoked by the NE tone suppressing spikes evoked by the BD tone. Similarly, the reduction in spiking that occurred when the BD and NE tones overlapped in time to form a single composite tone with an amplitude pedestal is the neural equivalent to simultaneous masking and was caused by the sustained inhibition evoked by the NE tone suppressing spikes evoked by the BD tone. The reduction in spiking that occurred when the BD tone followed the NE tone is the neural equivalent to forward masking and was caused by the persistent inhibition evoked by the NE tone suppressing spikes evoked by the BD tone. Interestingly, psychophysical studies have shown that forward and backward masking lasts longer when humans are presented with monotic compared to dichotic stimuli (Elliott, 1962a,b). This behavioural finding mirrors our single-cell neurophysiological results: DTNs tested with monotic paired tone stimulation had greater amounts of leading, sustained and persistent inhibition than the same cells tested with dichotic paired tone stimulation (Figure 4.5). The

importance of these results to normal hearing is that leading, sustained and persistent inhibition are neural mechanisms that can help to explain temporal masking phenomena in human psychophysics.

References

Adams J (1979) Ascending projections to the inferior colliculus. J Comp Neurol 183:519–538.

Aubie B, Becker S, Faure PA (2009) Computational models of millisecond level duration tuning in neural circuits. J Neurosci 29:9255–9270.

Aubie B, Sayegh R, Faure PA (2012) Duration tuning across vertebrates. J Neurosci 32:6364–6372.

Bohn KM, Schmidt-French B, Ma ST, Pollak GD (2008) Syllable acoustics, temporal patterns, and call composition vary with behavioral context in mexican free-tailed bats. J Acoust Soc Am 124:1838.

Boudreau J, Tsuchitani C (1968) Binaural interaction in the cat superior olive s segment. J Neurophysiol 31:442–454.

Casseday JH, Ehrlich D, Covey E (1994) Neural tuning for sound duration: role of inhibitory mechanisms in the inferior colliculus. Science 264:847–850.

Casseday JH, Ehrlich D, Covey E (2000) Neural measurement of sound duration: control by excitatory-inhibitory interactions in the inferior colliculus. J Neurophysiol 84:1475–1487.

Chen GD (1998) Effects of stimulus duration on responses of neurons in the chinchilla inferior colliculus. Hearing Res 112:142–150.

Covey E, Kauer JA, Casseday JH (1996) Whole-cell patch-clamp recording reveals subthreshold sound-evoked postsynaptic currents in the inferior colliculus of awake bats. J Neurosci 16:3009–3018.

Denes P (1955) Effect of duration on the perception of voicing. J Acoust Soc Am 27:761–764.

Ehrlich D, Casseday JH, Covey E (1997) Neural tuning to sound duration in the inferior colliculus of the big brown bat, *Eptesicus fuscus*. J Neurophysiol 77:2360–2372.

Elliott LL (1962a) Backward and forward masking of probe tones of different frequencies. J Acoust Soc Am 34:1116–1117.

Elliott LL (1962b) Backward masking: Monotic and dichotic conditions. J Acoust Soc Am 34:1108–1115.

Faure PA, Fremouw T, Casseday JH, Covey E (2003) Temporal masking reveals properties of sound-evoked inhibition in duration-tuned neurons of the inferior colliculus. J Neurosci 23:3052–3065.

Faure PA, Hoy RR (2000) Auditory symmetry analysis. J Exp Biol 203:3209–3223.

Frederiksen E (1977) Condenser microphones used as sound sources. Bruël Kjær Technical Review 3:3–23.

Fremouw T, Faure PA, Casseday JH, Covey E (2005) Duration selectivity of neurons in the inferior colliculus of the big brown bat: tolerance to changes in sound level. J Neurophysiol 94:1869–1878.

Fuzessery ZM, Hall JC (1999) Sound duration selectivity in the pallid bat inferior colliculus. Hearing Res 137:137–154.

Gadziola MA, Grimsley JM, Faure PA, Wenstrup JJ (2012) Social vocalizations of big brown bats vary with behavioral context. PLOS ONE 7:e44550.

Goldberg JM, Brown PB (1968) Functional organization of the dog superior olivary complex: an anatomical and electrophysiological study. J Neurophysiol 31:639–656.

Kiang NYS (1965) Discharge patterns of single fibers in the cat's auditory nerve MIT Press, Cambridge, MA.

Kuwada S, Batra R, Yin TC, Oliver DL, Haberly LB, Stanford TR (1997) Intracellular recordings in response to monaural and binaural stimulation of neurons in the inferior colliculus of the cat. J Neurosci 17:7565–7581.

Leary CJ, Edwards CJ, Rose GJ (2008) Midbrain auditory neurons integrate excitation and inhibition to generate duration selectivity: an *in vivo* whole-cell patch study in anurans. J Neurosci 28:5481–5493.

Li N, Gittelman JX, Pollak GD (2010) Intracellular recordings reveal novel features of neurons that code interaural intensity disparities in the inferior colliculus. J Neurosci 30:14573–14584.

Lu Y, Jen PHS (2003) Binaural interaction in the inferior colliculus of the big brown bat, *Eptesicus fuscus*. Hearing Res 177:100–110.

Pollack GS, Hoy RR (1979) Temporal pattern as a cue for species-specific calling song recognition in crickets. Science 204:429–432.

Pollak G (2012) Circuits for processing dynamic interaural intensity disparities in the inferior colliculus. Hearing Res 288:47–57.

Rayleigh L (1907) XII. On our perception of sound direction. Philos Mag 13:214–232.

Sayegh R, Aubie B, Fazel-Pour S, Faure PA (2012) Recovery cycle times of inferior colliculus neurons in the awake bat measured with spike counts and latencies. Front Neural Circuits 6:56.

Sayegh R, Aubie B, Faure PA (2011) Duration tuning in the auditory midbrain of echolocating and non-echolocating vertebrates. J Comp Physiol A 197:571–583.

Shimozawa T, Suga N, Hendler P, Schuetze S (1974) Directional sensitivity of echolocation system in bats producing frequency-modulated signals. J. Exp. Biol. 60:53–69.

Simmons J, Kick S, Lawrence B, Hale C, Bard C, Escudie B (1983) Acuity of horizontal angle discrimination by the echolocating bat, *Eptesicus fuscus*. J Comp Physiol A 153:321–330.

Tan ML, Borst JGG (2007) Comparison of responses of neurons in the mouse inferior colliculus to current injections, tones of different durations, and sinusoidal amplitude-modulated tones. J Neurophysiol 98:454–466.

Tollin DJ, Yin TC (2002a) The coding of spatial location by single units in the lateral superior olive of the cat. I. Spatial receptive fields in azimuth. J Neurosci 22:1454–1467.

Tollin DJ, Yin TC (2002b) The coding of spatial location by single units in the lateral superior olive of the cat. II. The determinants of spatial receptive fields in azimuth. J Neurosci 22:1468–1479.

Yost WA (2007) Fundamentals of hearing: An introduction Academic Press, 5th edition.

Zook JM, Casseday JH (1982) Origin of ascending projections to inferior colliculus in the mustache bat, *Pteronotus parnellii*. J Comp Neurol 207:14–28.

Figure 4.1 *(following page)*: Measuring the timecourse of inhibition with paired tone stimulation. (***A***) Dot raster display illustrating how changes in the number and timing of action potentials were used to calculate the onset (T_1) and offset (T_2) of the inhibition evoked by the NE tone with the equations given at the *bottom*. The BD and NE tones and are illustrated with *black bars*, with short bars representing the roving 3 ms BD tone and a single long bar representing the stationary 30 ms NE tone. On every trial the cell was presented with a BD and NE tone that were randomly varied in ISI (for clarity, the NE tone is drawn only once at the bottom), and there were 15 stimulus repetitions per ISI tested. The *grey box* indicates the range of times over which the BD and NE tones were temporally contiguous or overlapping. Note the gap in the cell's response when the BD and NE tones were sufficiently close in time. Circled responses are the 10 trials that were used to calculate the mean $\pm$ SD baseline spike count (1.70 $\pm$ 1.02 spikes per stimulus), baseline FSL (L_{first} = 13.85 $\pm$ 1.19 ms re BD tone onset), and the baseline LSL (L_{last} = 16.09 $\pm$ 1.40 ms re BD tone onset). For this cell, the first ISI with a significant deviation from the baseline spike count or latency was T_1 = -5 ms (determined by LSL), and the longest ISI with a significant deviation from the baseline spike count or latency was T_2 = 37 ms (consensus from all measures). The calculated inhibition start time (T_{start}) was 8.09 ms and the inhibition end time (T_{end}) was 47.85 ms, resulting in an effective duration of inhibition of 39.76 ms. The cell has 5.76 ms of leading inhibition and 9.76 ms of persistent inhibition (see text). (***B***) Mean $\pm$ SE spikes per stimulus as a function of the offset of the BD tone relative to the onset of the NE tone. The *dotted line* represents 50% of the baseline spiking count. The leftmost open circle is the first ISI where the spike count drops to $\leq$50% of baseline with a consecutive data point also $\leq$50% of baseline; this point represents the onset of spike suppression measured with spike counts (T_1 = -3 ms). The rightmost open circle represents the longest ISI, starting from T_1, where the spike count was $\leq$50% of baseline and with the two next consecutive data points also $>$50% of baseline; this point represents the offset of spike suppression measured with spike counts (T_2 = 37 ms). (***C***) Mean $\pm$ SE FSL as a function of the offset of the BD tone relative to the onset of the NE tone. *Dotted lines* represent $\pm$1 SD re baseline FSL. The leftmost open circle is the first ISI with a FSL that deviates by $>$1 SD from baseline with a consecutive data point also $>$1 SD from baseline; this point represents the onset of spike suppression measured with FSL (T_1 = 25 ms). The rightmost open circle is the longest ISI, starting from T_1, where the FSL deviates by $>$1 SD from baseline with the two next consecutive data points within 1 SD of baseline; this point represents the offset of spike suppression measured with FSL (T_2 = 37 ms). (***D***) Mean $\pm$ SE LSL as a function of the offset of the BD tone relative to the onset of the NE tone. *Dotted lines* represent $\pm$1 SD re baseline LSL. The leftmost open circle is the first ISI with a LSL that deviates by $>$1 SD from baseline with a consecutive data point also $>$1 SD from baseline; this point represents the onset of spike suppression measured with LSL (T_1 = -5 ms). The rightmost open circle is the longest ISI, starting from T_1, where the FSL deviates by $>$1 SD from baseline with the two next consecutive data points within 1 SD of baseline; this point represents the offset of spike suppression measured with LSL (T_2 = 37 ms).

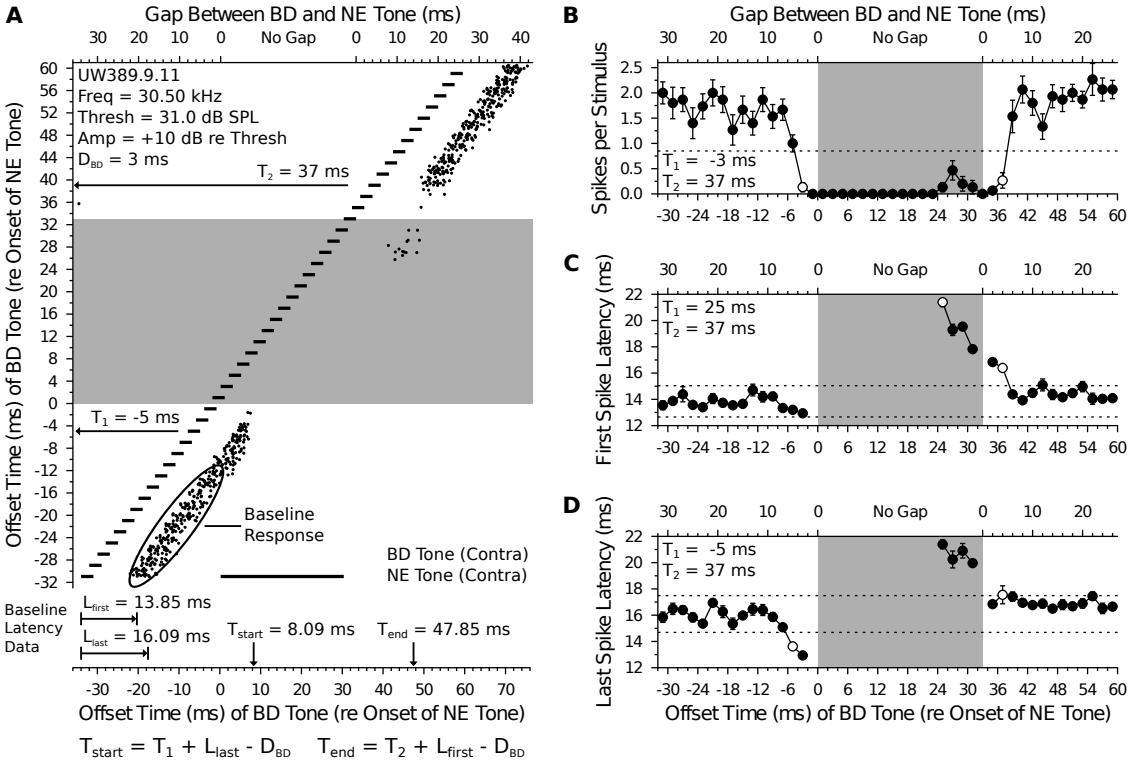
A
Gap Between BD and NE Tone (ms)
UW389.9.11
Freq = 30.50 kHz
Thresh = 31.0 dB SPL
Amp = +10 dB re Thresh
D_BD = 3 ms
T2 = 37 ms
T1 = -5 ms
Baseline Response
BD Tone (Contra)
NE Tone (Contra)
Baseline Latency Data
L_first = 13.85 ms
L_last = 16.09 ms
T_start = 8.09 ms
T_end = 47.85 ms
Offset Time (ms) of BD Tone (re Onset of NE Tone)
T_start = T1 + L_last - D_BD
T_end = T2 + L_first - D_BD
B
Spikes per Stimulus
T1 = -3 ms
T2 = 37 ms
C
First Spike Latency (ms)
T1 = 25 ms
T2 = 37 ms
D
Last Spike Latency (ms)
T1 = -5 ms
T2 = 37 ms

Figure 4.2 *(following page)*: Comparing monotic and dichotic paired tone stimulation. Dot raster display illustrating the spiking responses of a shortpass DTN to monotic (*left*) and dichotic (*right*) paired tone stimulation. (***A***) Spike suppression occurs when the 1 ms BD tone and 10 ms NE tone were presented sufficiently close in time. (***B***) Mean $\pm$ SE spikes per stimulus as a function of the ISI between the BD and NE tones. The first ISI where the spike count was $\leq$50% of baseline was T_1 = 1 ms. The longest IPI where the spike count was $\leq$50% of baseline spike count was T_2 = 49 ms. (***C***) Mean $\pm$ SE FSL as a function of the ISI between the BD and NE tones. The shortest ISI where the FSL deviated by $>$1 SD from baseline was T_1 = 3 ms and the longest ISI where the FSL deviated by $>$1 SD from baseline was T_2 = 49 ms. (***D***) Mean $\pm$ SE LSL as a function of the ISI between the BD and NE tone. The shortest and longest ISIs where the LSL deviated by $>$1 SD from baseline was T_1 = T_2 = 3 ms. In the monotic condition, the shortest T_1 time was 1 ms, calculated with spike counts, and the longest T_2 time was 49 ms, calculated with FSL. (***E***) Dot raster display illustrating the responses of the same DTN to dichotic paired tone stimulation. There was no significant reduction in the (***F***) spike count, (***G***) FSL or (***H***) LSL throughout all ISIs tested. This example shows that there was no ipsilateral-evoked inhibition, therefore the inhibition that creates the duration-selective response in this neuron was purely monaural. In this example the latency of inhibition measured lagged behind the excitatory FSL by 0.79 ms, and the inhibition persisted for 37.21 ms after the offset of the NE tone that evoked it.

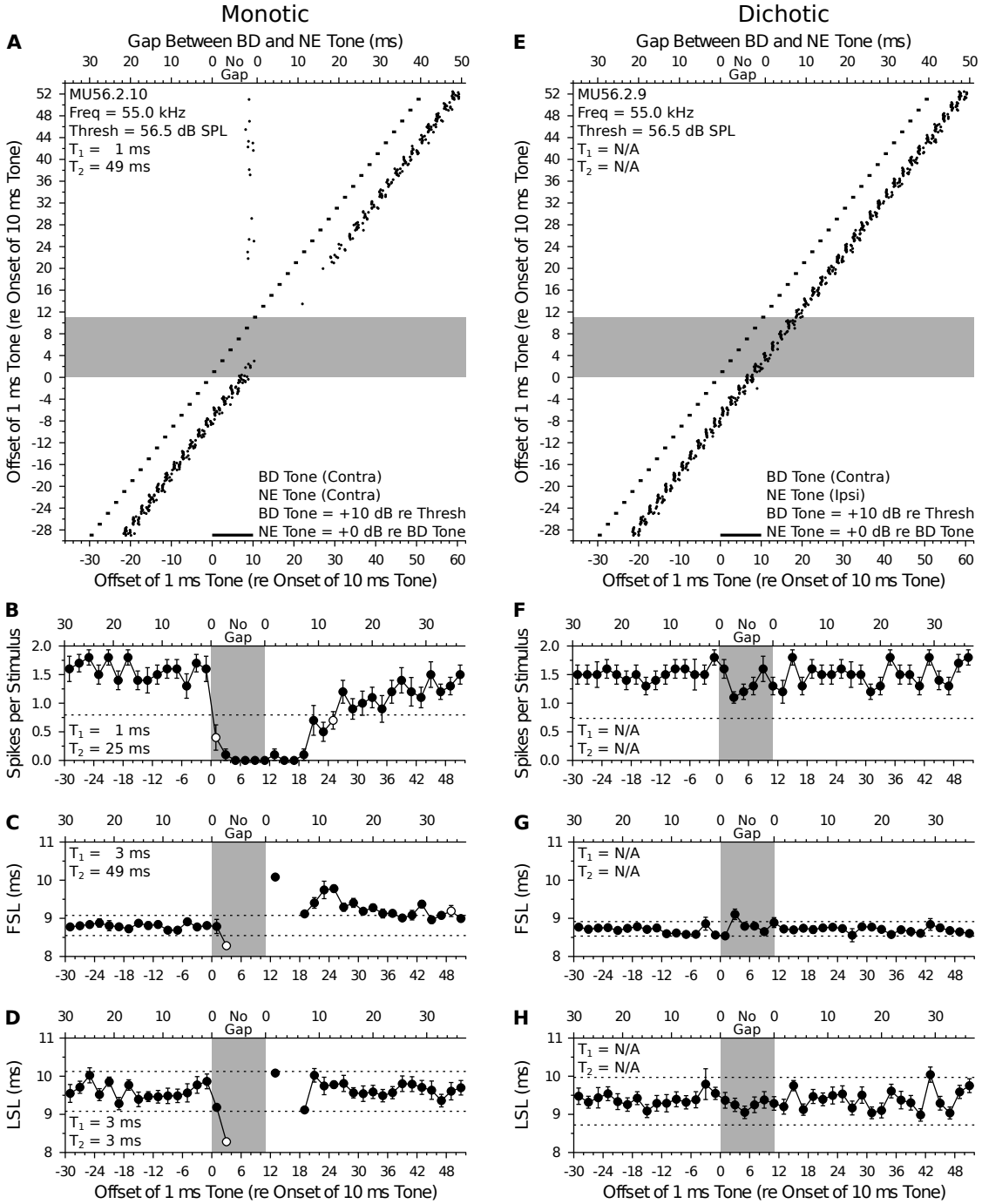
Monotic
Dichotic
A
E
Gap Between BD and NE Tone (ms)
MU56.2.10
Freq = 55.0 kHz
Thresh = 56.5 dB SPL
T1 = 1 ms
T2 = 49 ms
MU56.2.9
T1 = N/A
T2 = N/A
BD Tone (Contra)
NE Tone (Contra)
NE Tone (Ipsi)
BD Tone = +10 dB re Thresh
NE Tone = +0 dB re BD Tone
Offset of 1 ms Tone (re Onset of 10 ms Tone)
B
F
Spikes per Stimulus
T1 = 1 ms
T2 = 25 ms
C
G
FSL (ms)
T1 = 3 ms
T2 = 49 ms
D
H
LSL (ms)
T1 = 3 ms
T2 = 3 ms
No Gap

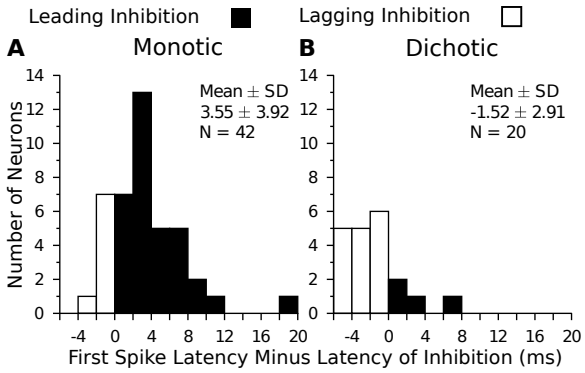

Figure 4.3: Distribution of the difference between the excitatory FSL and the latency of inhibition evoked by the NE tone for DTNs tested with monotic and dichotic paired tone stimulation. Cells with a positive latency difference are illustrated with *solid bars* and represent neurons where the onset of inhibition preceded the baseline FSL (i.e. leading inhibition). Cells with a negative latency difference are illustrated with *open bars* and represent neurons where the onset of inhibition followed the baseline FSL (i.e. lagging inhibition). (***A***) A majority of DTNs tested with monotic paired tone showed leading inhibition. (***B***) A majority of DTNs tested with dichotic paired tone stimulation showed lagging inhibition. The distribution of L_{first} - T_{start} for the monotic and dichotic conditions was significantly different (Mann-Whitney U = 742.00, $p \ll 0.001$).

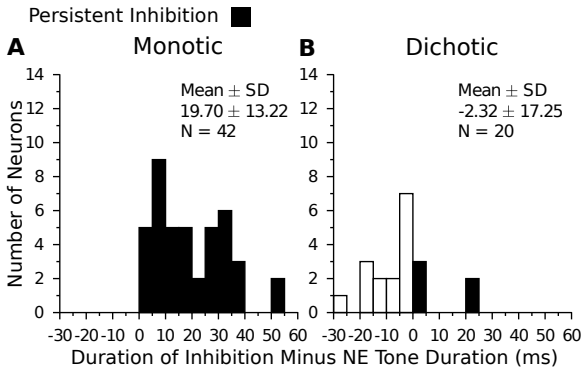

Figure 4.4: Distribution of the difference between the duration of inhibition evoked by the NE tone and the NE tone duration for DTNs tested with monotic and dichotic paired tone stimulation. Cells with a positive latency difference are illustrated with *solid bars* and represent neurons where the duration of inhibition was longer than the duration of the NE tone that evoked the inhibition (i.e. persistent inhibition). Cells with a negative latency difference are illustrated with *open bars* and represent neurons where the duration of inhibition was shorter than the duration of the NE tone that evoked the inhibition (***A***) Every DTN tested with monotic paired tone stimulation showed persistent inhibition (i.e. the duration of inhibition was longer than the duration of the NE tone presented to the contralateral ear). (***B***) The majority of DTNs tested with dichotic paired tone stimulation showed durations of inhibition that were shorter than the duration of the NE tone presented to the ipsilateral ear. The distribution of T_{end} - T_{start} - D_{NE} for the monotic and dichotic conditions was significantly different (Mann-Whitney U = 787.00, $p \ll 0.001$).

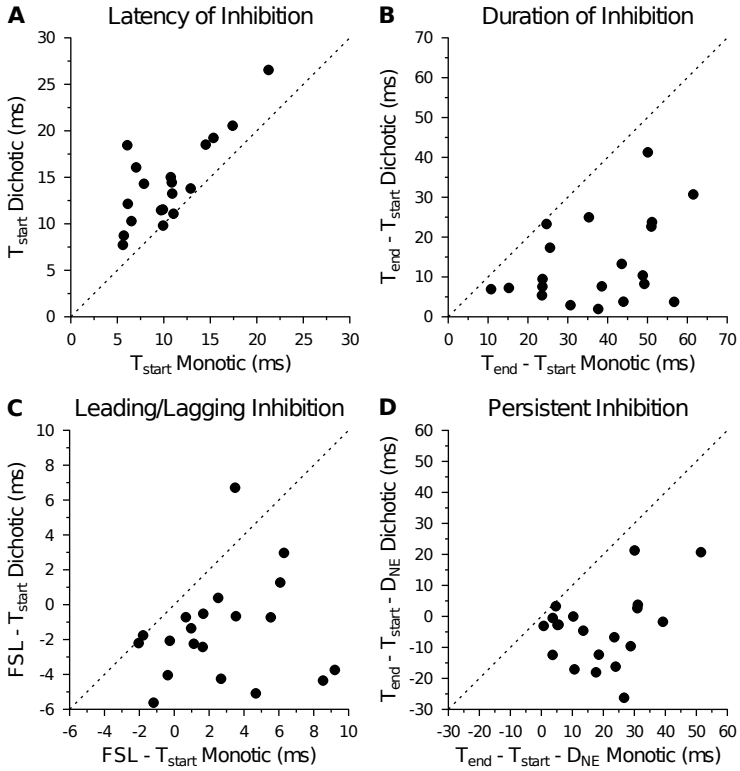

Figure 4.5: Comparing the latency and duration of inhibition evoked in DTNs by monotic and dichotic paired tone stimulation. Only cells that exhibited measurable inhibition in both the monotic and dichotic conditions were included in this paired analysis (n = 20). For each panel, the inhibition recruited monaurally is plotted on the *x-axis* and the inhibition recruited binaurally is plotted on the *y-axis*. The *dotted lines* is the unity line (y=x) and indicates the point monaural inhibition = binaural inhibition. (***A***) The latency of inhibition (T_{start}) recruited by the NE tone was significantly longer in the dichotic condition (Wilcoxon signed-rank test Z = -3.845, $p \ll 0.001$), as evidenced by the majority of points falling above the unity line. (***B***) The duration of inhibition (T_{end} - T_{start}) evoked by the NE tone was significantly longer in the monotic condition (t(19) = 4.605, $p \ll 0.001$), as evidenced by the majority of points falling below the unity line). (***C***) Leading inhibition (L_{first} - T_{start}) was significantly longer for DTNs tested in the monotic condition (Wilcoxon signed-rank test Z = -3.920, $p \ll 0.001$). (***D***) Persistent inhibition (T_{end} - T_{start} - D_{NE}) was significantly longer for DTNs tested in the monotic condition (t(19) = 6.934, $p \ll 0.001$).

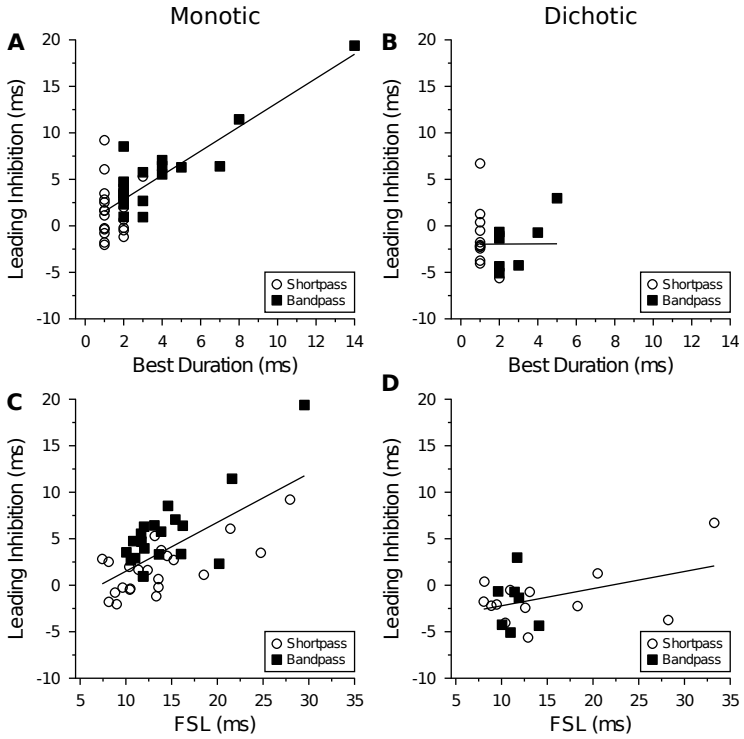

Figure 4.6: Relation of leading inhibition to BD, FSL and duration filter characteristic measured with monotic and dichotic paired tone stimulation. (***A***) The amount of time that inhibition leads excitation, as measured with monotic paired tone stimulation, increases in DTNs tuned to longer BDs ($r^2 = 0.62$; $p \ll 0.001$; $n = 42$). (***B***) In contrast, there was no relation between leading inhibition and BD in DTNs where the latency of NE tone evoked inhibition was measured with dichotic paired tone stimulation ($r^2 = 0.01$; $p = 0.67$; $n = 20$). (***C***) The amount of time that inhibition leads excitation, as measured with with monotic paired tone stimulation, also increases in DTNs with longer baseline FSLs ($r^2 = 0.46$; $p \ll 0.001$; $n = 42$); however, (***D***) there was no relation between leading inhibition and baseline FSL in DTNs where the latency of NE tone evoked inhibition was measured with dichotic paired tone stimulation ($r^2 = 0.18$; $p = 0.065$; $n = 20$).

Figure 4.7 *(following page)*: Effect of increasing the amplitude of the ipsilateral NE tone during dichotic paired tone stimulation. (***A***) Schematic of the stimulus paradigm. A constant amplitude BD tone was presented to the contralateral (excitatory) ear and a variable amplitude NE tone was presented to the ipsilateral ear (dB increase not to scale). (***B***) Mean $\pm$ SE spikes per stimulus as a function of the ISI between the BD and NE tones when the amplitude of the NE tone was +0 *top*, +10 *middle* and +20 dB *bottom* re BD tone. For this shortpass DTN there was no effect of increasing the amplitude of the ipsilateral stimulus on BD tone evoked responses until the NE tone was +20 dB re BD tone. D_{BD} = 2 ms; D_{NE} = 20 ms; Frequency = 32 kHz; Threshold = 32.5 dB SPL; BD tone amplitude = +10 dB re threshold; Repetitions per stimulus = 20. (***C***) Mean $\pm$ SE spikes per stimulus as a function of the ISI between the BD and NE tones when the amplitude of the NE tone was +0 *top*, +10 *middle* and +20 dB *bottom* re BD tone. For this bandpass DTN there was no effect of increasing the amplitude of the ipsilateral stimulus on BD tone evoked responses. D_{BD} = 2 ms; D_{NE} = 20 ms; Frequency = 23 kHz; Threshold = 33 dB SPL; BD tone amplitude = +10 dB re threshold; Repetitions per stimulus = 20. (***D***) Mean + SE duration of inhibition evoked by the ipsilateral NE tone when the amplitude of the NE tone was +0, +10 and +20 dB re BD tone. Increasing the amplitude of the NE tone caused a significant increase on the duration of inhibition evoked through ipsilateral central auditory pathways (Friedman test $\chi^2(2, N = 21) = 24.947$, $p \ll 0.001$).

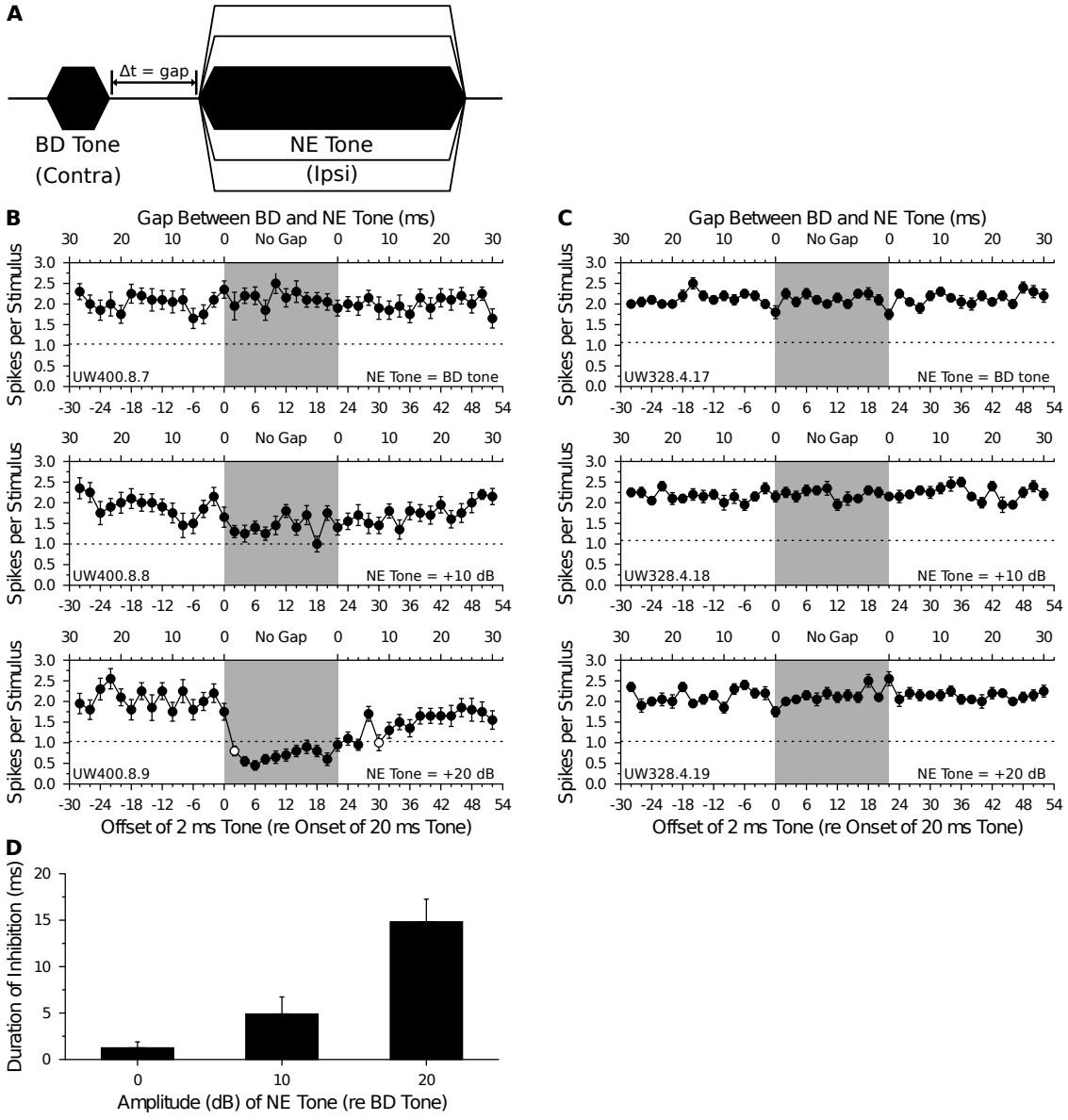
A
Δt = gap
BD Tone
(Contra)
NE Tone
(Ipsi)
B
Gap Between BD and NE Tone (ms)
30 20 10 0 No Gap 0 10 20 30
Spikes per Stimulus
UW400.8.7
NE Tone = BD tone
UW400.8.8
NE Tone = +10 dB
UW400.8.9
NE Tone = +20 dB
-30 -24 -18 -12 -6 0 6 12 18 24 30 36 42 48 54
Offset of 2 ms Tone (re Onset of 20 ms Tone)
C
Gap Between BD and NE Tone (ms)
UW328.4.17
NE Tone = BD tone
UW328.4.18
NE Tone = +10 dB
UW328.4.19
NE Tone = +20 dB
Offset of 2 ms Tone (re Onset of 20 ms Tone)
D
Duration of Inhibition (ms)
0 10 20
Amplitude (dB) of NE Tone (re BD Tone)

5 Dichotic Sound Localization Properties of Duration-Tuned Neurons in the IC of the Big Brown Bat

5.1 Abstract

Electrophysiological studies on duration-tuned neurons (DTNs) in the auditory midbrain (inferior colliculus; IC) have typically used monaural or free-field stimulation focused on the contralateral ear. The proposed mechanisms, inferred from electrophysiological recordings, that underlie duration selectivity do not take binaural stimulation into account. The IC receives convergent input from lower auditory nuclei that process sound from each ear and therefore many neurons in the IC respond to binaural stimulation. Furthermore, DTNs are found in both echolocating and non-echolocating vertebrates and the function(s) that DTNs play in hearing is(are) unknown. One hypothesis is that DTNs are involved in processing echolocation calls in echolocating species and communication calls in non-echolocating species. Processing binaural sound localization cues is thought to be important in echolocation for determining target location. Here we explore some binaural properties of DTNs and compare them to non-DTNs in the IC by measuring responses to dichotic sound localization cues by varying the relative stimulus amplitude presented to each ear (interaural level difference; ILD) and varying the relative time of arrival of the stimulus to each ear (interaural time difference). We then compare the binaural direction-dependent responses of DTNs to non-duration selective neurons in the IC in an attempt to elucidate the role that each ear plays in duration-tuning and the function of DTNs in hearing. We found that a majority of neurons, both DTNs and non-DTNs, in the IC were selective to sound localization stimuli with an emphasis on selectivity to ILDs. Duration-tuned neurons also showed

slightly more ILD selectivity in comparison to non-DTNs. This study provides evidence that DTNs are especially suited to process echolocation calls in the bat. We also discuss the potential role that DTNs might play as spectrotemporal filters in auditory stream segregation in both the bat and in non-echolocating animals.

5.2 Introduction

Neurons throughout the auditory pathway respond selectively to the frequency and amplitude of auditory stimuli. A class of neurons found in the auditory midbrain (inferior colliculus; IC) has been shown to respond to a third auditory parameter: the duration of the auditory stimulus. These so-called duration-tuned neurons (DTNs) have first been observed in the frog (Potter, 1965; Narins and Capranica, 1980), but most thoroughly studied in bat species (Pinheiro et al., 1991; Casseday et al., 1994; Ehrlich et al., 1997; Fuzessery and Hall, 1999; Casseday et al., 2000; Faure et al., 2003; Mora and Kössl, 2004). The presence of DTNs in bats and the finding that their temporal tuning generally matches the duration of echolocation calls has naturally led to the hypothesis that DTNs are involved in echolocation (Ehrlich et al., 1997; Sayegh et al., 2011). Duration-tuned neurons are also found in non-echolocating species (mouse: Brand et al. 2000; Xia et al. 2000, rat: Pérez-González et al. 2006, chinchilla: Chen 1998, guinea pig: Wang et al. 2006, cat:He et al. 1997) tuned to species-specific vocalization durations. Therefore DTNs must play a role outside of echolocation, at least in non-echolocating species. The temporal acuity demands of an echolocating system may have driven the sharpness of duration-tuning in bat DTNs over evolutionary time when compared to sharpness of tuning in non-echolocating species. For a review of duration-tuning across echolocating and non-echolocating vertebrates see Sayegh et al. (2011).

Bats echolocate by vocalizing a biosonar pulse and listening to the returning echoes generated when the biosonar pulse collides with an object. By comparing the time between the onset of the outgoing biosonar pulse and the incoming echoes, the distance between the bat and the object that returned the echo can be calculated neurally (Griffin, 1958; Simmons, 1973). Bats can also glean information about the texture of the object returning the echoes through spectral cues (Simmons et al., 1974; Habersetzer and Vogler, 1983). Some bats

can also detect moving targets by exploiting the physical phenomenon known as Doppler shift (Simmons, 1974). Binaural comparison of the returning echoes reaching each ear is thought to provide cues for localizing target location in azimuth (Shimozawa et al., 1974; Simmons et al., 1983) and spectral cues are exploited for localizing the target in elevation (Wotton et al., 1995; Wotton and Simmons, 2000). Other studies suggest a combination of binaural and spectral cues are involved in localizing targets both in azimuth and elevation (Grinnell and Grinnell, 1965; Fuzessery and Pollak, 1984; Aytekin et al., 2004).

Two binaural cues for azimuthal sound localization are interaural level difference (ILD) and interaural time difference (ITD) (Rayleigh, 1907). When sound originates from a source directly in front of an observer (midline), the amplitude (sound pressure level) of the sound will be equal in both ears. Similarly, the time it takes for the sound to travel to each ear will also be equal. When a sound source is moved to the left of midline, the left ear will receive a larger amplitude sound compared to the right ear and the sound will also reach the left ear before the right ear. The case is opposite for a sound source located to the right of midline. The differences between the level and timing of the sound in each ear can then be used by the central nervous system to compute location of the sound source. ILD and ITD cues are first processed in the superior olivary complex. In mammals, ITD cues are first processed in the medial superior olive (Goldberg and Brown, 1969; Yin and Chan, 1990) and ILD cues are first processed in the lateral superior olive (Boudreau and Tsuchitani, 1968; Park et al., 1996; Tollin and Yin, 2002; Tollin, 2003). Both regions send afferents to the IC (Zook and Casseday, 1982), where ILD seems to also be recalculated in a subset of neurons (Li et al., 2010; Pollak, 2012).

According to the duplex theory of sound localization, ILD cues dominate the localization of high-frequency sounds whereas ITD cues dominate the localization of low-frequency sounds (Rayleigh, 1907). As bat echolocation calls are primarily ultrasonic, we would expect bats to favour ILD cues over ITD cues for sound localization. A behavioural study on

the discrimination ability of *Eptesicus fuscus* (Koay et al., 1998) to differentiate left-source sounds from right-source sounds supports this hypothesis. Our study therefore focused on ILD tuning over ITD, though we explore potential tuning to both cues when possible.

Studies on duration-tuning in the IC have typically used monaural stimulation presented to the contralateral ear (e.g. Fremouw et al., 2005; Pérez-González et al., 2006) or a free-field speaker positioned in the direction of the contralateral sound field (e.g. Jen and Feng, 1999; Jen and Wu, 2006). Prior to this dissertation only two reports in the IC of the mouse and bat has employed dichotic stimulus presentations to elucidate the effect of binaural stimulation on duration-selectivity (Brand et al., 2000; Covey and Faure, 2005). Here we attempt to elucidate the function of DTNs by comparing the response physiology of temporally-selective DTNs and non-temporally-selective neurons to binaural sound localizing cues such as ILD and ITD. If bat DTNs serve a function in echolocation, as the range of temporal tuning and best durations of bat DTNs would suggest, then we expect to find that DTNs are selective to sound localizing cues.

5.3 Methods

5.3.1 Surgical procedures

Electrophysiological recordings were obtained from both male and female big brown bats, *Eptesicus fuscus*. To facilitate multiple recordings and to precisely replicate the position of the bat's head between sessions, a stainless steel post was glued to the skull. Prior to the head-posting surgery, bats were given a subcutaneous injection of buprenorphine (0.03 mL; 0.025 mg/kg). For surgery, bats were first placed in an anaesthesia induction chamber (12 x 10 x 10 cm) where they inhaled a 1 to 5% isofluorane:oxygen mixture (1 L/min). Anesthetized bats were then placed in a foam-lined body restraint within a stereotaxic alignment system with a custom mask for continuous isoflurane inhalation (David Kopf Instru-

ments Model 1900). The hair covering the skull was shaved and the skin disinfected with Betadine® surgical scrub. Local anesthetic (0.2 mL bupivicaine; 5 mg/mL) was injected subcutaneously prior to making a midline incision in the scalp. The temporal muscles were reflected, the skull was scraped clean and swabbed with ethanol, and the post was glued to the skull overlying the cortex with cyanoacrylate superglue (Henkel Loctite Corporation) cured with liquid acrylic hardener (Zipkicker; Pacer Technology). A chlorided silver wire attached to the head post was placed under the temporal muscles and served as the reference electrode. Recordings began 1 to 4 days after surgery. Each bat was used in 1 to 8 sessions lasting ca. 6 to 8 hrs. Recordings were terminated if a bat showed signs of discomfort. Between sessions, the electrode penetration site was covered with a piece of contact lens and Gelfoam coated in Polysporin®. Bats were housed individually in a temperature- and humidity-controlled room. All procedures were approved by the McMaster University Animal Research Ethics Board and were in accordance with the Canadian Council on Animal Care.

5.3.2 Electrophysiological recordings

Electrophysiological recordings were conducted inside a double-walled, sound attenuating booth with electrical shielding (Industrial Acoustics Co., Inc.). Prior to recording, each bat was given a subcutaneous injection of a neuroleptic (0.3 mL; 1:1 mixture of 0.05 mg/mL fentanyl citrate and 2.5 mg/mL droperidol; 19.1 mg/kg). Bats were then placed in a foam-lined body restraint that was suspended by springs within a small animal stereotaxic frame customized for bats (ASI Instruments) mounted atop of an air vibration table (TMC Migro-g). The bat's head was immobilized by securing the headpost to a stainless steel rod attached to a manipulator (ASI Instruments) mounted on the stereotaxic frame. The dorsal surface of the IC was exposed for recording by making a small hole in the skull and dura mater using a scalpel and a sharpened wire. Single-unit extracellular recordings were made with thin-wall

borosilicate glass microelectrodes with a capillary filament (o.d. = 1.2 mm; A-M Systems, Inc.) and filled with 3M NaCl. Typical electrodes resistances ranged from 10 to 30 MΩ. Electrodes were positioned over the dorsal surface of the IC with manual manipulators (ASI Instruments), and were advanced into the brain with a stepping hydraulic micropositioner (Kopf Model 2650). Action potentials were recorded with a Neuroprobe amplifier (A-M Systems Model 1600) whose 10x output was bandpass filtered and further amplified (500 to 1000x) by a Tucker Davis Technologies spike pre-conditioner (TDT PC1; lowpass f_c = 7 kHz; high-pass f_c = 300 Hz). Spike times were logged on a computer by passing the PC1 output to a spike discriminator (TDT SD1) and an event timer (TDT ET1) synchronized to a timing generator (TDT TG6).

5.3.3 Stimulus generation and data collection

Stimulus generation and on-line data collection were controlled with custom software that displayed spike-times as dot raster displays ordered by the acoustic parameter that was varied (see Faure et al., 2003). Briefly, sound pulses (e.g. pure tones) were digitally generated with a two-channel array processor (TDT Apos II; 357 kHz sampling rate) optically interfaced to two digital-to-analog (D/A) converters (TDT DA3-2) whose individual outputs were fed to a low-pass anti-aliasing filter (TDT FT6-2; f_c = 120 kHz), two programmable attenuators (TDT PA5) and two signal mixers (TDT SM5) with equal weighting. The output of each mixer was fed to a manual attenuator (Leader LAT-45) before final amplification (Krohn-Hite Model 7500). Unless stated otherwise, all stimuli were presented monaurally, contralateral to the IC being recorded, using a Brüel & Kjær $\frac{1}{4}$ inch condenser microphone (Type 4939; protective grid on), modified for use as a loudspeaker with a transmitting adaptor (B&K Type UA-9020) to correct for nonlinearities in the transfer function (Frederiksen, 1977). The loudspeaker was positioned ca. 1 mm in front of the external auditory meatus. The output of the speaker, measured with a B&K Type 4138 $\frac{1}{8}$ inch condenser microphone

(90^{o} incidence; grid off) connected to a measuring amplifier (B&K Type 2606) and band-pass filter (K-H Model 3500), was quantified with a sound calibrator (B&K Type 4231) and expressed as decibels sound pressure level (dB SPL re 20 μPa) equivalent to the peak amplitude of continuous tones of the same frequency. The loudspeaker transfer function was flat $\pm$6 dB from 28 to 118 kHz, and there was at least 30 dB attenuation at the ear opposite the source (Ehrlich et al., 1997). For presentation of dichotic stimuli, two matched Brüel & Kjær $\frac{1}{4}$ inch condenser microphones were used. All stimuli had rise/fall times of 0.4 ms shaped with a square cosine function and were presented at a rate of 3 Hz.

Single units were found by searching with short duration pure tones and/or downward FM sweeps. Upon isolation, we determined each cell's best excitatory frequency (BEF), spike threshold, first-spike latency (re signal onset), and for DTNs the cell's best duration (BD) and duration selective response class (i.e. shortpass, bandpass or longpass; see Faure et al. 2003; Fremouw et al. 2005).

5.3.4 Measuring neural responses to sound localization cues

After determining basic monaural response characteristics, we recorded the response of each neuron to varying binaural cues (ILD/ITD). We presented each cell with an excitatory tone at the neuron's BEF, and in the case of DTNs the signal duration was set to the BD of the cell. When measuring the ILD response of a cell, the amplitude of the contralateral stimulus was kept at +10 dB re threshold while the amplitude of the ipsilateral stimulus was varied in 5 dB steps from -30 dB to +30 dB re contralateral stimulus. We then increased the level of the contralateral stimulus to +20 dB re threshold, and again varied the intensity of the ipsilateral ear in 5 dB steps from -30 dB to +30 dB re contralateral stimulus. When measuring the ITD response of a cell, both the contralateral and ipsilateral stimuli were kept at +10 dB threshold. The onset time of the contralateral stimulus was kept constant while the onset of the ipsilateral stimulus was varied in 10 μs steps from -250 μs to 250 μs relative

to the contralateral stimulus. We also measured the ITD function when the stimuli were +20 dB re threshold. The spiking response of each cell to varying binaural cues (ILD/ITD) was normalized by dividing the spiking response by the peak spiking response. This was done so that we could directly compare the response across cells. For completeness, the range of peak spiking responses as a function of cell type is provided in Table 5.1 for ILD cues and Table 5.2 for ITD cues.

For neurons that exhibited a monotonic response to ILD and/or ITD stimuli we fitted a four-parameter sigmoid function in a manner similar to Tollin et al. (2008) and Karcz et al. (2012) using the following equation:

$$F(x) = ((A - D)/(1 + ((x/C)^B))) + D, \tag{5.1}$$

where x is the ILD or ITD value, A is the minimum asymptote, B is the slope factor, C is the inflection point and D is the maximum asymptote. Using the fitted curves, we then determined the ILD_{50} and ITD_{50} point as the ILD/ITD cue eliciting 50% of the maximum spiking response (Wise and Irvine, 1985; Park and Pollak, 1993). We also examined the slope factor (Eq. 5.1 - B variable) to compare the ILD and ITD slopes of DTNs to other non-duration-selective neurons in the IC.

5.4 Results

5.4.1 Response properties

We obtained single unit extracellular recordings of 55 IC neurons from 4 male and 17 female big brown bats. Of these, 28 neurons responded selectively to stimulus duration (28/55; 51% DTNs), while 27 neurons were not duration-selective (27/55; 49% non-DTNs). Duration-tuned neurons were further divided into three categories based on their duration-

tuning responses. Bandpass DTNs respond maximally to a best duration (BD), and the spiking response of these neurons drops to below 50% of maximum spike count at durations both longer and shorter than BD. Shortpass DTNs are similar to bandpass neurons in that they respond maximally to a BD stimulus, but their spiking response only drops below 50% of maximum at durations longer but not shorter than the BD (minimum stimulus duration tested = 1 ms). Longpass DTNs do not have a BD and spike only when the stimulus duration meets or exceeds some minimum duration. Longpass neurons are separate from typical sensory integrating neurons in that they do not respond to stimuli with higher amplitudes (and thus more energy) with more spikes per stimulus and/or a shortening of first-spike latency (Brand et al., 2000; Faure et al., 2003; Pérez-González et al., 2006). In our dataset of 28 DTNs, 20 cells were shortpass, 6 cells were bandpass and 2 cells were longpass. Our non-DTN category consisted of neurons with a spiking response that always remained above 50% of maximum at all durations tested (typically 1 to 25 ms). These non-duration-selective neurons typically responded in a phasic fashion, spiking in response to the onset and/or offset of the stimulus (21/27 neurons; 19 onset responding cells, 2 onset and offset responding cells), or had a sustained response throughout the duration of the stimulus (6/27 neurons).

We observed three general binaural response properties in the population of IC neurons tested. All neurons showed an excitatory response (E) to stimuli presented to the ear contralateral to the recording site. Stimulation of the ear ipsilateral to the recording site elicited either an excitatory response (E), an inhibitory response (I), or no response (O). Of 55 IC neurons tested, 36 cells (65.5%) showed an EI response (excitation to contralateral ear, inhibition to ipsilateral ear), 11 cells (20.0%) showed an EE response and 7 cells (12.7%) showed an EO response.

5.4.2 ILD selectivity

We observed variation of three response profiles when we presented IC neurons with binaural ILD stimuli (Figure 5.1). A number of neurons did not show any selectivity to ILD stimuli as evidenced by the spiking response never dropping below 50% of the maximum (13 of 54 cells at +10 dB; 14 of 47 cells at +20 dB; example DTN, Figure 5.1A). Other neurons had a peaked (maximum) response to a specific ILD value that dropped below 50% of the maximum at positive (contralateral ear louder) and negative (ipsilateral ear louder) ILDs (6 of 54 cells at +10 dB; 5 of 47 cells at +20 dB; example DTN, Figure 5.1B). The final and the most common response type was a monotonic (or near-monotonic) response with eventual saturation to changing ILD values (34 of 54 cells at +10 dB; 28 of 47 cells at +20 dB; example non-DTN, Figure 5.1C). The distribution of ILD response types separated by duration selectivity is reported in Table 5.3. The ILD function is measured as the stimulus level in the contralateral ear minus the stimulus level in the ipsilateral ear. A monotonic-responding neuron was considered contralateral-favouring if its ILD function increased toward positive values. A monotonic-responding cell was considered ipsilateral-favouring if its ILD function increased as the ILD stimulus became increasingly negative. To compare the ILD selectivity of monotonic responding neurons, we fit a four-parameter sigmoid function to each curve and compared the half maximal spiking response (ILD_{50}) and slope factor (See gray curve in Figure 5.1C and Equation 5.1).

Figure 5.2 presents individual neuron responses and the population averages to changing ILD stimuli for both DTNs and non-DTNs. The stimulus level presented to the contralateral ear was fixed at +10 dB (Figure 5.2A,B) or +20 dB re threshold (Figure 5.2C,D), while the stimulus level presented to the ipsilateral ear was varied in 5 dB steps to form binaural ILD stimuli that varied from +30 dB to -30 dB (ILD cue = contralateral stimulus level - ipsilateral stimulus level). The gray region represents the range of biologically relevant

ILD values for an adult *Eptesicus fuscus* (Jen and Chen, 1988). Only neurons that displayed a monotonic or near-monotonic response to varying ILDs were included in this figure and subsequent analyses.

Table 5.3 compares the response parameters of DTNs and non-DTNs tested with ILD stimuli. On average both DTNs and non-DTNs were located at similar electrode depths (dorsal-ventral direction), and had similar acoustic thresholds; however, DTNs exhibited significantly higher BEFs. Table 5.3 also presents the input/output (I/O) response types of DTN and non-DTNs to ILD stimuli. We found that both DTNs and non-DTNs had a similar distribution of ILD-selective and non-ILD selective neurons at +10 dB re threshold (Fisher's exact test, p = 0.5256); however, DTNs were more likely than non-DTNs to be selective for ILDs at +20 dB re threshold (Fisher's exact test, p = 0.0533). To determine the extent to which BEF could account for differences in ILD selectivity between DTNs and non-DTNs, we averaged the BEF of ILD-selective and non-ILD selective neurons regardless of the cell's duration tuning selectivity and found that both groups had similar BEFs (ILD-selective: 45.0 kHz$\pm$2.39, non-ILD-selective: 44.5 kHz$\pm$2.90, p=0.9060). Both DTNs and non-DTNs that had monotonic or near-monotonic responses to ILD cues (see Figure 5.2) had similar ILD_{50} points (Figure 5.3A,B) and slope factors (Figure 5.3C,D) at both +10 dB and +20 dB re threshold.

5.4.3 ITD selectivity

The biologically relevant range of ITDs in the big brown bat are determined by the time it takes for a sound wave to travel from one ear to the other. We measured the interaural distance of five bats and found that it was 12.08 ± 0.84 mm. The largest possible ITD occurs for a sound stimulus at 90° to the left or right and can be calculated using the formula

$$ITD = \frac{d}{c}, \tag{5.2}$$

where d is the interaural distance and c is the speed of sound. Assuming a speed of sound of 344 m/s, and given a mean interaural distance of 12.08 mm, the maximum ITD would be 35.12 μs. Maximum ITD values are larger if the Woodworth formula is used to calculate the travel time around a spherical head

$$ITD = \frac{r}{c}(sin\theta + \theta), \tag{5.3}$$

where r is the spherical radius, c is the speed of sound and θ is the azimuthal sound source angle (Woodworth, 1938). The maximum ITD calculated with the Woodworth equation was 45.14 μs. Therefore, we rounded our estimate of the maximal biologically relevant ITD range to be $\pm$50 μs to account for any additional ITD-amplification potentially caused by the snout and/or pinna as well as to account for variation in the head size of bats.

We observed five response profiles when IC neurons were tested with dichotic ITD stimuli (Figure 5.4). The most common response profile to ITD stimuli recorded was non-selective, characterized by the spiking response never dropping below 50% of the maximum spike count (24 of 45 cells at +10 dB; 15 of 33 cells at +20 dB; example DTN, Figure 5.4A). The least common profile recorded was a peaked response, characterized by a maximum in spiking that dropped below 50% of the maximum at more positive and negative ITD values (1 of 45 cells at +10 dB; 0 of 33 cells at +20 dB; example DTN, Figure 5.4B). We also observed neurons with a monotonic-like profile, characterized by increasing spike counts as the ITD increased (6 of 45 cells at +10 dB; 7 of 33 cells at +20 dB; example DTN, Figure 5.4C). The monotonic/peaked ITD profile was similar to a monotonic-like ITD response, but the ITD response peaked at a limited range of ITDs before the spiking response dropped at more negative ITDs (2 of 45 cells at +10 dB; 3 of 33 cells at +20 dB; example DTN, Figure 5.4D). The final response profile we observed was a cyclical spiking response to increasing ITD cues (12 of 45 cells at +10 dB; 8 of 33 cells at +20 dB; example non-DTN,

Figure 5.4E). A cyclical response was characterized by repeating peaks and troughs where the troughs regularly dropped below 50% of the maximum spike count. We also calculated and plotted an ITD_{50} and slope factor of the fitted four-parameter sigmoid function for neurons that showed a monotonic response to ITD stimuli (Figure 5.4F). One unit was not included in this plot as the neuron did not respond to ITD stimuli until the contralateral stimulus lead by $+500$ μs, which is well outside the biologically relevant range.

Table 5.4 compares the response parameters of DTNs and non-DTNs tested with ITD stimuli. On average, both DTNs and non-DTNs were found at similar electrode depths and had similar acoustic spike thresholds. Cells that were duration-tuned were more likely to have a higher BEF (p=0.0322) than non-DTNs. When we compared the two neuron groups selectivity to ITD-stimuli (monotonic, peaked, a combination of the two, or cyclical) versus non-selectivity with a Fisher's exact test we found both groups had a similar level of ITD selectivity at both $+10$ dB and $+20$ dB above threshold.

5.5 Discussion

Our results show that DTNs in the IC of the big brown bat selectively respond to binaural sound localization cues such as interaural level differences and interaural time of arrival differences. Duration-tuned neurons were as likely as non-temporally-selective neurons in the IC to respond selectively to sound localization cues. This finding suggests that DTNs respond selectively not only to duration, frequency and amplitude but also to the direction of the sound source. Combined with previous findings that DTNs are able to respond to both outgoing pulses and returning echoes (Sayegh et al., 2012), our results strengthen the hypothesis that DTNs in the bat play a role in processing echolocation calls and their returning echoes.

5.5.1 ILD selectivity

The biologically relevant range of ILD values in the big brown bat are determined by the sound shadow created by the size of the bats' head and the amplification of the signal by the pinnae. This head-related transfer function is dependent on stimulus frequency as lower frequency sounds have longer wavelengths and will diffract more easily around the head creating smaller ILDs. Amplification of the external signal by the pinnae is also frequency dependent (Obrist et al., 1993). By placing a small microphone in the ear of a bat and presenting sounds at varying locations we can begin to form a picture of the biologically relevant ILD values to the bat. Koay et al. (1998) found that for a speaker placed 30 degrees from midline, the corresponding ILD was 10 dB for a 32 kHz sound. With a speaker placed 90 degrees from midline, Jen and Chen (1988) found the corresponding ILD to be around 15 dB for 25 kHz and 20-25 dB for sounds of higher frequencies (45-85 kHz). In the IC neurons we tested with monotonic response functions to ILD stimuli (Figure 5.2), the steepest slope of mean the population curve was within the biologically relevant ILD range. We also found that the ILD_{50} values for both DTNs and non-DTNs had a slight ipsilateral bias (negative average ILD_{50}; Figure 5.3A,B), a finding consistent with electrophysiology data from the IC of the Mexican free-tailed bat (Park, 1998; Park et al., 2004). If the slope of the ILD response is important for determining sound source location, then these findings suggest that these neurons are most sensitive to differences in sound sources located around the ipsilateral side of the midline.

5.5.2 ITD selectivity

Previous studies examining the ITD selectivity of bat central auditory neurons have used larger stimulus step sizes and tested a larger range of values (Harnischfeger et al., 1985; Pollak, 1988; Fuzessery, 1997). We opted to test for ITD selectivity using smaller step

sizes (10 μs) within a range that included the biologically relevant ITD cues as well as ITD cues that lie outside of the biologically relevant range. We found that IC neurons in the big brown bat could be categorized in a similar fashion to neurons found in the IC of the pallid bat (Fuzessery, 1997). Our distribution of ITD-selective neurons in the monotonic, peaked and cyclical categories were similar to those reported by Fuzessery (1997). For example, peaked ITD selectivity (Figure 5.4B) was quite rare, with only one neuron falling into that category in both studies. Cyclical neurons were more common (Figure 5.4E), but it is unclear what role cyclical neurons play in bat sound localization as the spiking response varied greatly and unpredictably with small changes in ITDs. Perhaps cyclical neurons play a role in discriminating sound sources separated by very small time delays corresponding to short distances or angles of separation (Simmons, 1973; Simmons et al., 1983). Another common type was the monotonic response, where increasing the stimulus ITD resulted in an increase in spike count (Figure 5.4C). Similar to our analysis on ILD selectivity, we fit the monotonic response with a four-parameter sigmoid function to determine the ITD_{50} and slope factors. We found that nearly half of the ITD_{50} values (Figure 5.4F) fell within the biological ITD range. This finding, combined with a lack of neurons with peaked ITD selectivity, suggests that the slope of the ITD response function through the biologically relevant range is most important for sound localization (McAlpine et al., 2001; Grothe, 2003; Hancock and Delgutte, 2004).

5.5.3 Time-intensity trade-off

We attempted to characterize the ILD and ITD selectivity of DTNs in the IC of *Eptesicus fuscus* in isolation. That is, when we varied the ILD of a stimulus, the ITD was held constant at 0 μs (source located directly in front, 0°). Similarly, when we varied the ITD of a stimulus, the ILD was held constant at 0 dB (source located directly in front, 0°). When bats are actively echolocating in the real world, ITD and ILD are concordant with

one another along with other sound localizing cues (e.g. head-related transfer function). A concordant combination of all sound localization cues might alter the response properties of direction-selective neurons in the IC; however both the duplex theory of sound localization (Rayleigh, 1907) and a behavioural study on the discrimination of sound-localizing cues in the big brown bat (Koay et al., 1998) suggest that the bat primarily relies on ILD cues for localizing high-frequency sounds. Perhaps surprisingly, our data suggest that a subset of neurons in the IC of the big brown bat are able to process ITD information at high frequencies. Other studies on ILD and ITD selectivity in bats have revealed that some ITD stimuli can modulate the response of neurons to ILD cues, and that stimulus ILDs can modulate the response of cells to ITDs (Harnischfeger et al., 1985; Pollak, 1988; Fuzessery, 1997). In *Molossus ater*, this time-intensity trade-off was found to range between 8-50 μs/dB (Harnischfeger et al., 1985), in *Tadarida brasiliensis* the trade-off averaged 47 μs/dB (Pollak, 1988) and in *Antrozous pallidus* the average trade-off was 18 μs/dB (Fuzessery, 1997). This time-intensity trade-off has led to the hypothesis that the mechanism underlying high-frequency ILD sensitivity is based on the relative latencies of the inputs from the excitatory (contralateral) and the inhibitory (ipsilateral) ears (Fuzessery, 1997). Therefore, varying the time of arrival of sound to each ear would directly affect this mechanism. This leads to the idea that the ITD selectivity observed in high-frequency neurons of echolocating bats may simply be a by-product of the relative latency comparison underlying ILD selectivity (Pollak, 1988) rather than an integrative mechanism that combines ILD and ITD selectivity to enhance auditory spatial source discrimination (Harnischfeger et al., 1985). The time-intensity trade-off of neurons in the IC of the big brown bat has yet to be characterized.

5.5.4 Comparing responses of temporally-selective and non-temporally-selective neurons

In this manuscript we have compared the response physiology of temporally-selective DTNs with non-temporally-selective neurons in an attempt to further elucidate the mechanisms of duration selectivity and the function(s) of duration tuning in hearing. We have previously compared the recovery cycle times of DTNs and non-DTNs by measuring the response properties of IC neurons to pairs of excitatory pulses (Sayegh et al., 2012). The recovery cycle time of a neuron is the minimum interstimulus interval required for the responses evoked by the second pulse in a pair to reach 50% of the average response evoked by the first pulse. Recovery cycle times represent the minimum temporal separation required for a cell to effectively respond to both sounds in a pair of pulses, and the recovery time of a cell is influenced by the effects of synaptic inhibition (Lu et al., 1997; Zhou and Jen, 2003). Our previous comparison of the recovery cycle times of temporally-selective and non-temporally-selective neurons revealed that in a subset of DTNs (bandpass neurons) longer-lasting inhibition was evoked following the presentation of an excitatory stimulus compared to the evoked inhibition in a general population of IC neurons that were not temporally-selective (Sayegh et al., 2012). We also showed that the range of recovery cycle times in both DTNs and non-DTNs correlate with biologically relevant echolocation pulse and echo delays. In a review on duration tuning neural responses across vertebrates, we have also shown that the range of durations that DTNs respond to in echolocating bats match the range of vocalization durations emitted during foraging (Sayegh et al., 2011), leading to the hypothesis that DTNs may be especially well-suited for processing echolocation signals. Binaural timing and level cues are thought to be especially relevant for localizing the source of the faint returning echoes (Shimozawa et al., 1974; Simmons et al., 1983). We examined the response physiology of DTNs and non-DTNs to the binaural

sound localizing cues of ITD and ILD and found that DTNs and non-DTNs had similar ILD_{50} tuning and similar slopes in the ILD response curves; however, DTNs were more likely than non-DTNs to show ILD selectivity when we increased the amplitude of the contralateral stimulus to +20 dB re threshold (see Table 5.3) – a finding that is consistent with this hypothesis. Future studies comparing the responses of DTNs and non-DTNs should consider testing the robustness of ILD selectivity at even higher stimulus amplitudes above threshold.

5.5.5 Possible function(s) of DTNs in echolocation

Duration-tuned neurons in the IC of *E. fuscus* were more likely to show ILD selectivity compared to non-DTNs. Bat DTNs have previously been shown to respond to pairs of stimulus pulses that mimic the outgoing biosonar pulses and later returning echoes at pulse-echo intervals (delays) typical of echolocation (Sayegh et al., 2012). Selectivity to ILD cues in the bat IC have previously been shown to be more tolerant to changes in stimulus amplitude compared to ILD selective neurons in the LSO (Park et al., 2004). Tolerance to changing stimulus amplitude allows for a consistent response to returning echoes that vary in attenuation. These findings suggest that DTNs may be fully equipped to meet the signal processing demands of the central auditory system of an echolocating animal because they can respond to both outgoing pulses and incoming echoes as well as respond selectively to the location of the echo source. The IC has efferents that project to a number of auditory and non-auditory nuclei including, but not limited to, the medial geniculate body, the auditory cortex, the central gray, the lateral pontine nuclei, the superior colliculus, and the contralateral IC (Schweizer, 1981; Powell and Hatton, 2004). Although the efferent projections of the sub-population of duration-selective neurons in the IC have not been studied, doing so may give us greater insight as to their possible function(s) in the central auditory system. It is possible, that DTNs provide other upstream neurons with a mechanism by

which to segregate successive echolocation calls and their echoes by the duration of the acoustic stimulus. By discovering where DTNs in particular project their axons to, we can begin to understand where DTNs play a role and perhaps what role DTNs play in hearing.

In the lab, bats have been trained to discriminate simulated echoes that were successively increased or decreased in echo delay from simulated echoes with randomized echo delays (Moss and Surlykke, 2001). This suggests that bats can keep track of the delay of successive echoes and also suggests that their auditory system may be capable of auditory stream segregation to track multiple acoustic objects in three dimensional space. Auditory stream segregation is normally thought to occur when successive sounds are sufficiently separated in frequency (high vs. low frequency) and/or when the sounds are presented rapidly (Bregman and Campbell, 1971). Responses of DTNs may provide an alternative form of temporal stream segregation.

A number of bat species, including *Eptesicus fuscus*, have been observed to separate successive echolocation pulses by shifting the frequency of one pulse from the frequency of the second pulse, especially if the returning echoes might overlap in time (Kössl et al., 1999; Moss and Surlykke, 2001; Petrites et al., 2009; Hiryu et al., 2010; Ratcliffe et al., 2011; DiCecco et al., 2013). For example, *Saccopteryx bilineata* use low-high echolocation "strobe group pairs" when hunting (Ratcliffe et al., 2011), perhaps because the acoustic demands of foraging require the bat to localize multiple targets (i.e. to capture moving prey and to avoid stationary obstacles), whereas the processing demands outside of foraging might be less severe (e.g. obstacle avoidance only). To our knowledge, no behavioural experiments have been conducted on humans or non-human animals to test the hypothesis that auditory stream segregation could occur on the basis of stimulus duration alone. As frequency tuning at the level of auditory nerve fibres and beyond could provide a neural mechanism for segregating streams of sounds differing in frequency, DTNs could provide a neural mechanism for the segregating streams of sounds (or components thereof) differing

in duration.

5.6 Summary

1. Although not unique to bats, we hypothesized that DTNs might be especially suited for processing echolocation calls and their echos, as the durations that DTNs are tuned to correlate with the durations of their echolocation signals. Accurately localizing the source of the returning echoes is important for echolocating bats to navigate in roosting sites and while hunting. Bats use ILDs and ITDs to localize returning echoes in azimuth.

2. We compared the ILD selectivity of DTNs and non-DTNs in the IC of the big brown bat and found that the distribution of ILD_{50} response curves and their slopes did not vary significantly across cell types (i.e. DTN vs. non-DTN); however, DTNs were more likely than non-DTNs to respond selectively to ILD stimuli when the stimulus amplitude at the contralateral ear was +20 dB above threshold.

3. Both DTNs and non-DTNs showed a similar level of ITD selectivity. Nearly half of the neurons with monotonic ITD response functions had ITD_{50} points that fell between the estimated biological range of ITD cues, meaning that the steepest slopes of the spiking response to ITD was within the biological range.

4. Here we show that many DTNs have responses that are selective to ITD or ILD cues and thus the cells are sensitive to the location of a sound source. Thus, the role that DTNs play in echolocation may be to segregate outgoing biosonar pulses and their returning echoes by stimulus frequency, amplitude, duration and source location. In non-echolocating animals, including humans, DTNs may serve as spatio-spectro-temporal filters and provide a potential neural mechanism underlying auditory stream segregation.

References

Aytekin, M., Grassi, E., Sahota, M., and Moss, C. F. (2004). The bat head-related transfer function reveals binaural cues for sound localization in azimuth and elevation. *J Acoust Soc Am*, 116(6):3594–3605.

Boudreau, J. and Tsuchitani, C. (1968). Binaural interaction in the cat superior olive s segment. *J Neurophysiol*, 31(3):442–454.

Brand, A., Urban, A., and Grothe, B. (2000). Duration tuning in the mouse auditory midbrain. *J Neurophysiol*, 84(4):1790–1799.

Bregman, A. and Campbell, J. (1971). Primary auditory stream segregation and perception of order in rapid sequences of tones. *J. Exp. Psychol.*, 89(2):244–249.

Casseday, J. H., Ehrlich, D., and Covey, E. (1994). Neural tuning for sound duration: role of inhibitory mechanisms in the inferior colliculus. *Science*, 264(5160):847–850.

Casseday, J. H., Ehrlich, D., and Covey, E. (2000). Neural measurement of sound duration: control by excitatory-inhibitory interactions in the inferior colliculus. *J Neurophysiol*, 84(3):1475–1487.

Chen, G.-D. (1998). Effects of stimulus duration on responses of neurons in the chinchilla inferior colliculus. *Hearing Res*, 112:142–150.

Covey, E. and Faure, P. A. (2005). Neural mechanisms for analyzing temporal patterns in echolocating bats. In Pressnitzer, D., Cheveigné, A. d., McAdams, S., and Collet, L., editors, *Auditory signal processing: physiology, psychoacoustics, and models*, pages 251–257. Springer Verlag, New York.

DiCecco, J., Gaudette, J. E., and Simmons, J. A. (2013). Multi-component separation and analysis of bat echolocation calls. *J Acoust Soc Am*, 133:538.

Ehrlich, D., Casseday, J. H., and Covey, E. (1997). Neural tuning to sound duration in the inferior colliculus of the big brown bat, *Eptesicus fuscus*. *J Neurophysiol*, 77(5):2360–2372.

Faure, P. A., Fremouw, T., Casseday, J. H., and Covey, E. (2003). Temporal masking reveals properties of sound-evoked inhibition in duration-tuned neurons of the inferior colliculus. *J Neurosci*, 23(7):3052–3065.

Frederiksen, E. (1977). Condenser microphones used as sound sources. *Bruël Kjær Technical Review*, 3:3–23.

Fremouw, T., Faure, P. A., Casseday, J. H., and Covey, E. (2005). Duration selectivity of neurons in the inferior colliculus of the big brown bat: tolerance to changes in sound level. *J Neurophysiol*, 94(3):1869–1878.

Fuzessery, Z. (1997). Acute sensitivity to interaural time differences in the inferior colliculus of a bat that relies on passive sound localization. *Hearing Res*, 109(1):46–62.

Fuzessery, Z. M. and Hall, J. C. (1999). Sound duration selectivity in the pallid bat inferior colliculus. *Hearing Res*, 137(1-2):137–154.

Fuzessery, Z. M. and Pollak, G. D. (1984). Neural mechanisms of sound localization in an echolocating bat. *Science*, 225(4663):725–728.

Goldberg, J. and Brown, P. (1969). Response of binaural neurons of dog superior olivary complex to dichotic tonal stimuli: some physiological mechanisms of sound localization. *J Neurophysiol*.

Griffin, D. R. (1958). *Listening in the Dark: The acoustic orientation of bats and men*. Yale University Press, New Haven.

Grinnell, A. and Grinnell, V. (1965). Neural correlates of vertical localization by echolocating bats. *J. Physiol.*, 181(4):830.

Grothe, B. (2003). New roles for synaptic inhibition in sound localization. *Nat. Rev. Neurosci.*, 4(7):540–550.

Habersetzer, J. and Vogler, B. (1983). Discrimination of surface-structured targets by the echolocating batmyotis myotis during flight. *J Comp Physiol A*, 152(2):275–282.

Hancock, K. and Delgutte, B. (2004). A physiologically based model of interaural time difference discrimination. *J Neurosci*, 24(32):7110–7117.

Harnischfeger, G., Neuweiler, G., and Schlegel, P. (1985). Interaural time and intensity coding in superior olivary complex and inferior colliculus of the echolocating bat molossus ater. *J Neurophysiol*, 53(1):89–109.

He, J., Hashikawa, T., Ojima, H., and Kinouchi, Y. (1997). Temporal integration and duration tuning in the dorsal zone of cat auditory cortex. *J Neurosci*, 17(7):2615–2625.

Hiryu, S., Bates, M., Simmons, J., and Riquimaroux, H. (2010). FM echolocating bats shift frequencies to avoid broadcast–echo ambiguity in clutter. *Proc. Natl. Acad. Sci. USA*, 107(15):7048–7053.

Jen, P. and Chen, D. (1988). Directionality of sound pressure transformation at the pinna of echolocating bats. *Hearing Res*, 34(2):101–117.

Jen, P. H.-S. and Feng, R. B. (1999). Bicuculline application affects discharge pattern and pulse-duration tuning characteristics of bat inferior collicular neurons. *J Comp Physiol A*, 184:185–194.

Jen, P. H.-S. and Wu, C. H. (2006). Duration selectivity organization in the inferior colliculus of the big brown bat, *Eptesicus fuscus*. *Brain Res.*, 1108(1):76–87.

Karcz, A., Rübsamen, R., and Kopp-Scheinpflug, C. (2012). Low-threshold potassium currents stabilize IID-sensitivity in the inferior colliculus. *Front Neural Circuits*, 6.

Koay, G., Kearns, D., Heffner, H., and Heffner, R. (1998). Passive sound-localization ability of the big brown bat (*Eptesicus fuscus*). *Hearing Res*, 119(1):37–48.

Kössl, M., Mora, E., Coro, F., and Vater, M. (1999). Two-toned echolocation calls from *Molossus molossus* in Cuba. *J. Mammal.*, pages 929–932.

Li, N., Gittelman, J. X., and Pollak, G. D. (2010). Intracellular recordings reveal novel features of neurons that code interaural intensity disparities in the inferior colliculus. *J Neurosci*, 30(43):14573–14584.

Lu, Y., Jen, P. H.-S., and Zheng, Q. Y. (1997). GABAergic disinhibition changes the recovery cycle of bat inferior collicular neurons. *J Comp Physiol A*, 181(4):331–341.

McAlpine, D., Jiang, D., Palmer, A., et al. (2001). A neural code for low-frequency sound localization in mammals. *Nat. Neurosci.*, 4(4):396–401.

Mora, E. C. and Kössl, M. (2004). Ambiguities in sound duration selectivity by neurons in the inferior colliculus of the bat *Molossus molossus* from Cuba. *J Neurophysiol*, 91:2215–2226.

Moss, C. F. and Surlykke, A. (2001). Auditory scene analysis by echolocation in bats. *J Acoust Soc Am*, 110(4):2207–2226.

Narins, P. M. and Capranica, R. R. (1980). Neural adaptations for processing the two-note call of the Puerto Rican treefrog, *Eleutherodactylus coqui*. *Brain Behav. Evol.*, 17(1):48–66.

Obrist, M., Fenton, M., Eger, J., and Schlegel, P. (1993). What ears do for bats: a comparative study of pinna sound pressure transformation in chiroptera. *J. Exp. Biol.*, 180(1):119–152.

Park, T. (1998). IID sensitivity differs between two principal centers in the interaural intensity difference pathway: the LSO and the IC. *J Neurophysiol*, 79(5):2416–2431.

Park, T., Grothe, B., Pollak, G., Schuller, G., and Koch, U. (1996). Neural delays shape selectivity to interaural intensity differences in the lateral superior olive. *J Neurosci*, 16(20):6554–6566.

Park, T., Klug, A., Holinstat, M., and Grothe, B. (2004). Interaural level difference processing in the lateral superior olive and the inferior colliculus. *J Neurophysiol*, 92(1):289–301.

Park, T. and Pollak, G. (1993). Gaba shapes sensitivity to interaural intensity disparities in the mustache bat's inferior colliculus: implications for encoding sound location. *J Neurosci*, 13(5):2050–2067.

Pérez-González, D., Malmierca, M. S., Moore, J. M., Hernández, O., and Covey, E. (2006). Duration selective neurons in the inferior colliculus of the rat: topographic distribution and relation of duration sensitivity to other response properties. *J Neurophysiol*, 95(2):823–836.

Petrites, A. E., Eng, O. S., Mowlds, D. S., Simmons, J. A., and DeLong, C. M. (2009). Interpulse interval modulation by echolocating big brown bats (*Eptesicus fuscus*) in different densities of obstacle clutter. *J Comp Physiol A*, 195:603–617.

Pinheiro, A. D., Wu, M., and Jen, P. H. (1991). Encoding repetition rate and duration in the

inferior colliculus of the big brown bat, *Eptesicus fuscus*. *J Comp Physiol A*, 169(1):69–85.

Pollak, G. (1988). Time is traded for intensity in the bat's auditory system. *Hearing Res*, 36(2):107–124.

Pollak, G. (2012). Circuits for processing dynamic interaural intensity disparities in the inferior colliculus. *Hearing Res*, 288(1):47–57.

Potter, H. D. (1965). Patterns of acoustically evoked discharges of neurons in the mesencephalon of the bullfrog. *J Neurophysiol*, 28(6):1155–1184.

Powell, E. and Hatton, J. (2004). Projections of the inferior colliculus in cat. *J Comp Neurol*, 136(2):183–192.

Ratcliffe, J., Jakobsen, L., Kalko, E., and Surlykke, A. (2011). Frequency alternation and an offbeat rhythm indicate foraging behavior in the echolocating bat, *Saccopteryx bilineata*. *J Comp Physiol A*, 197(5):413–423.

Rayleigh, L. (1907). XII. On our perception of sound direction. *Philos Mag*, 13(74):214–232.

Sayegh, R., Aubie, B., and Faure, P. A. (2011). Duration tuning in the auditory midbrain of echolocating and non-echolocating vertebrates. *J Comp Physiol A*, 197:571–583.

Sayegh, R., Aubie, B., Fazel-Pour, S., and Faure, P. A. (2012). Recovery cycle times of inferior colliculus neurons in the awake bat measured with spike counts and latencies. *Front Neural Circuits*, 6:56.

Schweizer, H. (1981). The connections of the inferior colliculus and the organization of the brainstem auditory system in the greater horseshoe bat (*Rhinolophus ferrumequinum*). *J Comp Neurol*, 201(1):25–49.

Shimozawa, T., Suga, N., Hendler, P., and Schuetze, S. (1974). Directional sensitivity of echolocation system in bats producing frequency-modulated signals. *J. Exp. Biol.*, 60(1):53–69.

Simmons, J. (1973). The resolution of target range by echolocating bats. *J Acoust Soc Am*, 54(1):157–173.

Simmons, J. (1974). Response of the doppler echolocation system in the bat, rhinolophus ferrumequinum. *J Acoust Soc Am*, 56(2):672–682.

Simmons, J., Kick, S., Lawrence, B., Hale, C., Bard, C., and Escudie, B. (1983). Acuity of horizontal angle discrimination by the echolocating bat, *Eptesicus fuscus*. *J Comp Physiol A*, 153(3):321–330.

Simmons, J., Lavender, W., Lavender, B., Doroshow, C., Kiefer, S., Livingston, R., Scallet, A., and Crowley, D. (1974). Target structure and echo spectral discrimination by echolocating bats. *Science*, 186(4169):1130.

Tollin, D. (2003). The lateral superior olive: a functional role in sound source localization. *The neuroscientist*, 9(2):127–143.

Tollin, D., Koka, K., and Tsai, J. (2008). Interaural level difference discrimination thresholds for single neurons in the lateral superior olive. *J Neurosci*, 28(19):4848–4860.

Tollin, D. J. and Yin, T. C. (2002). The coding of spatial location by single units in the lateral superior olive of the cat. I. Spatial receptive fields in azimuth. *J Neurosci*, 22(4):1454–1467.

Wang, J., van Wijhe, R., Chen, Z., and Yin, S. (2006). Is duration tuning a transient process in the inferior colliculus of guinea pigs? *Brain Res.*, 1114(1):63–74.

Wise, L. and Irvine, D. (1985). Topographic organization of interaural intensity difference sensitivity in deep layers of cat superior colliculus: implications for auditory spatial representation. *J Neurophysiol*, 54(2):185–211.

Woodworth, R. (1938). *Experimental psychology*. Holt, New York.

Wotton, J., Haresign, T., and Simmons, J. (1995). Spatially dependent acoustic cues generated by the external ear of the big brown bat, *Eptesicus fuscus*. *J Acoust Soc Am*, 98:1423.

Wotton, J. and Simmons, J. (2000). Spectral cues and perception of the vertical position of targets by the big brown bat, eptesicus fuscus. *J Acoust Soc Am*, 107:1034.

Xia, Y.-F., Qi, Z.-H., and Shen, J.-X. (2000). Neural representation of sound duration in the inferior colliculus of the mouse. *Acta Oto-laryngol.*, 120:638–643.

Yin, T. and Chan, J. (1990). Interaural time sensitivity in medial superior olive of cat. *J Neurophysiol*, 64(2):465–488.

Zook, J. and Casseday, J. (1982). Origin of ascending projections to inferior colliculus in the mustache bat, *Pteronotus parnellii*. *J Comp Neurol*, 207(1):14.

Table 5.1: Peak spikes per stimulus to ILD stimuli.

		Peak Spiking Response	
Cell Type	n	Range	Mean±SE
Shortpass	20	0.90-6.95	2.40±0.29
Bandpass	5	0.87-3.33	1.98±0.45
Longpass	2	3.20-6.35	4.78±1.57
Phasic	21	0.87-4.67	2.18±0.24
Sustained	6	0.65-2.30	1.54±0.22

Table 5.2: Peak spikes per stimulus to ITD stimuli.

		Peak Spiking Response	
Cell Type	n	Range	Mean±SE
Shortpass	16	1.10-7.40	2.44±0.37
Bandpass	5	0.73-2.50	1.61±0.35
Longpass	2	1.70-2.33	2.02±0.32
Phasic	18	1.10-7.40	1.56±0.23
Sustained	4	0.60-1.70	1.36±0.26

Table 5.3: Summary statistics of ILD-tuning in DTN and non-DTN neurons.

	DTN		Non-DTN			
Parameter	Mean±SE	n	Mean±SE	n	Test	Significance
Depth (μm)	1313.00±61.75	27	1209.11±69.39	27	t-test	p = 0.2775
Frequency (kHz)	48.26±2.63	27	40.30±2.40	27	t-test	**p = 0.0326**
Threshold (dB SPL)	45.63±2.31	27	40.85±3.57	27	t-test	p = 0.2754
Response Type	Shortpass	20/27	Phasic	21/27		
	Bandpass	5/27	Sustained	6/27		
	Longpass	2/27				
ILD Selectivity 10dB>thresh.	Monotonic	18/27	Monotonic	17/27	fisher's test	p = 0.5256
	Peaked	4/27	Peaked	2/27		
	Not-Selective	5/27	Not-Selective	8/27		
ILD_{50}(dB) 10dB>thres.	-2.33±2.98	18	-5.70±3.46	17	t-test	p = 0.4775
ILD Slope Factor 10dB>thres.	37.29±11.80	18	37.92±13.02	17	t-test	p = 0.9726
ILD Selectivity 20dB>thresh.	Monotonic	18/25	Monotonic	10/22	fisher's test	**p = 0.0533**
	Peaked	3/25	Peaked	2/22		
	Not-Selective	4/25	Not-Selective	10/22		
ILD_{50}(dB) 20dB>thres.	2.20±3.01	18	-2.33±5.45	10	t-test	p = 0.4529
ILD Slope Factor 20dB>thres.	35.05±9.31	18	15.26±8.78	10	t-test	p = 0.1879

Table 5.4: Summary statistics of ITD-tuning in DTN and non-DTN neurons.

	DTN		Non-DTN			
Parameter	Mean±SE	n	Mean±SE	n	Test	Significance
Depth (μm)	1303.83±61.04	23	1184.50±68.27	22	t-test	p = 0.2087
Frequency (kHz)	48.96±2.61	23	40.86±2.43	22	t-test	**p = 0.0322**
Threshold (dB SPL)	44.04±2.71	23	40.82±3.90	22	t-test	p = 0.5070
Response Type	Shortpass	16/23	Phasic	18/22		
	Bandpass	5/23	Sustained	4/22		
	Longpass	2/23				
ITD Selectivity 10dB>thresh.	Monotonic	5/23	Monotonic	1/22	fisher's test	p = 0.5544
	Peaked	1/23	Peaked	0/22		
	Monotonic/Peaked	1/23	Monotonic/Peaked	1/22		
	Cyclical	5/23	Cyclical	7/22		
	Not-Selective	11/23	Not-Selective	13/22		
ITD Selectivity 20dB>thresh.	Monotonic	6/17	Monotonic	1/16	fisher's test	p = 1.0000
	Peaked	0/17	Peaked	0/16		
	Monotonic/Peaked	1/17	Monotonic/Peaked	2/16		
	Cyclical	3/17	Cyclical	5/16		
	Not-Selective	7/17	Not-Selective	8/16		

Figure 5.1 *(following page)*: Example responses of IC neurons to binaural interaural level difference (ILD) stimuli. Responses are plotted as the ratio of the maximum spiking response $\pm$standard error (SE). The shaded gray region in each panel represents stimuli presented within the biological range of ILD cues. (A) An example of a DTN not selective to ILD-stimuli. Here we see a $>$50% of maximum spiking response at all ILDs tested. (B) An example of a DTN with a peak-type ILD response. Here we see a maximum response to a 0 ILD cue (contralateral stimulus amplitude = ipsilateral stimulus amplitude), and that spiking response drops to below 50% spiking rate at increasing positive and negative ILD cues. (C) An example of a non-DTN with a monotonic response to ILD stimuli. Here we see the neuron's spiking rate increases near-monotonically as the ILD value increases (contralateral stimulus amplitude $>$ ipsilateral stimulus amplitude). The gray curve represents the fitted four-parameter sigmoid function. The ILD_{50} of the fitted curve is $+9.66$ dB and the slope factor is 16.6696. The fitted four-parameter sigmoid function was highly correlated with the raw curve (r = 0.10, p$\ll$0.001).

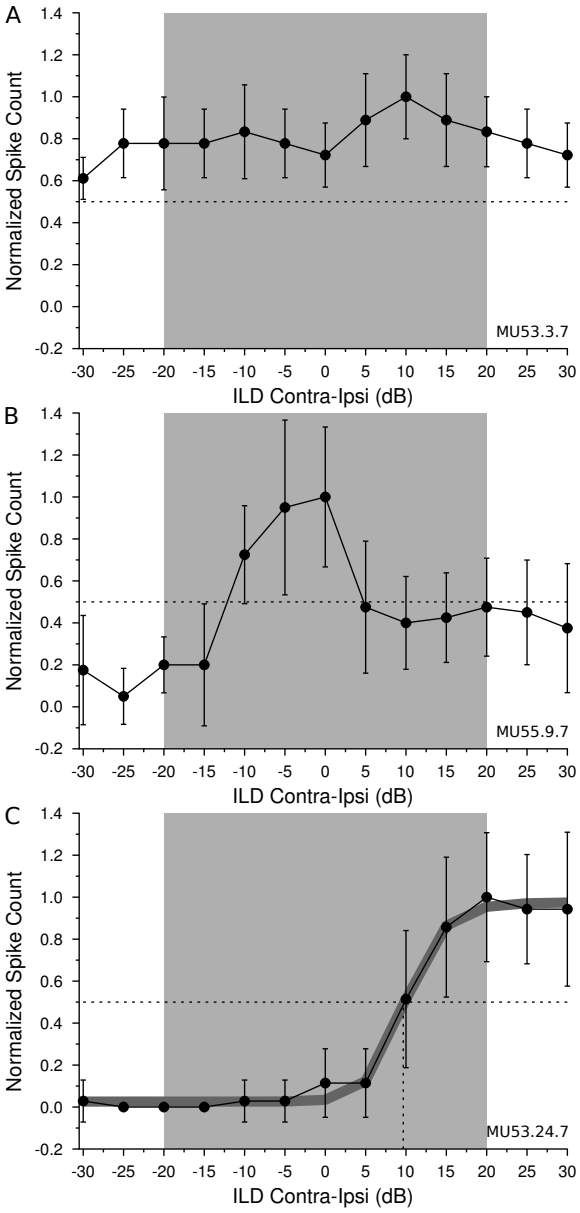
A
B
C
Normalized Spike Count
ILD Contra-Ipsi (dB)
MU53.3.7
MU55.9.7
MU53.24.7

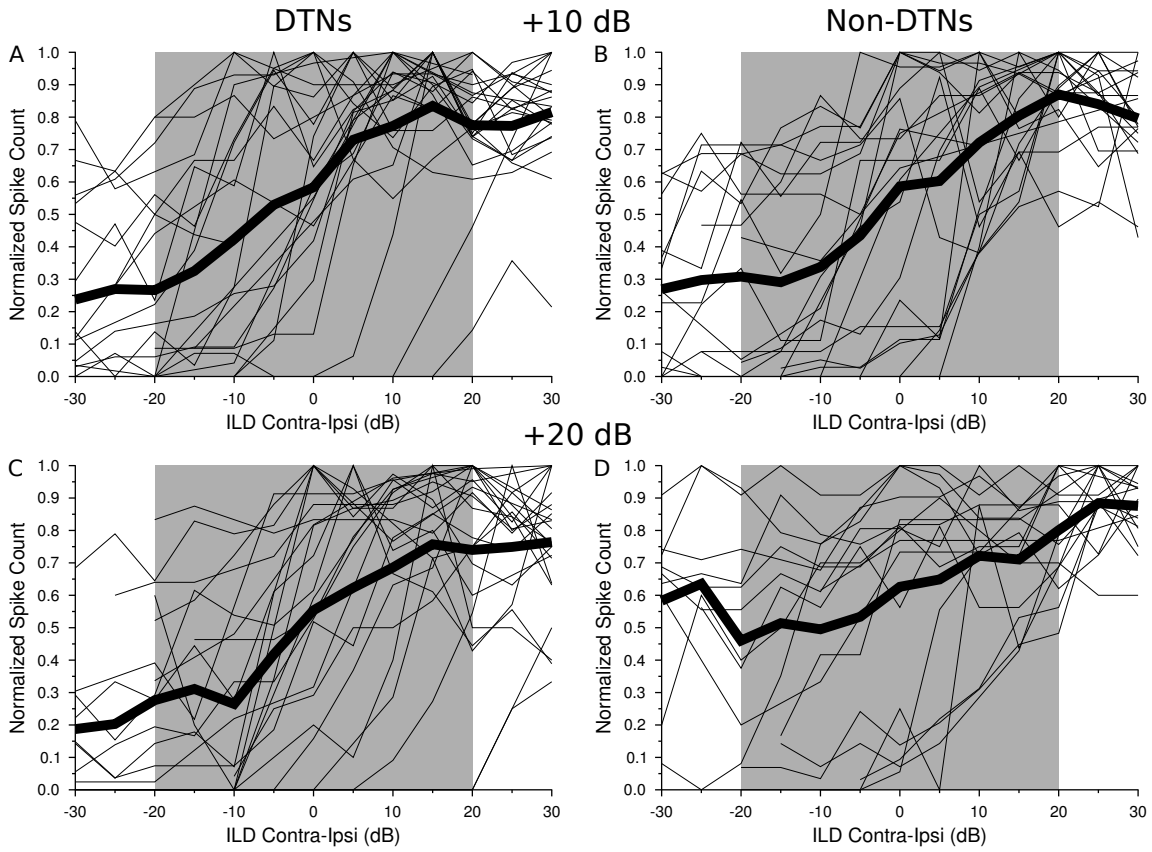

Figure 5.2: ILD sensitivity of IC neurons. Thin black traces represent the individual ILD-tuning curves of DTNs, while the thick black traces represent the average response across the population of (A,B) DTNs and (C,D) non-DTNs. The shaded gray region represents the estimated window of biological relevance (-20 to +20 ILD dB). The stimulus level presented to the contralateral ear was kept at (A,C) +10 dB and (B,D) +20 dB above threshold while the stimulus level presented to the ipsilateral ear varied in 5 dB steps to generate the ILD-tuning curves (ILD = contralateral stimulus level - ipsilateral level). We observed that on the population level the steepest portions of the averaged curves (both DTNs and non-DTNs) fell between the biological ILD range.

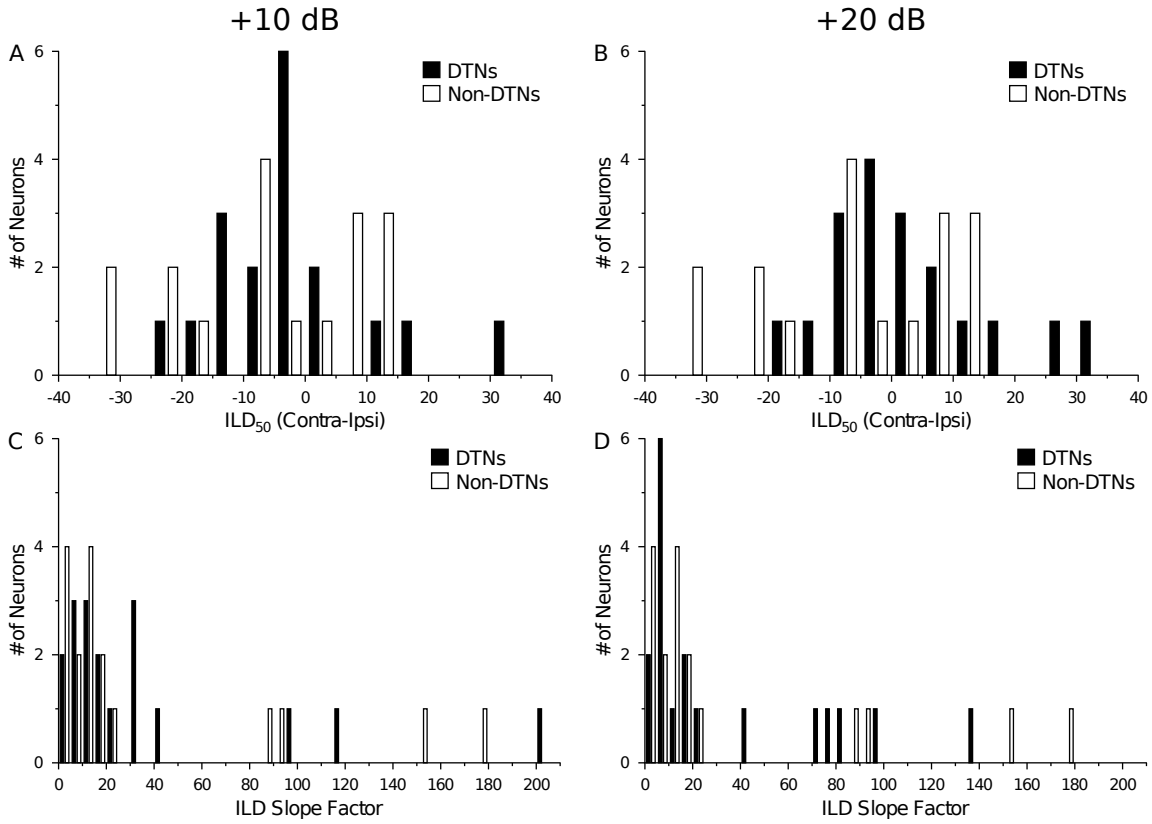

Figure 5.3: Histograms showing the distribution of ILD_{50} and slope factor values as a function of duration selectivity and stimulus amplitude above theshold. The ILD_{50} points of DTNs and non-DTNs were not significantly different at (A) +10 dB re threshold or (B) +20 dB re threshold. Both ILD_{50} distributions were centered between 0 to -10 dB, an ILD stimulus that simulates a sound from midline to the ipsilateral hemifield. The slope factors of the fitted ILD curves did not differ as a function of duration-selectivity at either (C) +10 dB or (D) +20 dB.

Figure 5.4 *(following page)*: Example responses of IC neurons to dichotic ITD stimuli. Responses are plotted as the spikes per stimulus divided by the maximum spiking response ±SE. The shaded gray region represents the estimated biologically relevant range of ITD values (±50 μs). (A) An example DTN not selective to ITD-stimuli. Here we see a >50% of maximum spiking response at all ITDs tested. (B) An example DTN with a peaked response to ITD-stimuli. The peak response occurs when the contralateral stimulus leads the ipsilateral stimulus by 180 μs, outside of the biological range. It is interesting to note that a trough occurs at the 0 ITD point, within the biological range. (C) An example DTN with a monotonic-like response to ITD stimuli. Here we see an increase in spiking response as the ipsilateral stimulus is further delayed relative to the contralateral stimulus. The gray curve represents the fitted four-parameter sigmoid function. The ITD_{50} of the fitted curve is 198.60 μs and the slope factor is 4.0302. The inflection point (maximum slope) occurs at 55.93 μs ITD. The fitted four-parameter sigmoid function was highly correlated with the raw curve ($r = 0.95$, $p \ll 0.001$). (D) An example DTN with a monotonic/peaked response to ITD stimuli. Here we see an increase in spiking response as the ITD cues increase, but peaks at an intermediate ITD before plateauing with a smaller spiking response at increasing ITD cues. (E) An example non-DTN with a cyclical response to ITD stimuli. A cyclical response is characterized by repeating peaks and troughs where the troughs spiking response is <50% of maximum spiking response. (F) ITD_{50} and slope factors of monotonic-responding ITD-sensitive neurons fitted with four-parameter sigmoid functions.

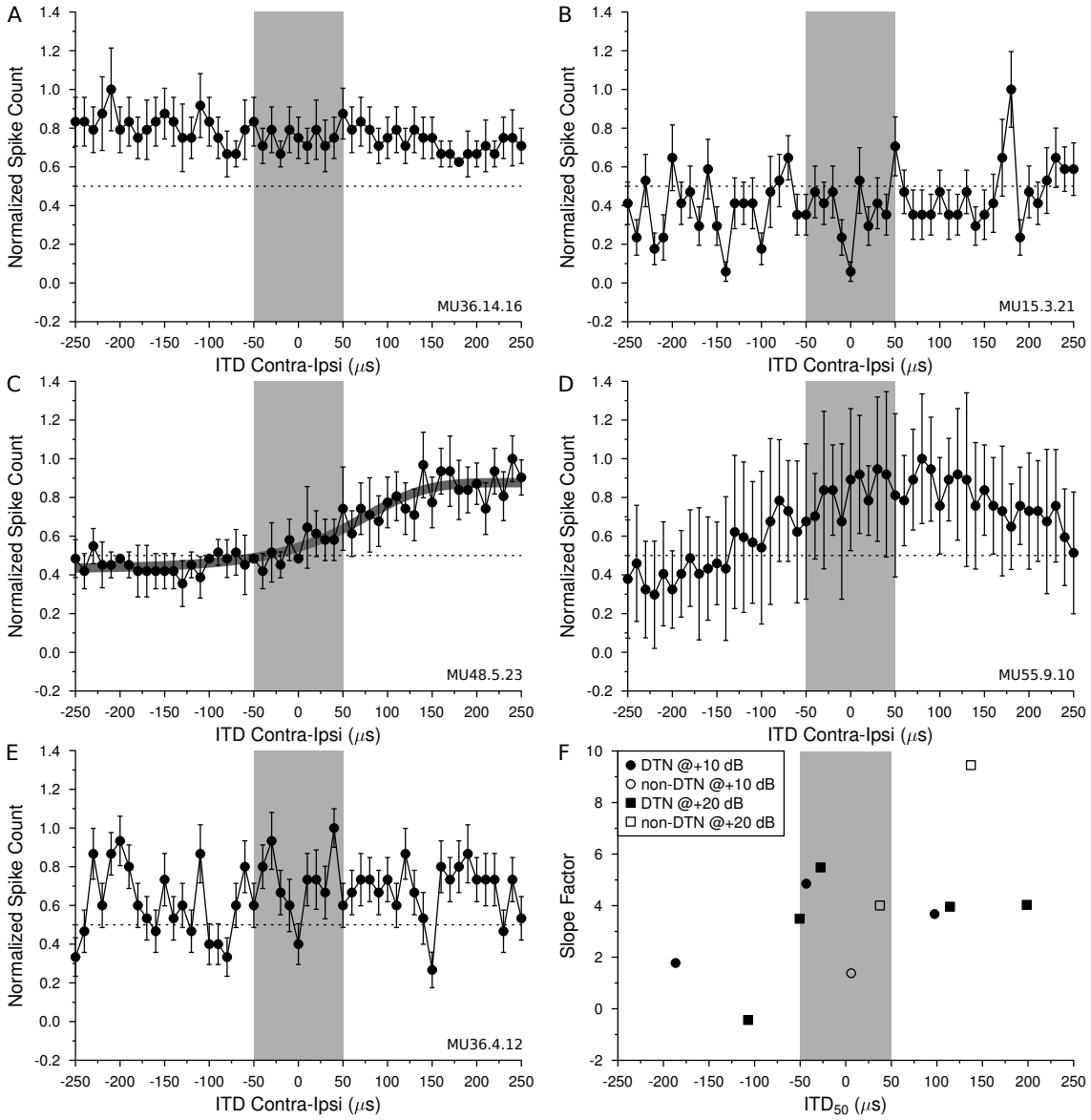
A
B
C
D
E
F
Normalized Spike Count
ITD Contra-Ipsi (μs)
MU36.14.16
MU15.3.21
MU48.5.23
MU55.9.10
MU36.4.12
DTN @+10 dB
non-DTN @+10 dB
DTN @+20 dB
non-DTN @+20 dB
Slope Factor
ITD50 (μs)

6 Discussion

6.1 Significance of dissertation

While the functional role that DTNs play in the central auditory system of the bat has been hypothesized to be involved in processing echolocation calls (Ehrlich et al., 1997), other researchers in the field are more skeptical. For example, Fuzessery and Hall (1999) reported that shortpass DTNs were found equally in both the high-frequency echolocation hearing range and the low-frequency passive listening range in the pallid bat, suggesting that DTNs play a role outside of echolocation in the bat. In non-echolocating animals, DTNs have been suggested to be involved in the processing of temporal components of within-species communication signals. Narins and Capranica (1980) attempted to correlate the range of durations that DTNs encoded and compared this to the durations of the Puerto Rican treefrogs' 100 ms vocalizations, but only reported that DTNs responded maximally to signals longer than the 100 ms vocalizations (response was maximum for pure tones between 100-150 ms). Chapter 2 of the present dissertation compiled the available evidence from the DTN literature and showed that the reported range of best durations of populations of DTNs in echolocating bats were correlated with the durations of their species-specific echolocation calls and the range of best durations of DTNs in non-echolcoating species were correlated with their species-specific vocalizations. This work provided evidence in favour of the argument that DTNs in echolocating animals are involved in processing echolocation calls and that DTNs in non-echolocating animals are involved in processing species-specific vocalizations.

The remaining chapters in this dissertation provided additional evidence supporting the potential role of DTNs in echolocation. Chapter 3 revealed that DTNs are able to respond to pairs of pulses that are separated by interpulse intervals within the range of times cor-

responding to the temporal patterns of emission of loud outgoing echolocation pulses and faint returning echoes. Chapters 4 and 5 explored the contribution of binaural inputs to the underlying neural circuitry that creates DTNs (Chapter 4), and the binaural response properties of DTNs (Chapter 5). If DTNs are involved in processing echolocation calls then it stands to reason that they should exhibit sound localizing properties for tracking of the source of returning echos. Chapter 4 revealed that a subset of DTNs receive inhibitory inputs from the ipsilateral ear, suggesting that at least a subset of DTNs are binaurally innervated. Chapter 5 showed that the majority of DTNs responded selectively to binaural sound localization stimuli, and this selectivity was as strong, if not stronger, than the sound localization selectivity of non-duration selective neurons in the IC. Taken together, it is very likely that DTNs play a role in bat echolocation.

Prior to this dissertation, nearly all research conducted on DTNs involved monaural or free-field binaural stimulation focused on the contralateral ear. Chapter 4 explored the contribution that each ear plays in duration selectivity and showed that non-excitatory tones presented to the contralateral ear (monotic condition) recruited significantly more inhibition than a non-excitatory tone presented to the ipsilateral ear (dichotic condition). In fact, in the dichotic condition only about 48% of neurons showed evidence for the recruitment of inhibition by stimulating the ipsilateral ear. In those neurons with ipsilaterally evoked inhibition, the duration of the inhibition was almost always shorter than the duration of the non-excitatory tone that evoked it – in stark contrast to the persistent inhibition commonly observed in DTNs tested with monaural paired tone stimulation. The ipsilaterally evoked inhibition was also delayed compared to the contralaterally evoked inhibition. Previous studies on DTNs have shown that inhibition is important for creating duration-selective responses. Together, these findings strongly suggest that the underlying mechanisms involved in forming duration selectivity are monaural in nature. Nevertheless, the fact that nearly half of the DTNs I tested showed some recruitment of inhibition in the binaural

condition suggests that, in at least a subset of DTNs, binaural inputs play some role in the response properties of DTNs.

Change in spike rate, as opposed to spike latency, is typically the measure used in electrophysiological studies. Spike rate neural models rely on integrating spike discharges over a period of time. Such a spike rate coding system would be less than ideal to account for rapidly performed sensorimotor tasks (VanRullen et al., 2005) and for processing echolocation calls at a single neuron level (Fontaine and Peremans, 2009). This is because spike rate neural models require an integration delay to account for multiple spikes. VanRullen et al. (2005) and Fontaine and Peremans (2009) argue that spike time neural coding, typically the first-spike latency time, can convey relevant information about the stimulus with a single spike. This dissertation examined changes in both spike count and spike latencies for determining the recovery cycle times (Chapter 3) and subsequently the inhibition times of DTNs (Chapter 4). The results obtained through evaluating changes in spike count and spike times were generally correlated, although this correlation was not perfect. Some neurons showed drastic differences in the results obtained through spike times versus spike counts in both recovery times and inhibition times. While the debate between the relative importance of these two neural codes is long from over, this dissertation highlighted some differences and similarities obtained through evaluating both methods.

6.2 Research limitations

Echolocation signals emitted by bats typically employ downward frequency modulated (FM) sweeps (Neuweiler, 1984); however most studies (including this dissertation) have characterized the response properties of DTNs using pure tones. This raises the obvious question of how DTNs process FM echolocation calls. One possibility is that DTNs also respond to downward FM sweeps, and in fact many do (Ehrlich et al., 1997). This does not

preclude DTNs that respond best to pure tones from playing a role in echolocation. Another possibility is that DTNs that respond best to pure tone may encode a portion of the FM sweep of the echolocation call. A population of DTNs that each respond to different bandwidths of stimulus frequency and stimulus duration may encode various portions of the outgoing FM echolocation pulse and the returning FM echo. Such population coding is often thought to increase the performance accuracy of the task at hand (Knight, 1972; Mason et al., 2001).

To better assess the binaural response properties of DTNs in the big brown bat I employed a pair of $\frac{1}{4}$ inch speakers that were positioned as close as possible to the external auditory meatus without touching the bat. The possibility exists that a loud sound stimulus from one speaker could "bleed-over" and stimulate the other ear via acoustic crosstalk. The amount of acoustic crosstalk that occurs will depend on the anatomy of the head of each bat and the positioning of the speakers. Although the amount of crosstalk was not directly measured in this dissertation, a previous study using similar $\frac{1}{4}$ inch speakers reported $>$30 dB of attenuation between the two ears (Ehrlich et al., 1997). To minimize the potential effect of acoustic crosstalk in my studies, auditory stimuli were typically presented at $+10$ to $+20$ dB relative to the threshold of the cell, or ± 30 dB relative to the threshold of the cell when measuring responses to changing ILD cues. It is important to note that the potential for crosstalk actually strengthens the finding that the circuitry underlying duration selectivity is monaural in nature (Chapter 4), as the effect of acoustic crosstalk should increase the amount of inhibition recruited in the binaural condition through inadvertent stimulation of the monaural pathway. This did not appear to happen for at least half of the cells I tested.

6.3 Alternate role of DTNs

As mentioned previously, the role of DTNs cannot solely be for echolocation as they are also found in non-echolocating species and also respond to frequencies outside the relevant range of echolocation signals. Each DTN responds to a specific range of stimulus frequencies, amplitudes and durations. This makes DTNs especially suited to act as auditory spectrotemporal filters for subsequent processing in ascending auditory nuclei. Spectrotemporal filters would allow for the brain to process highly specific information about the auditory environment. Spectrotemporal filters could also play a role in speech processing. For example, in the English language a number of phonemes share the same frequency information and differ only in the temporal domain (Denes, 1955), a processing problem that appears especially suited for DTNs to resolve.

The frequency tuning curves of auditory neurons can be thought of as spectral filters, and they have been implicated in playing a role in auditory stream segregation (Bregman, 1990; Beauvois and Meddis, 1991; Fishman et al., 2001; Pressnitzer et al., 2008). Auditory stream segregation is a phenomenon where auditory signals can be perceived as belonging to separate sources as opposed to a single source, depending on the physical parameters of the sounds. Stimulus frequency plays a primary role in auditory stream segregation because sounds with large frequency disparities are more likely to be reported as belonging to separate streams compared to sounds with small frequency disparities which are more likely to be reported as belonging to a single stream (Bregman and Campbell, 1971). Other factors have been shown to play a role in the perception of sound streams, including signal duration (Bregman, 1990; Bregman et al., 2000). To my knowledge, the potential for auditory stream segregation to occur on the basis of duration alone has yet to be tested. Nevertheless, DTNs provide a neural mechanism that could contribute to auditory stream segregation because DTNs can filter incoming signals in both the frequency and time domain.

Auditory stream segregation and echolocation are not mutually exclusive. Duration-tuned neurons in the bat may be involved in segregating successive echolocation calls and their incoming echoes into different streams, perhaps when the bat is attempting to locate multiple objects in three dimensional space. In fact, a recent study on echo-delay tuned neurons in the IC of the mustached bat has reported that a subset of these echo-delay neurons are also selective to stimulus duration (Macıas et al., 2013). A preliminary behavioural study has shown that the big brown bat is able to discriminate between echo delays that are systematically changing over time (successively increasing or decreasing) from randomized echo delays (Moss and Surlykke, 2001), suggesting that bats can keep track of the delay of successive echoes over time – a prerequisite for bats to segregate pulse-echo pairs into streams that vary in echo delay times. For example, if bats are tracking a prey item (figure) while simultaneously probing the environment for obstacles (ground), the echo delays that are generated as the bat approaches its prey would be shorter than the echo delays generated by obstacles that are further away. Stream segregation by echo delay would allow for parallel processing of prey echoes and obstacle echoes. A number of studies have reported that bat species send out echolocation pulses in pairs that are sometimes referred as "strobe groups" (Kössl et al., 1999; Moss and Surlykke, 2001; Petrites et al., 2009; Hiryu et al., 2010; Ratcliffe et al., 2011; DiCecco et al., 2013). These strobe groups typically vary in frequency; a strategy that would presumably facilitate auditory stream segregation through the most well-known stream segregating parameter – stimulus frequency (Bregman and Campbell, 1971). Should bat echolocation call strobe pairs be targeted at different objects, say a prey item and an obstacle, the returning echoes would also vary in echo delay and this could potentially further facilitate stream segregation. One particular bat species, *Saccopteryx bilineatta*, has been observed to only use strobe pair echolocation calls when foraging (Ratcliffe et al., 2011), perhaps because while hunting the bat is simultaneously tracking prey items and obstacles as opposed to tracking obstacles alone when navigating

in a roost site or after capturing a prey item.

6.4 Future directions

Compared to other types of central auditory neurons, DTNs have only recently been discovered in mammals (e.g. Jen and Schlegel, 1982; Pinheiro et al., 1991; Casseday et al., 1994) and have only been studied in a handful of research labs. There are many avenues yet to be explored with DTN physiology. For example, DTNs are typically tested with pure tones, and most DTNs respond well to pure tone stimuli, but bats employ FM sweeps in their echolocation pulses. At least a subset of DTNs have been reported to respond to FM stimuli (Ehrlich et al., 1997), but the parameters of the FM sweep stimuli that DTNs are selective to remain unknown. The potential differences between DTNs that respond to FM stimuli and those that don't also remains unexplored. A further understanding of how DTNs encode and respond to FM sweeps might provide additional insight on the role of DTNs in hearing in general and in echolocation by bats.

The inputs to and from the IC have been identified through a large number of tracer studies (e.g. Beyerl, 1978; Adams, 1979; Brunso-Bechtold et al., 1981; Schweizer, 1981; Zook and Casseday, 1982; Faye-Lund, 1986; Coleman and Clerici, 1987; Olaźbal and Moore, 1989; Caicedo and Herbert, 1993; Wenstrup et al., 1994; Marsh et al., 2002; Oliver et al., 1995; Winer Jeffery A and Hefti, 1998; Winer et al., 2002; Loftus et al., 2004). Although, these studies show that the IC receives and sends inputs to a number of brain regions, the afferents to and efferents of DTNs are unknown as the tracer studies did not selectively target neurons based on temporal selectivity. The IC does not only have connections with auditory regions but also has efferents that project to motor-areas (Wenstrup et al., 1994; Covey, 2005) and receives afferents from non-auditory regions such as the amygdala (Marsh et al., 2002) and the substantia nigra (Olaźbal and Moore, 1989). Should DTNs selectively re-

ceive inputs from certain regions and/or project efferents to certain regions we may get a glimpse on the role DTNs play and an idea of where DTNs play a role.

The behavioural role that DTNs play in discriminating sounds based on signal duration is unknown. Bats can be trained to indicate that they perceive differences in sound stimuli using a two-alternative forced choice paradigm (e.g. Simmons, 1971). Using similar training, we can test the temporal acuity of bats based on signal duration and then compare their behavioural temporal acuity with the physiological temporal acuity of DTNs (both single cells and populations of DTNs). The temporal acuity of other animals can also be tested and compared in a simialr manner. I predict that species with sharper neural duration tuning profiles would also have sharper behavioural temporal acuity.

In chapter 5 of this dissertation I explored the response properties of DTNs to sound localization stimuli presented dichotically. When DTNs were stimulated with varying ILDs, the ITD was kept constant and was equal in both ears (ITD = 0 μs). When DTNs were stimulated with varying ITDs, the ILD was kept constant and was 0 dB. In the real world, ILD and ITD cues covary with one another as well as other sound localization cues such as the head-related transfer function. By presenting sounds with a free-field speaker that can be positioned at various locations in azimuth and elevation, it is possible to characterize the sound localization response properties of DTNs to ILD and ITD stimuli that are more in line with the real world. Given that the results of chapter 4 showed that over half of the DTNs studied showed no recruitment of inhibition in the binaural condition, I predict that this subset of DTNs would have large spatial receptive fields and respond to sounds located within the entire acoustic hemifield, whereas DTNs that showed recruitment of ipsilaterally-evoked inhibition would have much narrower receptive fields and respond to a restricted location of sound space. It would be interesting to note whether the spatial receptive fields of DTNs are tolerant to changes in sound pressure level in a manner similar to the spatially-receptive auditory neurons found in the avian homolog of the IC of the barn

owl (Knudsen and Konishi, 1978) and the amplitude tolerance of duration tuning response curves (Fremouw et al., 2005), or if increasing the overall sound pressure level alters the shape and/or size of their spatial receptive fields.

References

Adams, J. (1979). Ascending projections to the inferior colliculus. *J Comp Neurol*, 183(3):519–538.

Au, W. W. (2000). Echolocation in dolphins. In Popper, A. and Fay, R., editors, *Hearing by whales and dolphins*, pages 364–408. Springer New York.

Aubie, B., Becker, S., and Faure, P. A. (2009). Computational models of millisecond level duration tuning in neural circuits. *J Neurosci*, 29(29):9255–9270.

Aubie, B., Sayegh, R., and Faure, P. A. (2012). Duration tuning across vertebrates. *J Neurosci*, 32(18):6364–6372.

Beauvois, M. W. and Meddis, R. (1991). A computer model of auditory stream segregation. *Q. J. Exp. Psychol-A.*, 43(3):517–541.

Beyerl, B. D. (1978). Afferent projections to the central nucleus of the inferior colliculus in the rat. *Brain Res.*, 145(2):209–223.

Brand, A., Urban, A., and Grothe, B. (2000). Duration tuning in the mouse auditory midbrain. *J Neurophysiol*, 84(4):1790–1799.

Bregman, A. and Campbell, J. (1971). Primary auditory stream segregation and perception of order in rapid sequences of tones. *J. Exp. Psychol.*, 89(2):244–249.

Bregman, A. S. (1990). *Auditory scene analysis: the perceptual organization of sound*. MIT Press, Cambridge.

Bregman, A. S., Ahad, P. A., Crum, P. A., and OReilly, J. (2000). Effects of time intervals and tone durations on auditory stream segregation. *Atten. Percept. Psychophys.*, 62(3):626–636.

Brunso-Bechtold, J., Thompson, G., and Masterton, R. (1981). HRP study of the organization of auditory afferents ascending to central nucleus of inferior colliculus in cat. *J Comp Neurol*, 197(4):705–722.

Caicedo, A. and Herbert, H. (1993). Topography of descending projections from the inferior colliculus to auditory brainstem nuclei in the rat. *J Comp Neurol*, 328(3):377–392.

Casseday, J. H., Ehrlich, D., and Covey, E. (1994). Neural tuning for sound duration: role of inhibitory mechanisms in the inferior colliculus. *Science*, 264(5160):847–850.

Casseday, J. H., Ehrlich, D., and Covey, E. (2000). Neural measurement of sound duration: control by excitatory-inhibitory interactions in the inferior colliculus. *J Neurophysiol*, 84(3):1475–1487.

Coleman, J. R. and Clerici, W. J. (1987). Sources of projections to subdivisions of the inferior colliculus in the rat. *J Comp Neurol*, 262(2):215–226.

Covey, E. (2005). Neurobiological specializations in echolocating bats. *Anat. Rec. A Discov. Mol. Cell. Evol. Biol.*, 287(1):1103–1116.

Covey, E. and Faure, P. A. (2005). Neural mechanisms for analyzing temporal patterns in echolocating bats. In Pressnitzer, D., Cheveigné, A. d., McAdams, S., and Collet, L., editors, *Auditory signal processing: physiology, psychoacoustics, and models*, pages 251–257. Springer Verlag, New York.

Covey, E., Kauer, J. A., and Casseday, J. H. (1996). Whole-cell patch-clamp recording reveals subthreshold sound-evoked postsynaptic currents in the inferior colliculus of awake bats. *J Neurosci*, 16(9):3009–3018.

Dear, S. P., Simmons, J. A., and Fritz, J. (1993). A possible neuronal basis for representation of acoustic scenes in auditory cortex of the big brown bat. *Nature*, 364(6438):620–623.

Denes, P. (1955). Effect of duration on the perception of voicing. *J Acoust Soc Am*, 27(4):761–764.

DiCecco, J., Gaudette, J. E., and Simmons, J. A. (2013). Multi-component separation and analysis of bat echolocation calls. *J Acoust Soc Am*, 133:538.

Ehrlich, D., Casseday, J. H., and Covey, E. (1997). Neural tuning to sound duration in the inferior colliculus of the big brown bat, *Eptesicus fuscus*. *J Neurophysiol*, 77(5):2360–2372.

Faure, P. A., Fremouw, T., Casseday, J. H., and Covey, E. (2003). Temporal masking reveals properties of sound-evoked inhibition in duration-tuned neurons of the inferior colliculus. *J Neurosci*, 23(7):3052–3065.

Faye-Lund, H. (1986). Projection from the inferior colliculus to the superior olivary complex in the albino rat. *J. Anat. Embryol.*, 175(1):35–52.

Fenton, M. B. (1984). Echolocation: implications for ecology and evolution of bats. *Q. Rev. Biol.*, 59:33–53.

Fishman, Y. I., Reser, D. H., Arezzo, J. C., and Steinschneider, M. (2001). Neural correlates of auditory stream segregation in primary auditory cortex of the awake monkey. *Hearing Res*, 151(1):167–187.

Fontaine, B. and Peremans, H. (2009). Bat echolocation processing using first-spike latency coding. *Neural Networks*, 22(10):1372–1382.

Fremouw, T., Faure, P. A., Casseday, J. H., and Covey, E. (2005). Duration selectivity of neurons in the inferior colliculus of the big brown bat: tolerance to changes in sound level. *J Neurophysiol*, 94(3):1869–1878.

Fuzessery, Z. M. and Hall, J. C. (1999). Sound duration selectivity in the pallid bat inferior colliculus. *Hearing Res*, 137(1-2):137–154.

Galazyuk, A. V. and Feng, A. S. (1997). Encoding of sound duration by neurons in the auditory cortex of the little brown bat, *Myotis lucifugus*. *J Comp Physiol A*, 180(4):301–311.

He, J. (2002). OFF responses in the auditory thalamus of the guinea pig. *J Neurophysiol*, 88(5):2377–2386.

He, J., Hashikawa, T., Ojima, H., and Kinouchi, Y. (1997). Temporal integration and duration tuning in the dorsal zone of cat auditory cortex. *J Neurosci*, 17(7):2615–2625.

Hiryu, S., Bates, M., Simmons, J., and Riquimaroux, H. (2010). FM echolocating bats shift frequencies to avoid broadcast–echo ambiguity in clutter. *Proc. Natl. Acad. Sci. USA*, 107(15):7048–7053.

Jen, P. H.-S. and Feng, R. B. (1999). Bicuculline application affects discharge pattern and pulse-duration tuning characteristics of bat inferior collicular neurons. *J Comp Physiol A*, 184:185–194.

Jen, P. H.-S. and Schlegel, P. A. (1982). Auditory physiological properties of the neurones in the inferior colliculus of the big brown bat, *Eptesicus fuscus*. *J Comp Physiol A*, 147(3):351–363.

Klump, G. M. and Gerhardt, H. C. (1987). Use of non-arbitrary acoustic criteria in mate choice by female gray tree frogs. *Nature*, 326:286–288.

Knight, B. W. (1972). Dynamics of encoding in a population of neurons. *J. Gen. Physiol.*, 59(6):734–766.

Knudsen, E. I. and Konishi, M. (1978). A neural map of auditory space in the owl. *Science*, 200(4343):795–797.

Kössl, M., Mora, E., Coro, F., and Vater, M. (1999). Two-toned echolocation calls from *Molossus molossus* in Cuba. *J. Mammal.*, pages 929–932.

Leary, C. J., Edwards, C. J., and Rose, G. J. (2008). Midbrain auditory neurons integrate excitation and inhibition to generate duration selectivity: an *in vivo* whole-cell patch study in anurans. *J Neurosci*, 28(21):5481–5493.

Loftus, W. C., Bishop, D. C., Saint Marie, R. L., and Oliver, D. L. (2004). Organization of binaural excitatory and inhibitory inputs to the inferior colliculus from the superior olive. *J Comp Neurol*, 472(3):330–344.

Lu, Y. and Jen, P. H.-S. (2003). Binaural interaction in the inferior colliculus of the big brown bat, *Eptesicus fuscus*. *Hearing Res*, 177(1):100–110.

Macıas, S., Hechavarrıa, J. C., Kossl, M., and Mora, E. C. (2013). Neurons in the inferior colliculus of the mustached bat are tuned both to echo-delay and sound duration. *Neuroreport*, 24(8):404–409.

Marsh, R. A., Fuzessery, Z. M., Grose, C. D., and Wenstrup, J. J. (2002). Projection to the inferior colliculus from the basal nucleus of the amygdala. *J Neurosci*, 22(23):10449–10460.

Mason, A. C., Oshinsky, M. L., and Hoy, R. R. (2001). Hyperacute directional hearing in a microscale auditory system. *Nature*, 410(6829):686–690.

Mauk, M. D. and Buonomano, D. V. (2004). The neural basis of temporal processing. *Annu. Rev. Neurosci.*, 27:307–340.

Moss, C. F. and Surlykke, A. (2001). Auditory scene analysis by echolocation in bats. *J Acoust Soc Am*, 110(4):2207–2226.

Narins, P. M. and Capranica, R. R. (1980). Neural adaptations for processing the two-note call of the Puerto Rican treefrog, *Eleutherodactylus coqui*. *Brain Behav. Evol.*, 17(1):48–66.

Neuweiler, G. (1984). Foraging, Echolocation and Audition in Bats. *Naturwissenschaften*, 71:446–455.

Olaźbal, U. and Moore, J. (1989). Nigrotectal projection to the inferior colliculus: horseradish peroxidase transport and tyrosine hydroxylase immunohistochemical studies in rats, cats, and bats. *J Comp Neurol*, 282(1):98–118.

Oliver, D. L., Beckius, G. E., and Shneiderman, A. (1995). Axonal projections from the lateral and medial superior olive to the inferior colliculus of the cat: a study using electron microscopic autoradiography. *J Comp Neurol*, 360(1):17–32.

O'Neill, W. E. and Suga, N. (1979). Target range-sensitive neurons in the auditory cortex of the mustache bat. *Science*, 203(4375):69–73.

Petrites, A. E., Eng, O. S., Mowlds, D. S., Simmons, J. A., and DeLong, C. M. (2009). Interpulse interval modulation by echolocating big brown bats (*Eptesicus fuscus*) in different densities of obstacle clutter. *J Comp Physiol A*, 195:603–617.

Pinheiro, A. D., Wu, M., and Jen, P. H. (1991). Encoding repetition rate and duration in the inferior colliculus of the big brown bat, *Eptesicus fuscus*. *J Comp Physiol A*, 169(1):69–85.

Pollack, G. S. and Hoy, R. R. (1979). Temporal pattern as a cue for species-specific calling song recognition in crickets. *Science*, 204(4391):429–432.

Pressnitzer, D., Sayles, M., Micheyl, C., and Winter, I. M. (2008). Perceptual organization of sound begins in the auditory periphery. *Curr. Biol.*, 18(15):1124–1128.

Ratcliffe, J., Jakobsen, L., Kalko, E., and Surlykke, A. (2011). Frequency alternation and an offbeat rhythm indicate foraging behavior in the echolocating bat, *Saccopteryx bilineata*. *J Comp Physiol A*, 197(5):413–423.

Rayleigh, L. (1907). XII. On our perception of sound direction. *Philos Mag*, 13(74):214–232.

Schweizer, H. (1981). The connections of the inferior colliculus and the organization of the brainstem auditory system in the greater horseshoe bat (*Rhinolophus ferrumequinum*). *J Comp Neurol*, 201(1):25–49.

Shannon, R. V., Zeng, F.-G., Kamath, V., Wygonski, J., and Ekelid, M. (1995). Speech recognition with primarily temporal cues. *Science*, 270:303–304.

Simmons, J. (1971). Echolocation in bats: signal processing of echoes for target range. *Science*, 171(974):925–928.

Simmons, J. A. (1973). The resolution of target range by echolocating bats. *J Acoust Soc Am*, 54(1):157–173.

Tan, M. L. and Borst, J. G. G. (2007). Comparison of responses of neurons in the mouse inferior colliculus to current injections, tones of different durations, and sinusoidal amplitude-modulated tones. *J Neurophysiol*, 98(1):454–466.

VanRullen, R., Guyonneau, R., and Thorpe, S. J. (2005). Spike times make sense. *Trends Neurosci.*, 28(1):1–4.

Wenstrup, J. J., Larue, D. T., and Winer, J. A. (1994). Projections of physiologically defined subdivisions of the inferior colliculus in the mustached bat: Targets in the medial geniculate body and extrathalamic nuclei. *J Comp Neurol*, 346(2):207–236.

Winer, J. A., Chernock, M. L., Larue, D. T., and Cheung, S. W. (2002). Descending projections to the inferior colliculus from the posterior thalamus and the auditory cortex in rat, cat, and monkey. *Hearing Res*, 168(1):181–195.

Winer Jeffery A, L. D. T. D. J. J. and Hefti, B. J. (1998). Auditory cortical projections to the cat inferior colliculus. *J Comp Neurol*, 400:147–174.

Zook, J. M. and Casseday, J. H. (1982). Origin of ascending projections to inferior colliculus in the mustache bat, *Pteronotus parnellii*. *J Comp Neurol*, 207(1):14–28.